

FLORIDA DEPARTMENT OF TRANSPORTATION – AVIATION OFFICE

STATEWIDE AIRPORT STORMWATER STUDY

FAA POND DESIGN CRITERIA

WATER TREATMENT MODELING

REPORT



CLEAN WATER – SAFE AIRPORTS

DECEMBER, 2010

STATEWIDE AIRPORT STORMWATER STUDY
FAA POND DESIGN CRITERIA –
WATER TREATMENT MODELING REPORT

TABLE OF CONTENTS

1	Executive Summary	1
2	Introduction	3
3	Purpose and Scope	5
4	Material and Methods.....	8
4.1	Hyetographs.....	8
	4.1.1 Study Hyetographs.....	8
4.2	Particle Size Distribution	12
	4.2.1 PSD Selection	12
	4.2.2 PSD Significance	13
4.3	Physical Model Description	14
	4.3.1 Transformation of Rainfall Hyetographs to Runoff Hydrographs	19
4.4	Wet pond at the Orlando Executive Airport.....	21
	4.4.1 Hydrologic-hydraulic simulation.....	22
4.5	Generic Rectangular and Triangular Quarry Ponds.....	30
4.6	Physical Model Methodology.....	30
	4.6.1 Description of the Equipment and Components.....	31
	4.6.2 Data Acquisition and Management.....	33
	4.6.3 Calibration Procedures and Verification.....	34
	4.6.4 Slurry Mixing and Injection System.....	36
	4.6.5 Sampling Methodology and Protocol	37
	4.6.6 Mass Recovery and Sample Protocol	37
	4.6.7 Laboratory Analysis.....	37
	4.6.8 Verification of Mass Balance for each Experimental Run.....	38
	4.6.9 Verification of PSD Balance for Each Run.....	39

4.7	CFD modeling	39
4.7.1	CFD governing equations	39
4.7.2	Discrete phase model (DPM)	41
4.7.3	Model Implementation.....	42
4.7.4	Boundary and Initial Conditions, Computational Parameters and Assumptions.....	50
4.7.5	Population Balance	51
4.7.6	Model validation.....	51
4.7.7	Computational resources	51
5	Results and Discussion	53
5.1	Experimental Results - FAA Linear Pond and Crenellated Pond Configurations ..	53
5.2	CFD Modeling – FAA Linear Pond and Crenellated Pond results	58
5.3	CFD Modeling – ORL Wet Pond Results.....	64
5.4	CFD Modeling - Triangular and Rectangular Quarry Ponds Results.....	75
6	Conclusions and Recommendations	82
7	References	85
8	Abbreviations and Symbols	88

1 Executive Summary

This document is the fourth publication of the *Florida Statewide Airport Stormwater Study*, which is jointly funded by the Federal Aviation Administration (FAA) and the Florida Department of Transportation (FDOT). Technical review and guidance for stormwater management is provided by the Florida Department of Environmental Protection (FDEP), and the five Water Management Districts (WMDs). The purpose of the program is to develop design options that promote aircraft safety through reducing wildlife attractants while meeting or exceeding water quality protection and water quantity management standards. Results of the efforts are being incorporated into Florida Administrative Code (FAC) as they demonstrate the ability to satisfy both sets of criteria.

This study focuses on the expected behavior of two wet pond designs that meet the generic guidance of the FAA and the United States Department of Agriculture (USDA) to minimize attraction of birds and other wildlife hazardous to aircraft operation. The significant damage caused to aircraft by bird and other wildlife strikes is documented, and dramatically illustrated by the downing of US Airways Flight 1549 in the Hudson River in January 2009. Additional to the two wet pond designs, the study includes preliminary examination of an existing airport pond located at Orlando Executive Airport (ORL), and two ponds formed by old quarries located on or near airports in Florida. The latter two quarry ponds are studied only for initial guidance on their probable behavior, since quarry ponds are located near a set of Florida airports.

Expected behavior of the pond configurations studied was evaluated with Computational Fluid Dynamic (CFD) models, validated with testing of scaled physical models of the FAA linear and crenellated pond designs. The existing airport and the quarry ponds are evaluated solely using CFD for comparative purposes only.

Results of the scaled physical models coupled with the validated CFD models demonstrate that a crenellated pond configuration significantly outperforms a conventional linear FAA Pond design for all hydrologic loadings tested. Note that the FAA linear design was predicted to outperform typical Florida presumptive pond design. This statistically significant improvement in water treatment function by the crenellated pond is shown by CFD to be a function of greatly improved

volumetric utilization (reduced dead zones) for the same pond surface area used by the FAA linear pond. Based on the prior and current model results, while an FAA linear pond will likely outperform a typical presumptively designed and permitted water management pond, a preferred solution will involve the insertion of baffles into the linear pond to create a crenellated pond. Full scale testing is planned to confirm the predicted behavior and validate the CFD modeling concept for establishing presumptive permitting and design criteria for ponds that minimize wildlife attraction.

Results of the CFD model for ORL demonstrate that for the existing deteriorated condition of the pond the re-placement of the earthed baffles could be improved to achieve a better utilization of volume and minimize the presence of dead zones. During influent flow rates up to approximately 3½ cfs (100 L/s), the earthed baffles exert their treatment function, constraining the flow to follow the path delimited by the baffles. For higher flow rates, the water level in the pond exceeds the top elevation of the baffles and a portion of the flow is able to bypass them. Under this condition the effect of the baffles is minimized with potential generation of short-circuiting and stagnant zones. Baffles must be elevated to preclude this under normal flow conditions.

The results of the CFD models for the quarry ponds indicate that volume (or mean residence time) alone is not an adequate index for pond behavior. More appropriately the utilization of the volume is more relevant with respect to formation of dead zones and short-circuiting. The area and volume of such Ponds is excessive without potentially providing any additional particulate matter (PM) separation and chemical conversion benefits beyond dilution. As CFD modeled results demonstrate in this report, the volumetric utilization of the two quarry ponds is very low and such extended Pond surface area could be optimized with the insertion of baffles.

While pond design will be unique for each set of airport conditions and time series loadings, results of this study indicate that (1) the distance between inlet and outlet should be hydrodynamically maximized while ensuring that scour velocities do not generate a bed shear stress capable of re-entraining previously-separated yet unconsolidated bed PM; (2) volumetric utilization of the pond is maximized; (3) maintenance is sufficient to ensure water chemistry benefits for the treatment functioning of the pond; and (4) these objective functions provide regulatory load reduction requirements that are achieved based on a cost-benefit function.

2 Introduction

As reported in the literature, the treatment effectiveness (as PM separation) of stormwater treatment structures based on gravitational settling primarily depends on the hydrodynamic conditions established within the system (Pathapati and Sansalone, 2009a; He et al., 2008; Wu, J.S. et al., 1996). In particular, PM removal is strongly affected by hydraulic detention times since longer detention time allow particles to have enough time to settle. A method to enhance PM separation is the placement of baffles through the system so that the flow across the cross-section of the Pond is evenly distributed, minimizing the potential for short-circuiting and increasing residence times; maximizing the hydrodynamic distance from inlet to outlet, and essentially creating a plug flow reactor (PFR) system. For this reason, a baffled FAA pond is proposed by placing baffles within the volumetric system, in order to potentially improve the performance of a standard linear pond and maintain the same surface area.

The hydraulic response and PM separation of stormwater systems have been traditionally studied using “lumped” parameters, such as surface overflow rate (SOR) defined as inflow divided by the surface area of the sedimentation Pond (Metcalf and Eddy, 2003). In the last decades, in contrast to these traditional methods, advanced tools such as CFD have become a defensible approach to model the hydraulic and pollutant behavior of stormwater treatment systems; with most conventional methods incapable of representing the coupled hydrodynamic and water chemistry complexity of such systems (Sansalone and Pathapati, 2009c; Pathapati and Sansalone, 2009b). The CFD method is based on numerically solving the fundamental equations of fluid flow, the Navier-Stokes (N-S) equations, is especially powerful when the system is subject to non-ideal conditions, such as complex flows typical of runoff, heterogeneous loadings and complex geometries which often are not possible to model accurately using the traditional methods. While a hydrodynamic model solves and simulates the flow field in CFD, a discrete phase model is used to model particle trajectories and simulate particle separation. The latter approach is coupled with granulometric data, such as particle size distribution (PSD), chemical distribution with PM [for example mg/g] and specific gravity (ρ_s) of PM in order to obtain the PM and PM-based treatment characteristics of the system.

The benefits offered by CFD modeling are numerous. Once the CFD model is calibrated/validated it can be utilized as a design tool comparing different geometrical configurations and layouts, avoiding the time and costs associated with physical testing of each configuration. Additionally, three-dimensional description of particle and pollutant trajectories and velocities which may not be determined in physical models, can be determined at each point within the system.

3 Purpose and Scope

The *Florida Statewide Airport Stormwater Study* is a multi-phase, multi-agency cooperative effort addressing requirements of successful airport stormwater management. As part of a public transportation facility, the stormwater management system must be consistent with safe and efficient air transportation. As a component of environmental protection, the stormwater management system must meet statutory and rule requirements intended to protect water quality, limit or prevent flooding, and promote healthy ecosystems in downstream receiving waters. Ultimately, the traveling and general public is the beneficiary of both requirements.

The *Florida Statewide Airport Stormwater Study* focuses on airside stormwater management. This is required since airside land uses are similar airport to airport, and the stormwater runoff from these has quantifiable quality characteristics. Contrarily, airport landside areas are highly variable in use, including golf courses, race tracks, industrial park and concentrated commercial lands. These landside uses are by their variability outside the scope of the *Statewide Airport Stormwater Study*.

Previous study findings demonstrated the efficacy of overland flow as a best management practice for most airport airside, stormwater management. The documentation in the *Best Management Practices Manual*, the *Technical Report for the Florida Statewide Airport Stormwater Study* and the *Application Assessment for the Florida Statewide Airport Stormwater Study* describe the conditions where overland flow can be the sole structural method of airside stormwater management and provide the supporting data. However, an estimated 20 to 30 percent of airport airside projects will not be able to use the overland flow BMP for stormwater management. In these cases, where continuously wet, stormwater management ponds will be required; the pond must be designed to minimize wildlife attractant features. Federal Aviation Administration (FAA) and United States Department of Agriculture (USDA) have set forth generic guidance for these type ponds in FAA Advisory Circular (AC) 150/5200-33B *Hazardous Wildlife Attractants On or Near Airports*. The generic guidance in the AC is for deep, steep-sided ponds without emergent vegetation. They do not conform to standard “presumptive” pond design criteria of the Water Management Districts or Florida Department of Environmental Regulation (FDEP). Further, detailed design criteria from FAA or the United

States Department of Agriculture (USDA) do not exist for these ponds, only generic features intended to discourage bird and wildlife use are given. This study examines the hydrodynamic and treatment behavior of two wet ponds configured consistent with the generic guidance of the *Hazardous Wildlife Attractant* circular. The purpose is to characterize their potential for load reduction, refining the expected water management behavior of the concept, and provide data for detailed design. Prior to incorporation in rule, a full scale test pond configured to FAA/USDA guidelines will need to demonstrate that the concept will meet Florida and federal environmental regulatory standards. Accordingly, the model study provides guidance to help assure a first time successful design for the full scale test pond.

This study is carried out using scaled physical models and numerical (CFD) models. These efforts quantify the behavior of the standard, linear FAA pond design and a baffled (crenellated) pond design of similar surface area, with deep, steep sided channels. Final components of the study model an existing crenellated pond at the ORL, illustrating the existing functionality of the pond; and two pond configurations typical of the quarry ponds adjacent to a number of Florida airports.

CFD is an advanced, numerical modeling tool previously used for aerodynamic behavior for rocket and aircraft component design. Increases in computer power and speed have made feasible the extension of the tool into the fluid dynamic problems describing the transport and settlement of particulates in water. This study uses CFD for hydrodynamic behavior of constituents, represented by a particle size distribution (PSD) of PM and PM-bound chemicals. For ponds designed to minimize avian or terrestrial wildlife attractants thereby minimizing aircraft strikes, CFD results clearly illustrate the volumetric and geometric utilization of each pond system examined and quantify pond behavior for load reduction benefits.

Study models use hydrologic loadings generated from a 25-year, 24-hour design storm, a historical, high intensity storm recorded July 8, 2008 and a moderate intensity, triangular and short duration event for the FAA linear and crenellated ponds. Pond pollutant reduction behavior is examined utilizing a hetero-disperse PM that has a distribution in size from colloidal to sand-size PM. The first component of this study analyzes the hydrodynamic and load separation behavior of a linear FAA and a crenellated pond subject to such PM and hydrologic

loadings utilizing CFD validated by physical models. As reported in the 2007 ***Application Assessment for the Florida Statewide Airport Stormwater Study*** the modeled behavior of an FAA linear pond illustrated the benefit of increasing the length to width ratio (maximize hydrodynamic separation of inlet and outlet) of a pond geometric design. The FAA linear pond exhibited improved pollutant removal characteristics when compared to ponds designed based on the typical presumptive design criteria published by Water Management Districts. Using the 2007 results as a starting point the linear FAA pond examined in this study has a length to width ratio of 8:1. The CFD model is validated with physical model data to ensure congruence with reality and to give confidence in the conclusions developed from the study. This avoids the “hydro-fantasy” that can and does result from improper use of numerical or analytical models.

As a second component of this project, the existing crenellated pond at the Orlando Executive Airport, in Orlando, Florida is studied in order to estimate its hydrodynamic and PM treatment behavior. A CFD model for the existing condition of the pond is developed and applied based on the existing bathymetry, geometrics and hydraulic configuration of the pond. The configured CFD model is loaded by the same hetero-disperse PSD as the scaled physical model ponds.

The final component of this study examines the peak flow behavior of two existing quarry pond configurations. The configurations are based on quarry ponds located near or on airports in Florida. The specific locations are confidential by airport request, and with concurrence of the project regulatory representatives.

4 Material and Methods

4.1 Hyetographs

4.1.1 Study Hyetographs

An initial component of this study is the definition of the hydrological loadings. The three hyetographs selected are:

1. **Triangular hyetograph** with 0.5 inch of runoff volume and duration of 15 minutes. This loading is selected as short and intense rainfall event during the wet season in Florida, where more than half of the events are likely to be less extreme. A triangular shape is used to define the design hyetograph as shown in Figure 1.

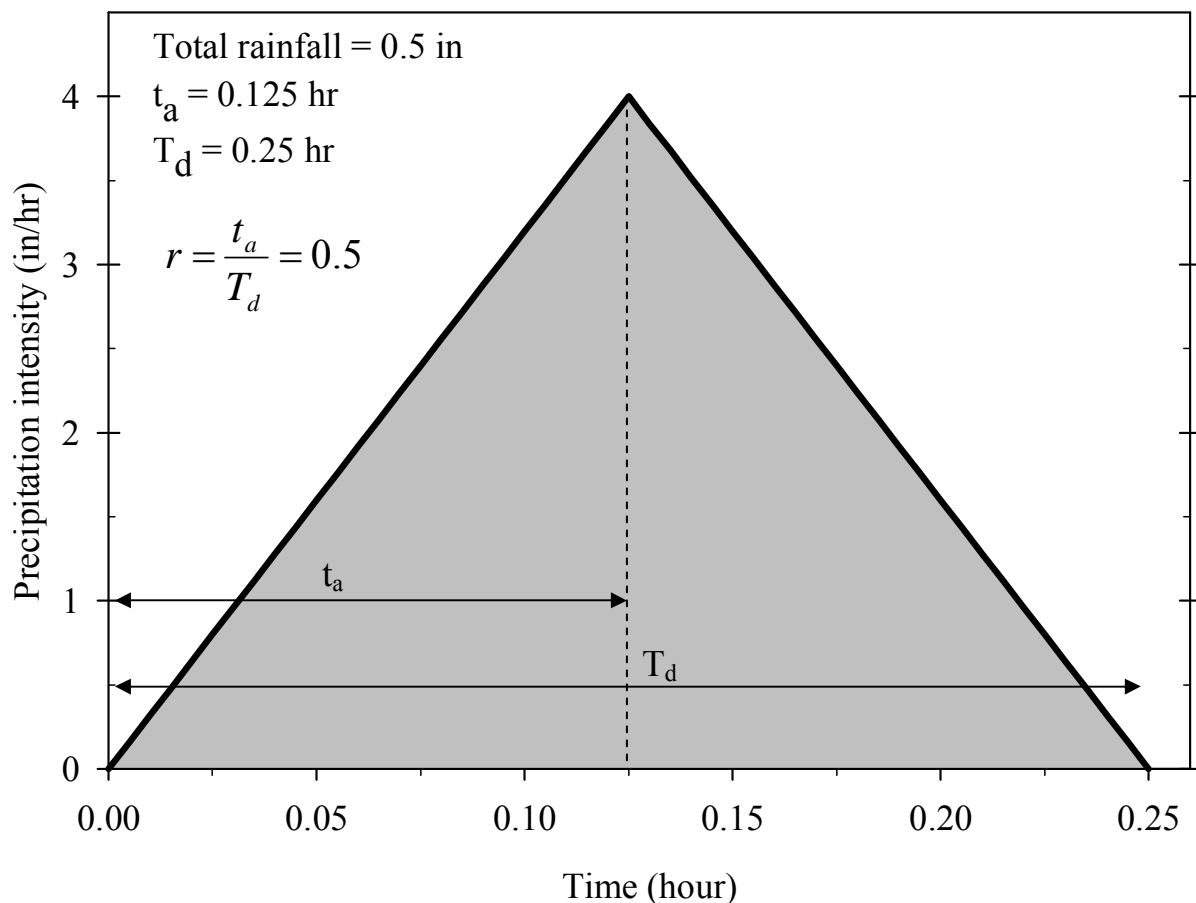


Figure 1 Triangular Design Hyetograph. T_d is the rainfall duration, t_a is the time to peak, and r is the storm advancement coefficient (Chow et al., 1988)

The maximum rainfall intensity of the triangular hyetograph is approximately 4 inches per hour and the total excess precipitation depth is 0.5 inches. This is the same intensity used in roadway “spread” calculations, since driving is considered difficult or impracticable at intensities above this (FDOT, 2010). The hyetograph selected is considered a fairly extreme event, since 80% of storm events occurring in Gainesville are characterized by a total precipitation depth equal or less than 0.5 in. Figure 2 reported below depicts the frequency distribution of 1999-2008 hourly rainfall data for Gainesville Regional Airport (GNV).

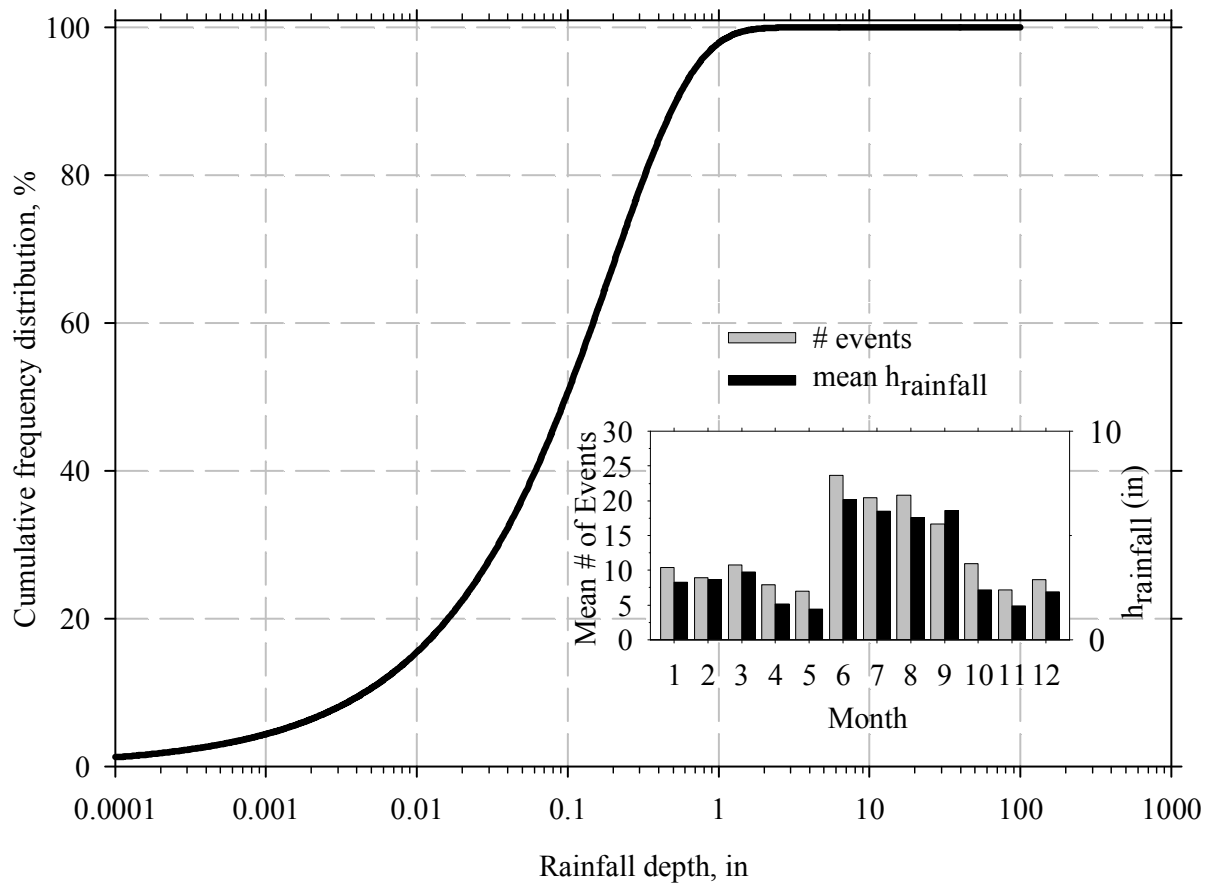


Figure 2 Frequency Distribution of Rainfall Precipitation for Gainesville, Florida on an hourly basis. The frequency distribution is obtained from a series of 1999-2008 hourly precipitation data for Gainesville Regional Airport (GNV)

- Historical event** collected on 8 July 2008 by UF with total rainfall depth of 2.9 inches. This event shown in Figure 3 is chosen since it is an extremely intense historical event, with a peak rainfall intensity of about 6.5 in/h. This value is higher than peak precipitation intensity of the 24 hour-25 year design storm described in the following paragraph.

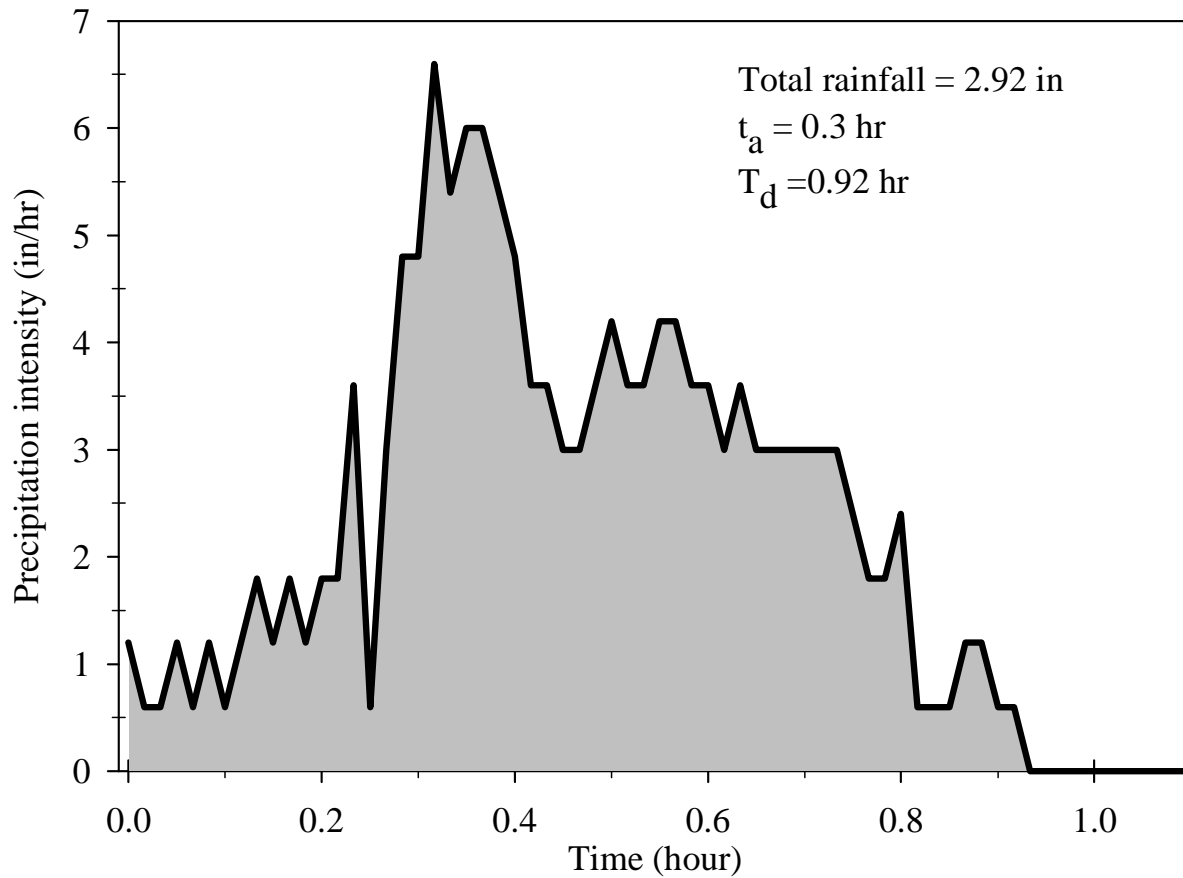


Figure 3 Historical event collected on 8 July 2008 by UF with total rainfall depth of 2.9 inches

- 25-year, 24-hour design event** for Orlando Executive Airport (ORL) rainfall region located near the center of peninsular Florida. From the 25 year-24 hour rainfall frequency distribution provided by St. John River Managemet District, it is found the precipitation depth ($P_{25yr,24h}$) for Orlando area is 8.4 in (St. John River Managemet District,1988) as shown in Figure 4. Then the synthetic hyetograph is developed based on rainfall distributions provided by the National Resource Conservation Service (NRCS) former, Soil Conservation Service (SCS) in 1986. Since Orlando is located in Central Florida, a Type II SCS rainfall distribution is used. The final design storm hyetograph obtained is reported in Figure 5.

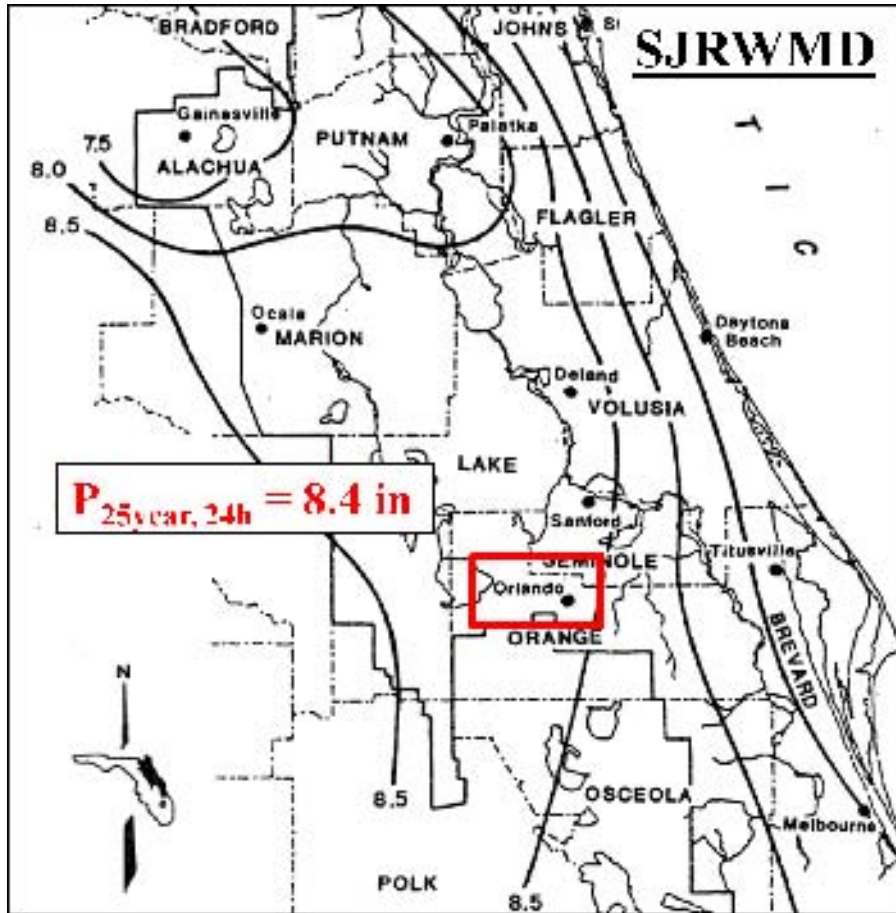


Figure 4 25 year- 24 hour Rainfall frequency distribution (St. John River Water Management District, 1988)

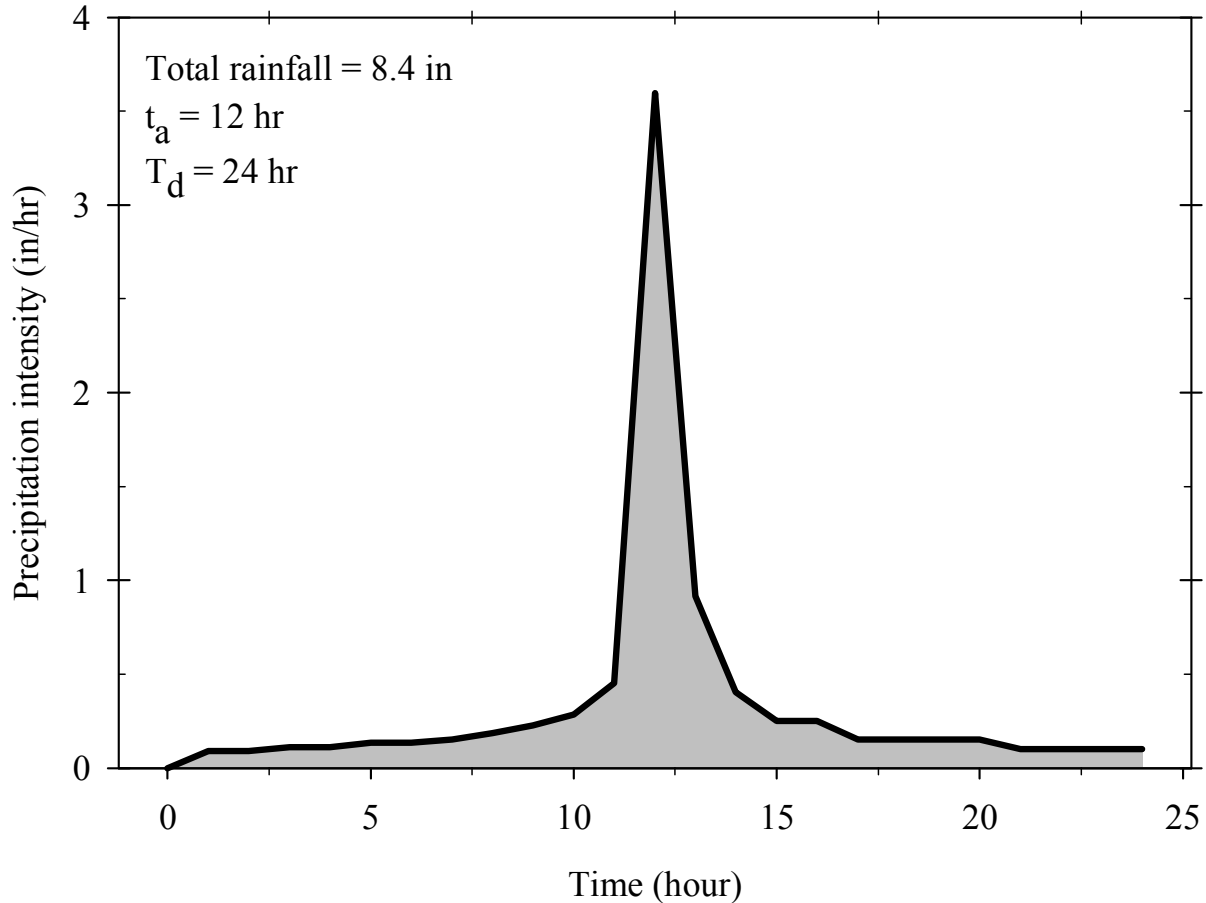


Figure 5 25 Year – 24 hour Design Storm from SCS type II rainfall distribution for Orlando, Florida

4.2 Particle Size Distribution

4.2.1 PSD Selection

The influent particulate loading used throughout the entire study for CFD wet-pond simulation runs and experimental full-scale physical model testing consists of a PSD that is in the silt-size range. The PSD, ranging from less than 1 to 75 μm is reported in Figure 6. The PM specific gravity is 2.63. The mass-based PSD is well described by a gamma distribution function (GF) (Sansalone and Ying, 2008). The probability density function is given by Equation 1 as a function of particle diameter d , where α is a distribution shape factor and γ a scaling parameter. The cumulative gamma distribution function is expressed in Equation 2.

$$f(d) = \frac{\left(\frac{d}{\alpha}\right)^{\gamma-1} e^{(-d/\alpha)}}{\alpha \cdot \Gamma(\gamma)} \quad (1)$$

$$F(x) = \int_0^x f(x) dx \quad (2)$$

4.2.2 PSD Significance

PM is widely recognized as a primary vehicle for the transport and partitioning of pollutants and PM is a pollutant itself that impacts the deterioration of receiving surface waters (EPA, 2000). The potential for water chemistry impairment strongly depends on PM loading and PSD. Furthermore, many PM-bound constituents, such as metals, nutrients and other pollutants, partition to and from PM while transported by PM through rainfall-runoff events (Sansalone et al., 2010; Ma and al., 2010; Dickenson et al., 2009; Sansalone and Buchberger, 1997). Therefore, PSD plays an important role in the transport and chemical processes occurring in runoff and its knowledge is crucial for the analysis and the selection of unit operations.

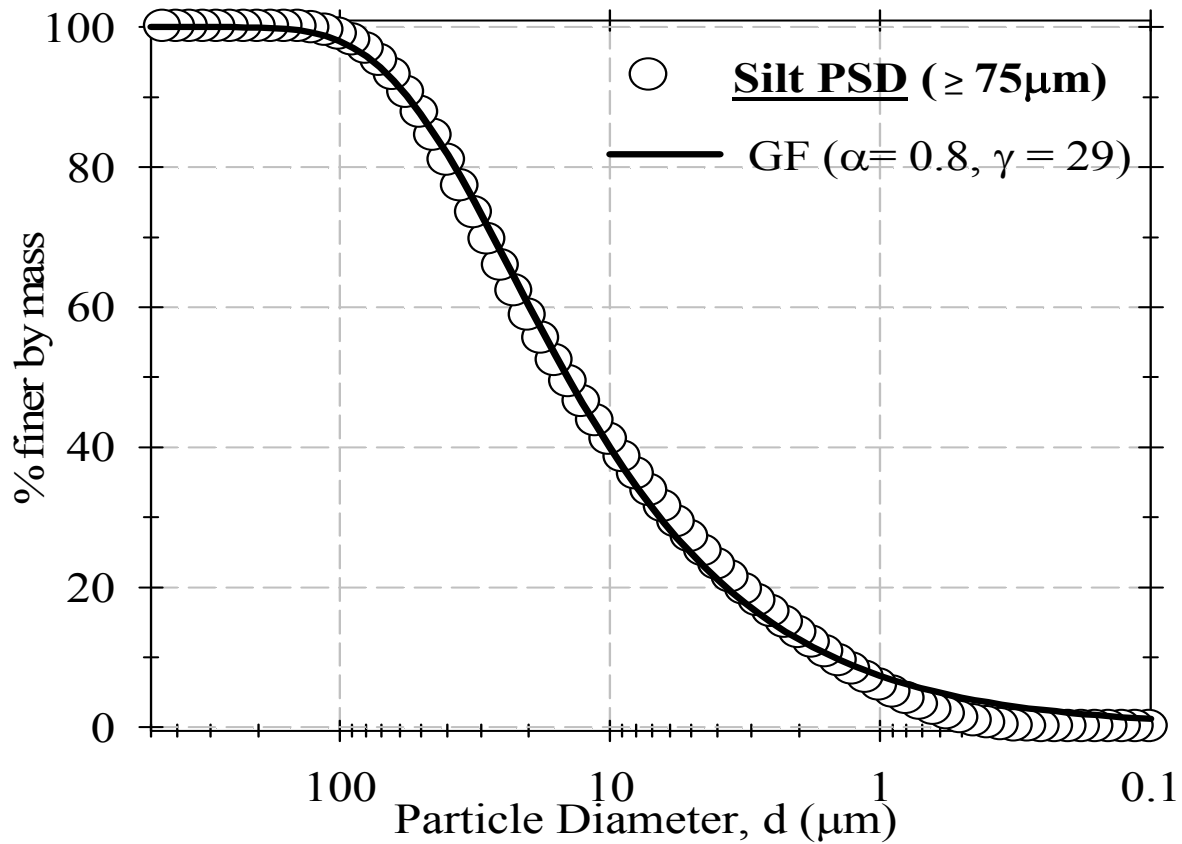


Figure 6 Influent Silt PM PSD. PSD data are fitted by Gamma Function (GF) based on its distribution parameters, α , shape factor and β , scale factor.

4.3 Physical Model Description

The linear FAA Pond physical model, illustrated in Figure 7, is a trapezoidal cross-section, approximately 5.31 feet (1.62 m) tall and 24 feet (7.31 m) long. The scaled physical model of Linear FAA Pond is designed with the following considerations:

- Total length to mid-depth width ratio is 8:1
- Trapezoidal section with bottom width 10% of top width (Top width = 6 feet)
- Side slopes are 2:1(horizontal to vertical)
- A maximum permanent pool depth of 4.3 feet

The Crenellated Pond physical model, illustrated in Figure 8, is a rectangular tank, approximately 6.13 feet (1.87 m) tall, 6 feet (1.8m) wide and 24 feet (7.31 m) long. Eleven baffles are placed within the unit to avoid the potential for short-circuiting. The pond is designed with the following considerations:

- Total length to mid-depth width ratio is 8:1
- Length to width ratio is 4:1 within the crenellations
- Side slopes are vertical within the rectangular crenellated sections
- A maximum permanent pool depth of 4.3 feet
- 11 Baffles (crenellations) with length of 4 feet (1.22 m) and inter-distance of 2 feet (0.61 m)

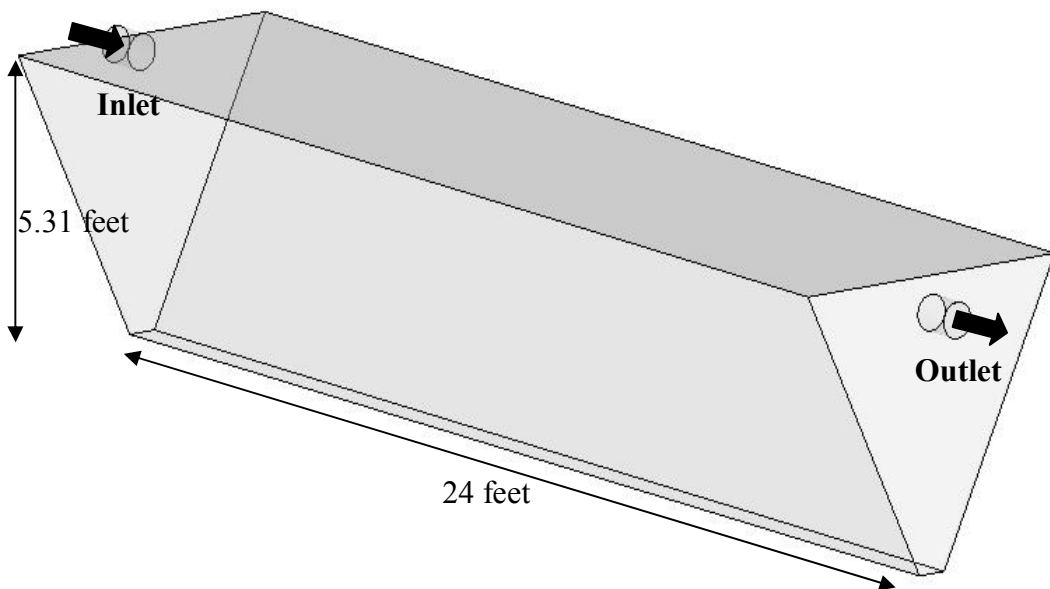


Figure 7 Isometric view of Pilot-scale Physical Model of the Linear FAA Pond Configuration Model

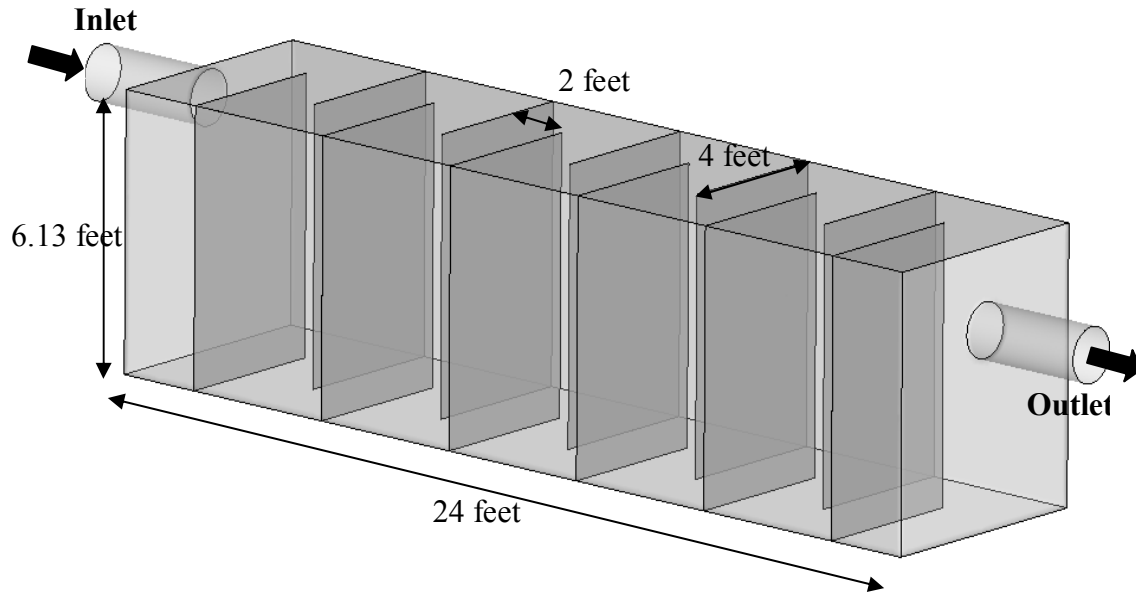


Figure 8 Isometric view of Pilot-scale Physical Model of the Crenellated Pond Configuration

The design flow rate of the physical model is determined to be ~ 1.77 cfs (790 gpm), corresponding to the hydraulic capacity of physical model as an open-channel system. The full-scale physical model is located at the site at the Stormwater Unit Operations and Processes Laboratory located at the University of Florida, in Gainesville Florida. A schematic process diagram of the experimental setup is reported in Figure 9. The following photograph in Figure 10 further illustrates the scaled physical model.

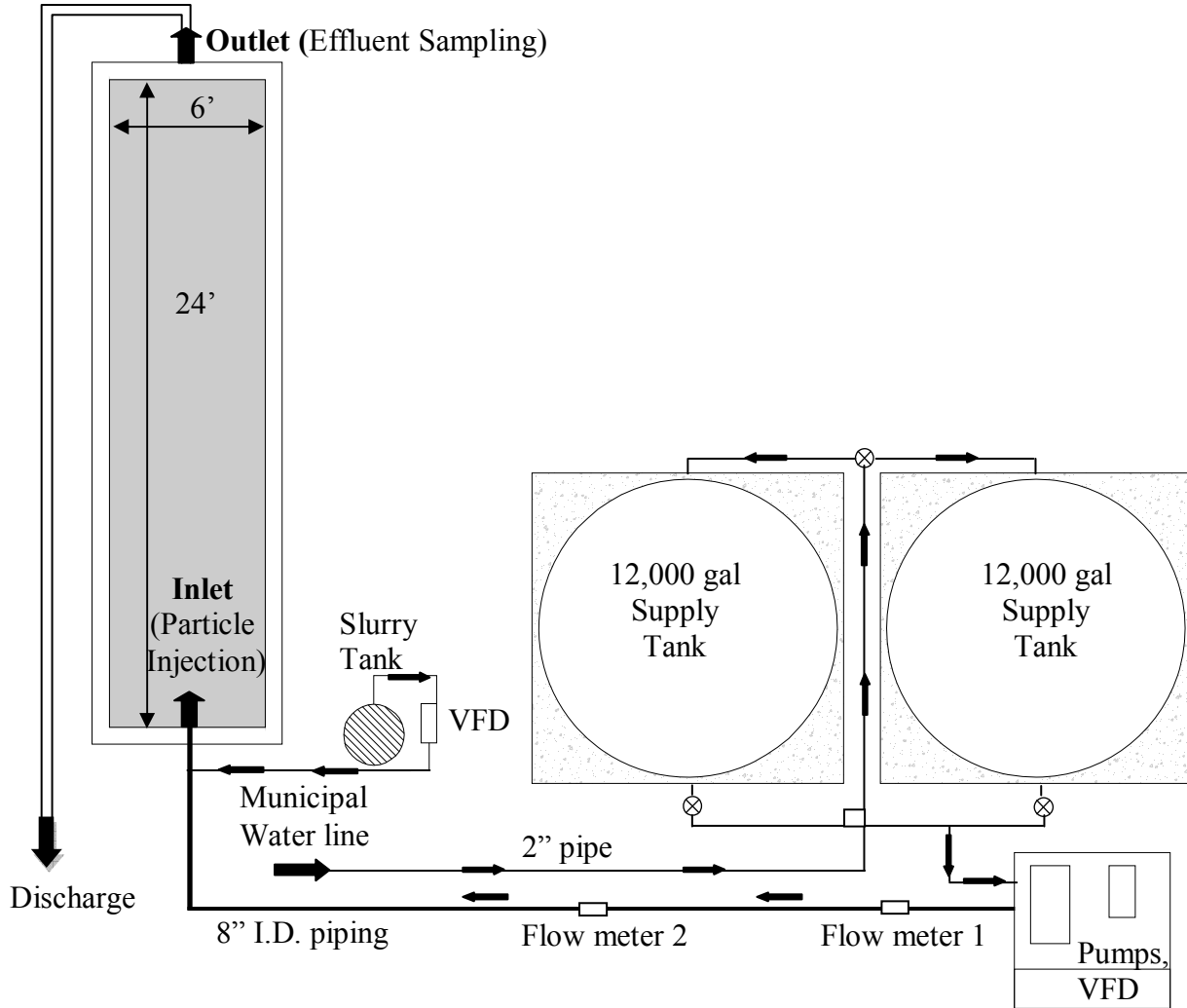


Figure 9 Schematic representation of experimental site setup



Figure 10 Photograph of the Linear FAA Pond physical scale model

4.3.1 Transformation of Rainfall Hyetographs to Runoff Hydrographs

The hyetographs reported in Figure 1, Figure 3 and Figure 5, are transformed as event-based hydrographs by using Storm Water Management Model (SWMM) for each physical and CFD model. The objective of the rainfall-runoff simulations is to generate unsteady runoff flow loadings for the scaled physical model and CFD model. SWMM translates rainfall in runoff given specific catchment properties (FDOT, 2007).

In this transformation from rainfall to runoff for the scaled physical Ponds the watershed area is matched to deliver peak runoff flow rate equal to the design flow rate of the unit operation (physical model of FAA pond). As shown in Section 3.1.1, the July 8th 2008 historical hyetograph is characterized by the highest rainfall peak intensity (approximately 6.5 in/h) in comparison to the other selected hyetographs. Therefore, the historical hyetograph is utilized as reference to perform the flow scaling of the physical testing model. Since the maximum hydraulic capacity of the physical models is ≈ 800 gallons/minute (1.8 cfs), the area of the catchment implemented in SWMM is defined to deliver peak flow rate approximately equal to 800 gallons/minute for the historical storm of 8 July 2008.

Modeling parameters adopted are based on an asphalt-pavement typical of a runway/taxiway. The Green-Ampt method is used to model the infiltration process (Teng and Sansalone, 2004; FDOT, 2007). The rainfall-runoff modeling results for the three hyetographs are shown in Figure 11.

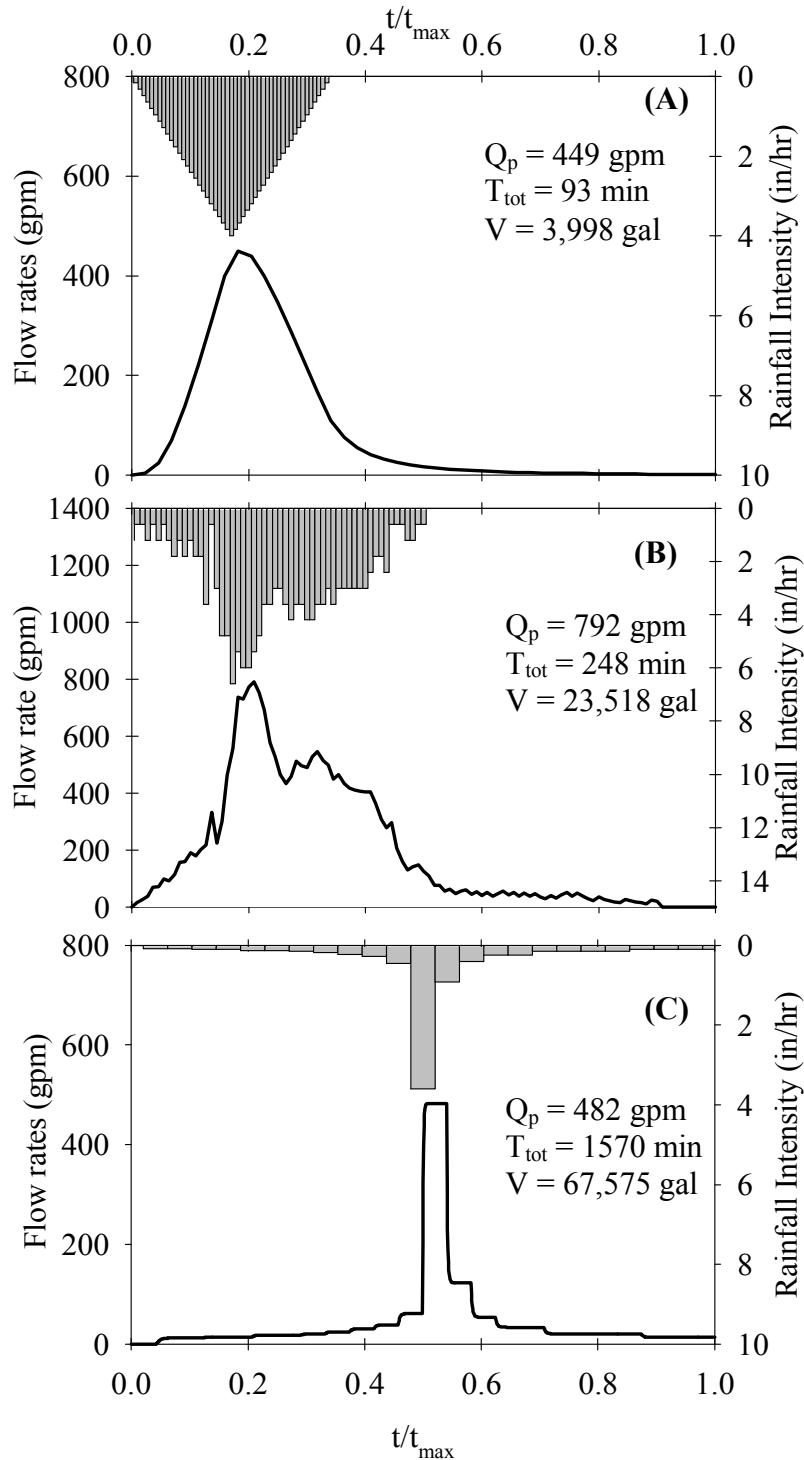


Figure 11 Loading Hydrologic Events utilized (Triangular Hyetograph (A), Historical 8 July 2008 Loading Hydrologic Event Collected by UF (B) and 24 Hour, 25 Year Loading Hydrologic Event (C)) for full-scale physical model of Linear FAA Pond and Crenellated Pond Configurations. The SWMM Rainfall-Runoff modeling is based on modeling parameters for asphalt-pavement of a typical airport runway/taxiway (FDOT, 2007).

Figure 11 illustrates the hydrograph (B) generated in SWMM for historical event presents a peak flow rate equal to the maximum hydraulic capacity of 1.77 cfs (50 L/s). The hyetograph (A) generates a peak flow rate of about 0.98 cfs (28 L/s), while hyetograph (C) generates a peak flow rate of 1 cfs (30 L/s).

4.4 Wet pond at the Orlando Executive Airport

The area of interest is the Orlando Executive Airport (ORL) located in Orlando, FL (28°32'44"N 081°19'59"W). It covers an area of 1,055 acres (427 ha) at an elevation of 113 feet (34 m) above mean sea level. It has two asphalt paved runways: 7/25 is 6,003 by 150 feet (1,830 x 46 m) and 13/31 is 4,638 by 100 feet (1,414 x 30 m). In 2009 ORL had more than 108,000 aircraft operations constituted by general aviation, air taxi and military. The ORL includes parking lots and commercial areas besides areas dedicated to airport activities. The ORL drainage system consists of a network of piping discharging into 4 wet ponds in series and Lake Underhill as the receiving water.

The pond of interest in this study is the downstream one named South Treatment Pond (STB). The area drained by this wet pond consists of 124 acres of pavement/impervious areas, 19 acres of roofs, 57 acres of vegetated areas and 31 acres of water (Figure 12). Details of the major downstream ponds are shown in Figure 13. Each upstream pond has multiple inlets and it is connected to the downstream ones through a system of 3-6' X 6' box culverts. The STB has a storage capacity of around 68 acre feet, a water depth of 97.4" at normal pool elevation and an area of around 11.4 acres (Figure 13). The conveyance system consists of 3-6' x 6' box culverts discharging into an open channel that directly flows into the lake. A flow/level control system consisting of a 90° V-notch weir is installed in the STB. The weir has a maximum elevation of 97.4". When the water level in the pond reaches this elevation, the system overflows the weir that is submerged and the conveyance system in this case consists of the box culverts as for the upstream ponds. Over this elevation the whole system hydraulically can be considered as 5 connected storage tanks controlled by the level of the downstream one that in this case is Lake Underhill.

4.4.1 Hydrologic-hydraulic simulation

The runoff flow rate at the inlet of the STB for different design storms is calculated through the SWMM model. The drained area is then subdivided in 8 catchments whose end sections are inlets to the upstream ponds, named north Ponds (NB1 and NB2) and mixing Pond (MB) as shown in Figure 14. Each catchment is subdivided in several sub-catchments as a function of the drainage system and elevations. A total number of 26 sub-catchments are considered and details on the land use of each one of these areas are reported in Table 1.

In Figure 15 the connectivity diagram of the SWMM model is shown with the major catchments highlighted in red.

The soil characterization of the drained area is reported in Figure 16. Three different soils, Millhopper, St. Lucie and Tavares characterize the area of interest.

Hydrologic characteristics of each area depending on the different soil are reported in Table 22 . The dynamic wave model is chosen for the flow routing while Green Ampt is chosen to model the infiltration.

The investigated hydrologic event is the 25 yr-24 hr storm. The resulting hydrograph simulated through SWMM is shown in Figure 17. The hydrograph is characterized by a peak flow rate equal to 241 cfs.



Figure 12 Plan View of Orlando executive airport (ORL) with the area drained by the wet pond of interest highlighted in red

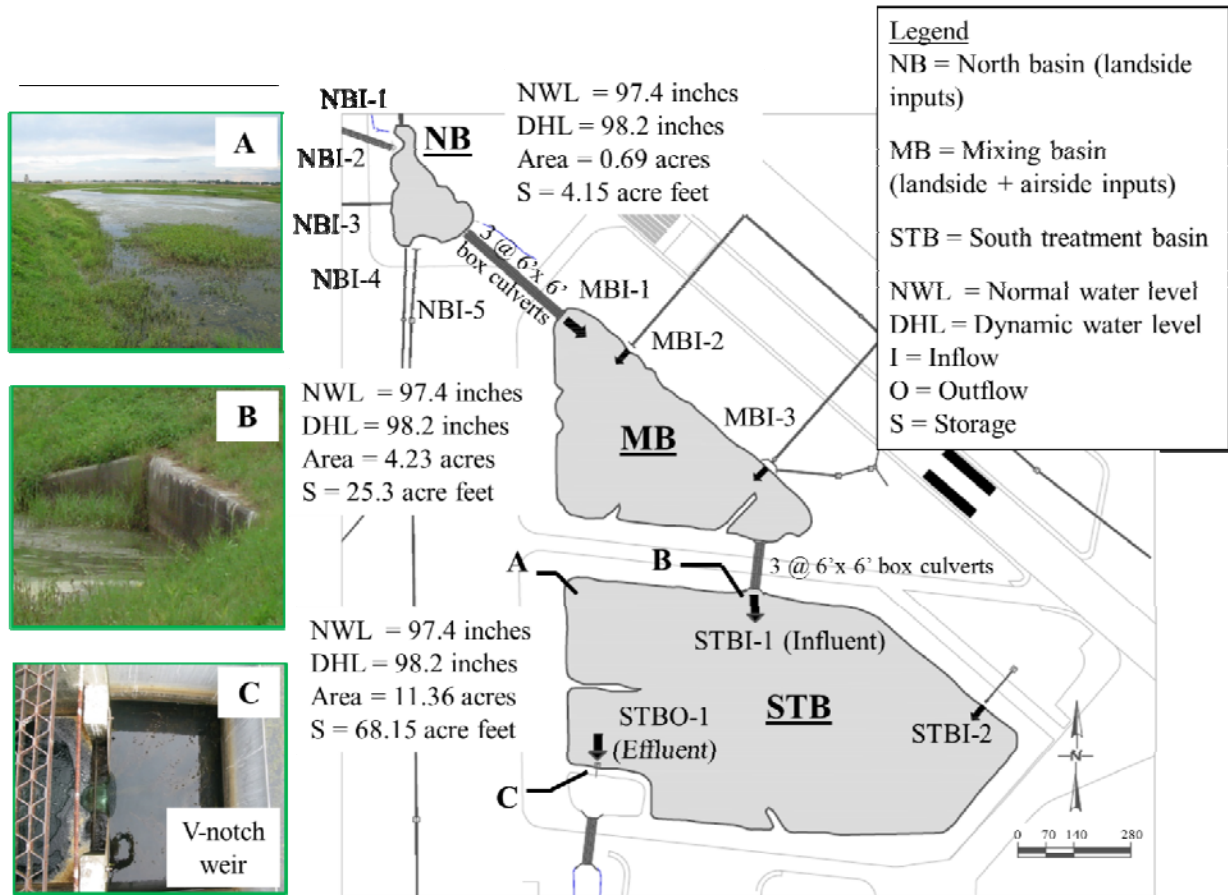


Figure 13 Plan view of Orlando Executive Airport (ORL) Pond system. Details of the three major ponds (NB = North Pond 2, MB = Mixing Pond, STB = South Treatment Pond, I = Inflow, O = Outlet, S= Storage) and the inlets and outlets of each pond.

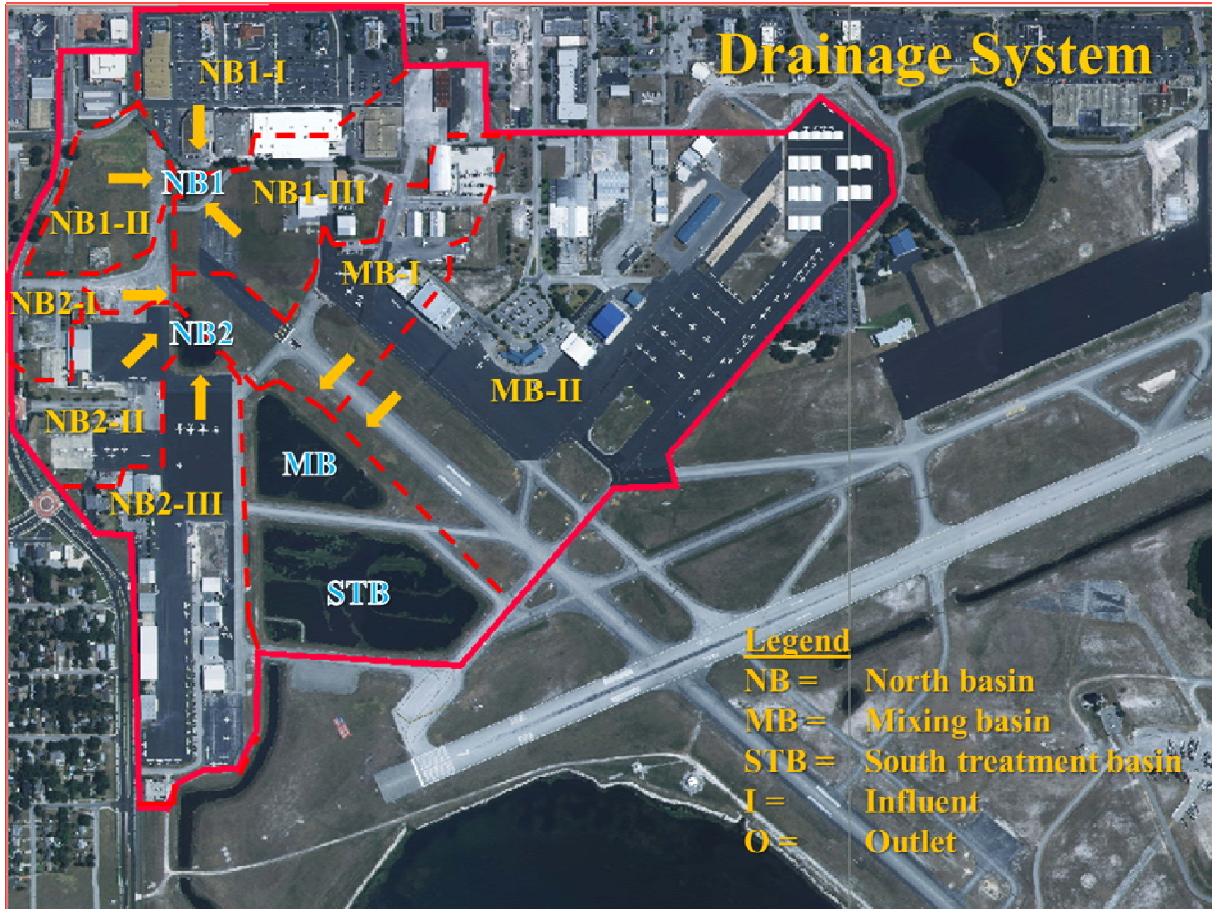


Figure 14 Drained area subdivision as a function of the drainage system. Each catchment end section is the inlet of the ponds

Catchments	Sub-catchments	Area (acre)	Roof (%)	Pavement (%)	Vegetated (%)
NB1-I	1	2.84	55.88	44.12	0.00
	2	16.25	6.27	93.73	0.00
NB1-II	1	8.78	0.00	2.26	97.74
NB1-III	1	12.60	12.30	23.55	64.15
	2	4.63	23.10	47.66	29.24
	3	3.90	32.97	67.03	0.00
NB2-I	1	3.72	10.46	84.64	4.91
	2	6.36	0.00	86.21	13.79
NB2-II	1	12.95	4.24	80.47	15.29
NB2-III	1	4.24	0.00	92.85	7.15
	2	6.54	19.18	77.12	3.70
	3	7.41	10.13	75.25	14.63
	4	7.49	9.41	90.59	0.00
MB-I	1	8.72	0.00	26.16	73.84
	2	8.10	12.14	71.44	16.42
	3	5.52	7.50	40.34	52.16
	4	2.97	9.11	46.65	44.24
MB-II	1	7.07	0.00	51.08	48.92
	2	10.50	0.00	23.68	76.32
	3	8.27	0.00	100.00	0.00
	4	8.73	0.00	100.00	0.00
	5	14.43	11.84	70.39	17.77
	6	10.48	24.82	60.11	15.06
	7	4.34	21.12	39.01	39.87
	8	8.81	5.21	41.16	53.64
	9	4.03	33.23	53.82	12.95

Table 1 Sub-catchment characteristics in terms of extensions and land uses

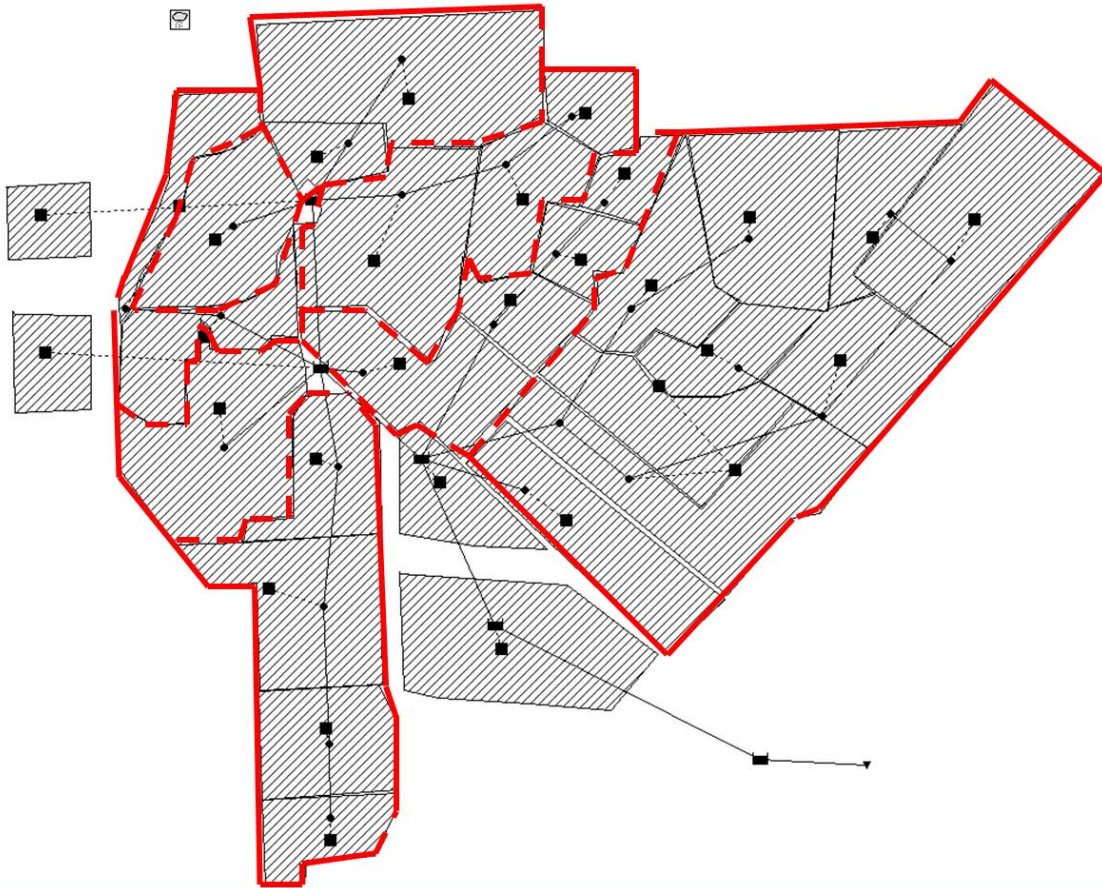


Figure 15 Connectivity diagram of the SWMM model with the catchments subdivision highlighted in red



Figure 16 Orlando Executive Airport soil characterization

Parameter	Soil Type		
	Millhopper	St. Lucie	Tavares
Area	97.33 acre	76.70 acre	25.70 acre
% Impervious	66.07	70.5	93.65
Evaporation	Daily	Daily	Daily
Design Storm	25-year, 24-hr	25-year, 24-hr	25-year, 24-hr
Total Precipitation	8.4 in	8.4 in	8.4 in
Rainfall Distribution	SCS Type II	SCS Type II	SCS Type II
Infiltration Algorithm	Green Ampt	Green Ampt	Green Ampt
Flow Routing	Dynamic Wave	Dynamic Wave	Dynamic Wave

Table 2 SWMM model information and algorithms utilized for hydrologic characteristics of the drained area as a function of the different soils.

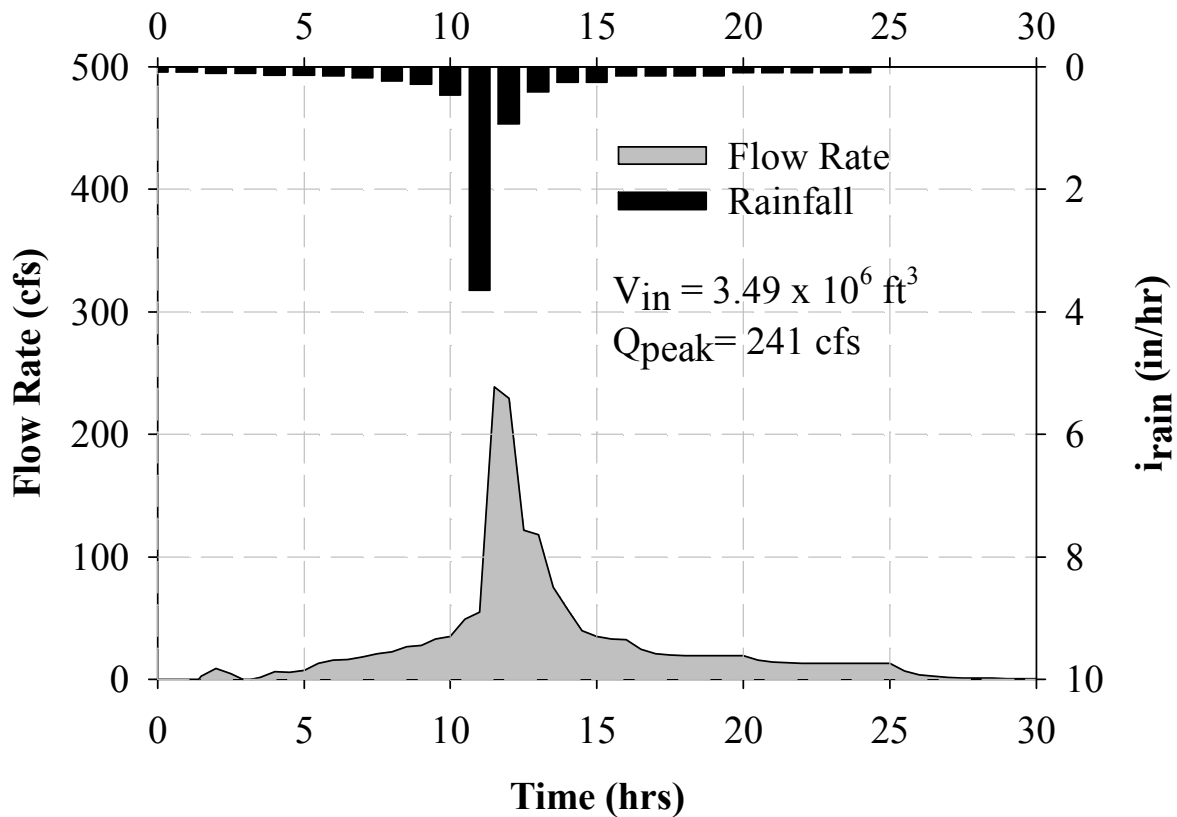


Figure 17 Hyetograph and simulated hydrograph for the 24 Hour, 25 Year Hydrologic Event.

4.5 Generic Rectangular and Triangular Quarry Ponds

The two generic rectangular and triangular quarry Ponds are selected to be modeled in CFD under steady conditions. The flow rates selected represent the peak flow rate of the 25 year – 24 hour design storm. In particular, the flow rate for the rectangular quarry Pond is 158 cfs, while the flow rate for the triangular quarry Pond is 821 cfs.

4.6 Physical Model Methodology

The data for this study are collected at the Stormwater Unit Operations and Processes Laboratory located at the University of Florida, in Gainesville Florida. The site footprint area is of 8,911 ft², consisting of a 40 by 60 feet concrete pad covered by a roof. A two storied 20 by 20 foot tower building is used as a multipurpose lab for engineered media preparation, particle mixture

preparation and as a storage space. There is a data acquisition room, 10 by 6 foot within the concrete pad, with A/C control for collecting the data during each run. The site is also provided with two 12,000-gallon water tanks fed by a pressured municipal water supply line and power (3 phase 208 volt 200 amps). Figure 18 is the basic layout of the experimental site:

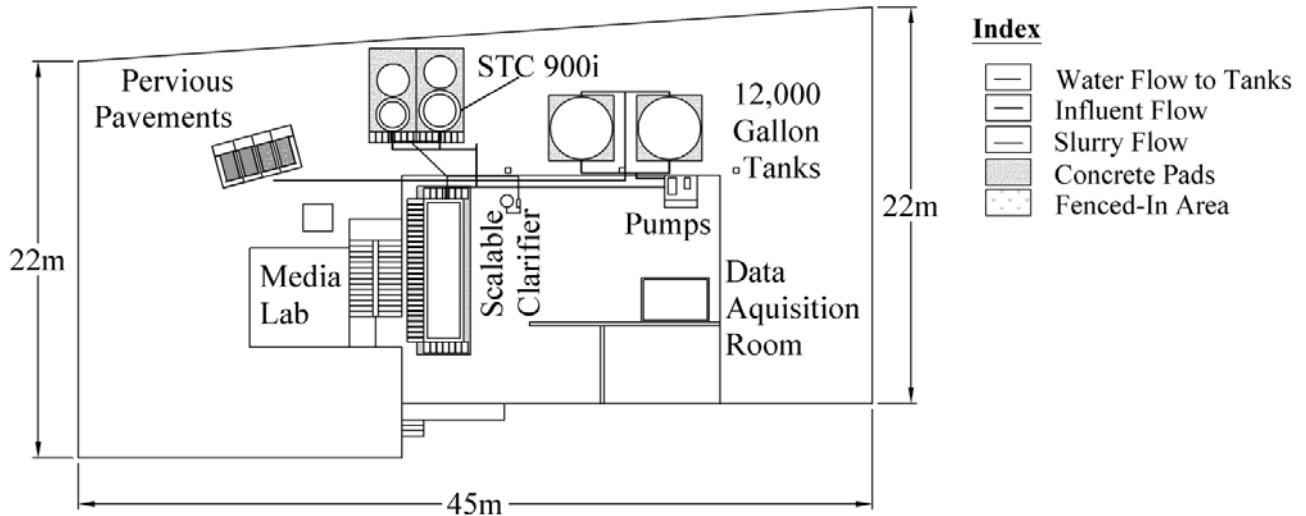


Figure 18 Site layout of the Stormwater Unit Operations and Processes Laboratory at the University of Florida

Experimental runs are performed on the full-scale physical models at unsteady influent hydraulic conditions at a temperature of 20 °C. The systems are hydraulically loaded with three hydrographs illustrated previously. Their formulation is based on the maximum hydraulic capacity for the given treatment system 1.76 cfs (50 L/s).

4.6.1 Description of the Equipment and Components

This section outlines the core components of the physical model hydraulic control system.

4.6.1.1 Duplexing Booster Pumping Station with Programmable Logic Control (PLC) System

The site is engineered with a low-head liquid/slurry delivery system which has capability to deliver accurate flow rates under low total dynamic head conditions for a wide range of flow rates from 33 to 1300 gallons per minute. Flow rates lower than 33 gpm are achieved by using a 2 inch feedline and valve. The system is equipped with a duplex, constant flow booster pumping station with two variable speed Berkley centrifugal pumps which operate in parallel (300 gpm,

4" Suction, 3" Discharge, 3 HP (horsepower) and 1000 gpm 8" Suction, 6" Discharge, 10 HP respectively) for controlling the water inlet into the physical model Pond. A series of two magnetic flow meters, valves, and VFDs (variable frequency drives) are integrated with the PLC to support the testing applications by providing a feedback control loop to maintain the desired flow rates and for logging real-time data. The flow rate measurements are recorded on a Micro-Logger with a logging frequency of 1 second. Before a run, the PLC is pre-programmed with the target influent unsteady flow rate.

4.6.1.2 Slurry Mixing and Feeding system

The slurry mixing and feeding system consists of a 65 gallon conical bottom HDPE slurry tank and two (one internal and one external) mixing pumps which provide vertical and horizontal mixing to keep the particles in suspension within the tank while slurry is being injected into the system. Internal mixing is provided by a 1HP 2" discharge ABS JC-11W submersible pump and external mixing is done with the help of a small straight centrifugal pump (3608 series). The slurry mixing system is located above the roof of the Stormwater Unit Operations and Processes Laboratory at an elevation of 15 feet above the facility slab. This slurry mixing system suspends the PM slurry and provides a consistent PM concentration and PSD profiles.

4.6.1.3 Mx Ultramag Meters for Flow Rate

The Mx UltraMag incorporates microprocessor technology which offers a broad range of flow rate tracking from low flows (30 gpm) to high velocity flows (well over the 1500 gpm capability of the system). The two flowmeters are equipped with a remotely mounted signal converter that indicates both rates of flow and total flow as well as providing analog and pulse outputs. The Mx UltraMag electromagnetic flow meter is an obstruction-less, volumetric flow measuring device that is capable of measuring the flow rate of almost all conducting liquids and slurries with a high degree of accuracy. Compact, high-density field coils generate a magnetic field across the flow tube. The moving flow generates a voltage which is then amplified and converted to give a direct flow rate reading with 4 to 20 mA and frequency outputs. The signal converter is remotely mounted up to 300 feet from the meter and is factory programmed for every meter. This signal is split by a multiplexor to simultaneously communicate with the PLC pump controller and the CR 3000 data logger.

4.6.1.4 MJK Level Transmitter

A 30 kHz ultrasonic sensor (model Shuttle Level Transmitter, manufactured by MJK Inc.) is placed at the effluent section of the physical model to acquire effluent water level measurements. After appropriate installation and calibration of the sensor, the ultrasonic sensor is utilized to record at 1 second intervals the effluent water levels. The water level data are then transformed to effluent flow rates according to a calibration curve previously obtained.

4.6.1.5 YSI 600 OMS Probe

YSI 600 OMS probe is a multi parameter water quality monitoring device equipped with a 6136 Turbidity Sensor for accurate, in-situ measurement of turbidity. The OMS also incorporates sensors for the measurement of conductivity and temperature. It has a built-in memory that can store the data it records. Temperature data is an important input variable for various types of models such as a CFD model and surface overflow rate (SOR) based-models. Conductivity data can be used to experimentally measure hydraulic residence time distributions. Influent and effluent turbidity data can be used to develop a relationship between particle concentration and turbidity which can be eventually used as a tool to continuously monitor the influent and effluent particle concentration profile throughout the entire duration of the treatment run under steady- or non-steady state conditions. The data stored in the YSI is downloaded after each run.

4.6.2 **Data Acquisition and Management**

All the necessary data for the experimental run are collected in the data acquisition room with help of the data acquisition notebook computer which has the necessary software platforms installed. The following primary data for the experiment are collected.

4.6.2.1 Downloading the Recorded Turbidity Data

The YSI is programmed before every run with field details and calibrated to start logging data. After each run the data are uploaded from the YSI with the data acquisition notebook computer which is installed with Eco Watch, a PC software interface for YSI.

4.6.2.2 The Programmable Micro-Logger for Flow Rate

The PLC is preset with a target flow rate for a particular test run. The CR3000 Micrologger is a data logger, manufactured by Campbell Scientific Inc. This is used as the real-time data monitoring and data collection unit. The CR3000 is powered for constant operation by 110-V AC power with a 12-V DC battery backup. Data are transferred from the data logger to a data acquisition notebook computer using a data transfer cable with the help of LoggerNet v3.0, a data monitoring and acquisition program compatible with the CR3000 Micrologger. This particular data logger system provides 4-20 mA current inputs via a 100 Ohm shunt resistor as well as multiple voltage inputs which enables it to simultaneously measure flow from two sensors, log sample events from two automatic water samplers, and log input from a high frequency velocity probe.

An initial Quality assurance/ Quality Control (QA/QC) check is performed following each data download to ensure that the acquired data is reasonable. This is done by routinely checking for any outliers, spikes, questionable values, or incomplete data in the logged data that would indicate erroneous measurement or configuration of the data logging system.

4.6.3 Calibration Procedures and Verification

4.6.3.1 Calibration of Flow Measurement Devices

As already mentioned the flow rate is motivated by a duplex, constant flow booster pumping station with a PLC. After initially installing the system it is volumetrically calibrated as follows. The data acquisition notebook computer is connected with CR3000 data logger, and real-time flow data in terms of mV are measured using the flow meter and monitored on the Logger Net c3.0 software and the graphical user interface. The rectangular container for volumetric calibration is characterized by a surface area of 22,200 in², and volume of 1,198,800 in³.

Prior to flow rate calibration at a specific flow rate, flow is directed to bypass the rectangular clarifier used for calibration unit until a steady flow rate is achieved. Once steady state is achieved flow is directed to the clarifier. The calibration curves obtained for each flow meter are shown in Figure 19.

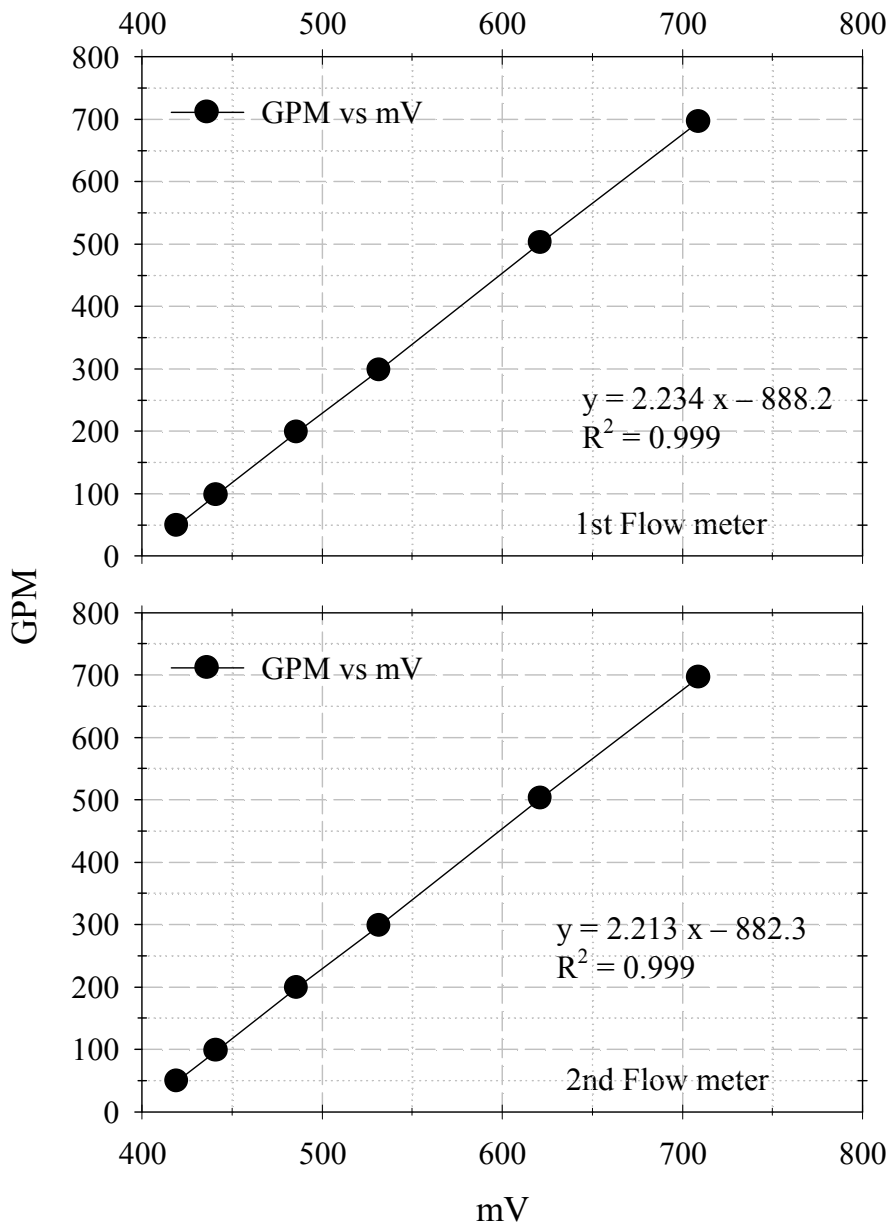


Figure 19 Flow calibration curves for the two Mx UltraMag flow meters developed from volumetric calibration at the Stormwater Unit Operations and Processes Laboratory at UF

4.6.3.2 Calibration of Slurry Mixing and Injection System

The slurry mixing and injection system is calibrated to deliver slurry composed of the NJCAT gradation. The rate of slurry addition to the drop box is controlled by a peristaltic pump manufactured by Eccentric Pumps driven by a VFD. The rate of slurry injection is controlled by the frequency of the VFD and is calibrated volumetrically.

Figure 20 is the result in liters per minute (LPM) and gallons per minute (GPM) of duplicate calibration experiments on the slurry injection system for flow rate for specified Hz input to the slurry pump VFD.

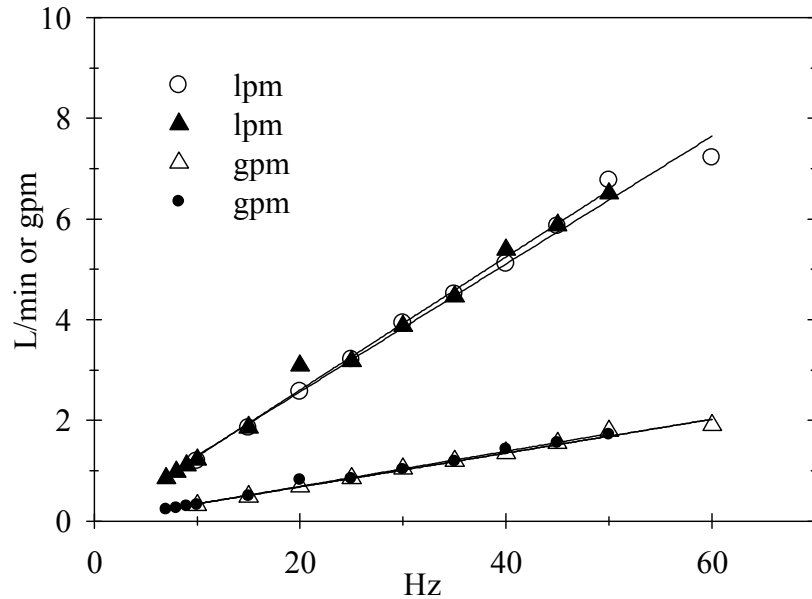


Figure 20 Calibration of Slurry Injection Pump by volumetric calibration at the Stormwater Unit Operations and Processes Laboratory

4.6.4 Slurry Mixing and Injection System

The experiments are conducted at constant concentration of 200 mg/L and constant influent particle size distribution (PSD) of PM. The PM influent gradation utilized is a silt gradation ranging from 0.1 to 75 μm with a d_{50} of 15 μm as shown in Figure 6. The particulate specific gravity is 2.63 g/cm^3 . The silica particles are purchased from US Silica. The slurry mixing and feeding system consists of a 65 gallon conical bottom HDPE slurry tank and two (one internal and one external) mixing pumps which provide vertical and horizontal mixing to keep the particles in suspension within the tank while slurry is being injected into the system. Internal mixing is provided by a 1HP 2” discharge ABS JC-11W submersible pump and external mixing is done with the help of a small straight centrifugal pump (3608 series). The slurry mixing system is located on the roof of the Stormwater Unit Operations and Processes Laboratory. This slurry mixing system suspends the silt slurry and makes the particle concentration profiles consistent. The slurry mixing and injection system is calibrated to deliver slurry composed of the

silt gradation. The rate of slurry addition to the drop box is controlled by a peristaltic pump manufactured by Eccentric Pumps driven by a VFD. The rate of slurry injection is controlled by the frequency of the VFD and is calibrated volumetrically. The VFD is also connected to the PLC system of the pumping station and controls the unsteady rate of slurry varying according to the flow rate.

4.6.5 Sampling Methodology and Protocol

The sampling is conducted according to the following procedure. During the test running time, representative effluent samples are taken manually across the entire cross section of the effluent section of the unit as discrete samples in 1L wide mouthed bottles. Samples are collected in duplicate through the entire duration of the run at variable time sampling frequency according to the flow rate gradients and event duration to provide a reasonable estimate of effluent variability of PM concentration and PSD. The minimum sampling time interval is 1 minute.

The sampling protocol used to characterize the supernatant PSD consists of taking a duplicate sample at the geometric midpoint of the supernatant after overnight settling. In particular, four PSD and SSC duplicate samples are taken at four evenly spaced intervals of height of the stored supernatant volume.

4.6.6 Mass Recovery and Sample Protocol

After the supernatant sample has been collected, the wet slurry from the system is recovered from the bottom of the unit by manually sweeping it through the washout points into buckets and taken to the laboratory where they are allowed to stand for quiescent settling and dried in glass trays at 105 degrees Celsius in an oven. After the slurry completely dries, the dry silica is disaggregated and collected in pre-weighed glass bottles and the gross weight is recorded to find the overall PM separation of the system based on mass and for the mass balance. Laser diffraction analysis for the collected dry sample is then performed to analyze the PSD of the captured particle.

4.6.7 Laboratory Analysis

The experimental analyses include PSD measurements for influent, effluent and captured PM by laser diffraction analysis, effluent gravimetric analysis based on PM concentration as suspended

solid concentration (SSC). SSC analysis is performed to quantify particle concentration for each effluent composite sample as collected from each run and to calculate the effluent mass load for the operating flow rates. Fully characterizing the entire PSD and utilizing SSC allow a mass balance to be conducted which is not possible when utilizing an index component and method of PM, such as total suspended solids, TSS. The protocol specifically followed for this laboratory analysis is the ASTM D 3977 (ASTM, 2002).

To perform the PSD analysis the Malvern Mastersizer 2000, a commercial laser diffraction analyzer is utilized in this experimental analysis. The instrument technology is based on laser diffraction, occurring when a laser beam passing through a dispersion of particles in air or in a liquid is diffracted at the particle surface. The angle of diffraction is influenced by the size and the shape of the particle. As the particle size decreases, the scattering angle increases (Jillavenkatesa et al., 2001). The Mastersizer 2000 detects particle sizes in the range of ~0.02 to 2000 μm in spherical diameter. The 10 duplicate samples are analyzed independently in the Mastersizer 2000 as 20 one liter samples. During a sample measurement, the instrument is programmed to characterize the PSD three times. These three PSD curves are then analyzed for stability to ensure that the measurement settings for the instrument are adequately suited for the sample and to ensure that any bubbles that might be present and affect the reliability of the measurement are purged from the system. The three measured and stable PSDs for the individual sample are averaged into a representative curve for that sample. An event mean PSD is generated from averaging the individual Mastersizer measurements (both A and B).

Finally, the captured PSD is measured with the laser diffraction analyzer in dry phase. In order to representatively sub-sample the dry mass the silica is uniformly mixed to obtain a sub-sample as representative as is physically obtainable. Duplicate 20 gram samples are taken for the dry phase of the laser diffraction analyzer. The dry dispersion cell is connected to the laser diffraction analyzer and the dry sample is measured by forming a PM aerosol with a high pressure, high velocity air stream. The PSDs measured are observed for stability and averaged.

4.6.8 Verification of Mass Balance for each Experimental Run

A mass balance evaluation is conducted to ensure representative and defensible event-based treatment performance results for the unit. The PM mass balance is calculated from dried

captured mass, effluent mass load, and supernatant mass load. The mass balance error (MBE) criterion is $\pm 10\%$ MBE and determined by the following equation (Kim and Sansalone, 2008):

$$MBE (\%) = \frac{(\text{Effluent mass load} + \text{Captured mass load}) - \text{Influent mass load}}{\text{Influent mass load}} \times 100 \quad (3)$$

4.6.9 Verification of PSD Balance for Each Run

The gravimetric PSD of the effluent, supernatant and recovered mass is measured and compared with that of the influent to verify the balance of influent and effluent PSDs. This QC measurement is performed by quantifying the deviation between the representative silt influent loading and the summation PSD of the effluent, recovered, and supernatant mass.

$$PSD_{\text{error}} = \frac{\sum_{i=1}^n |\text{Influent PSD}_i - (\text{Effluent PSD}_i + \text{Recovered PSD}_i + \text{Supernatant PSD}_i)|}{\sum_{i=1}^n \text{Influent PSD}_i} \quad (4)$$

In this expression each i is a discrete measurement at a specific particle size of the cumulative PSD.

Measured results including temporal effluent PSD, PM and SSC obtained from the physical modeling testing are utilized to validate the CFD model parametric analysis.

4.7 CFD modeling

CFD is a branch of the analysis of fluid dynamics widely used in many disciplines such as aerodynamics and airplane engineering design applications and it rapidly emerged with the development of computer-related technologies and the advancement of solving ordinary and partial differential equations (ODE and PDE). CFD represents a proven and versatile technology to model fluid flow field encountered in different applications, such as discrete particles, heat-transfer, mixed fluid flow, drag, combustion, and many other fluid phenomena.

4.7.1 CFD governing equations

CFD is based on numerically solving Navier-Stokes (N-S) equations across a computational domain. In this study, the Reynolds Averaged Navier Stokes (RANS) formulation is utilized to

solve the flow field with Fluent 12.1. The RANS conservation equations are obtained from the N-S equations, by applying the Reynolds decomposition which decomposes the fluid flow properties into their time-mean value and fluctuating component. The mean velocity is defined as a time average for a period T which is larger than the time scale of the fluctuations. The time average of the fluctuations over T tends to zero meaning the turbulence components do not contribute to the bulk mass transport. The time-dependent RANS equations for continuity and momentum conservation are reported below:

$$\frac{\partial}{\partial x_i} (\rho \bar{u}_i) = 0, \quad (5)$$

$$\rho \frac{\partial \bar{u}_i}{\partial t} + \rho \frac{\partial}{\partial x_j} (\overline{u_i u_j}) + \rho \frac{\partial}{\partial x_j} (\overline{u'_j u'_i}) = -\frac{\partial \bar{p}}{\partial x_i} + \mu \frac{\partial^2 \bar{u}_i}{\partial x_j^2} + \rho g_i \quad (6)$$

In these expressions ρ is fluid density, x_i is the i th direction vector, u_j is the Reynolds averaged velocity in the i th direction; p_j is the Reynolds averaged pressure; and g_i is the sum of body forces in the i th direction. The decomposition of the momentum equation with Reynolds decomposition generates the Reynolds stresses term, $-\rho \overline{u'_i u'_j}$, from the nonlinear convection component. Since the Reynolds stresses are unknown variables, the realizable k - ε model proposed by Shih et al. (1995) is used to resolve the closure problem. The realizable k - ε model consists of a turbulent kinetic energy equation and a turbulence energy dissipation rate equation, respectively reported below (Shih et al., 1995):

$$\frac{\partial k}{\partial t} + \overline{u_j} \frac{\partial k}{\partial x_j} = \frac{\partial}{\partial x_j} \left(\frac{\nu_T}{\sigma_k} \frac{\partial k}{\partial x_j} \right) - \overline{u'_i u'_j} \frac{\partial \bar{u}_i}{\partial x_j} - \varepsilon \quad (7)$$

$$\frac{\partial \varepsilon}{\partial t} + \overline{u_j} \frac{\partial \varepsilon}{\partial x_j} = \frac{\partial}{\partial x_j} \left(\frac{\nu_T}{\sigma_\varepsilon} \frac{\partial \varepsilon}{\partial x_j} \right) + C_1 S \cdot \varepsilon - C_2 \frac{\varepsilon^2}{k + \sqrt{\nu \varepsilon}} \quad (8)$$

where

$$C_1 = \max\left[0.43, \frac{\eta}{\eta + 5}\right], \eta = S \cdot \frac{k}{\varepsilon}, S = \sqrt{2 \cdot S_{ij} \cdot S_{ij}} \quad (9)$$

In these expressions the constants are: $\sigma_k = 1.0$, $\sigma_\varepsilon = 1.2$ and $C_2 = 1.9$. In these equations, k is the turbulent kinetic energy; ε is the turbulent energy dissipation rate; S is the mean strain rate; ν_T is the eddy viscosity; ν is the fluid viscosity; and u_{ji} and $u_j' u_i'$ are defined in Equations 7-9. Hence, the turbulent flow field is determined by solving a system of four equations including the governing equations (See Equation 5-6) and the k - ε turbulence model (See Equation 7-8). The numerical solver used in the current study is the pressure based solver, which is well-suited for incompressible flows governed by motion based on pressure gradients. The used spatial discretization schemes are the second order for the pressure, the second order upwind scheme for the momentum, the turbulence energy and the specific dissipation and the Semi-Implicit Method for Pressure-Linked Equations (SIMPLE) algorithm for pressure-velocity coupling. For temporal discretization of the governing equations the second-order implicit scheme is utilized. The solutions are considered converged when the scaled residuals for all governing equations are below $1 \cdot 10^{-3}$ (Ranade, 2001).

4.7.2 Discrete phase model (DPM)

In CFD, DPM is used to simulate three-dimensional trajectories of discrete phase particles through the computational domain and to model particle separation. DPM is based on Euler-Lagrangian approach. While the aqueous phase is treated as a continuum in an Eulerian frame and solved by integrating the time-averaged Navier-Stokes equations (Equation 5-6), the particulate phase is studied as a discrete phase in a Lagrangian reference frame. The assumptions of the Lagrangian particle tracking approach are:

- The particles are spherical
- The particle motion is influenced by the continuous fluid phase, but the continuous fluid phase is not affected by the particle motion (one-way coupled model)
- Particle-particle flocculation is neglected; therefore, dispersed phase is assumed to be sufficiently dilute by checking the volume fraction is less than 10-12% (Brennen, 2005)
- Particle-wall interaction is neglected except for reflection

DPM integrates the governing equation of motion for the dispersed phase and tracks individual particles through the flow field by balancing the forces acting on them, such as gravitational body force, drag force, inertial force, and buoyancy. The trajectory of particles is calculated by integrating the force balance equation written below in the i th-direction:

$$\frac{dv_{pi}}{dt} = F_{Di} \cdot (v_i - v_{pi}) + \frac{g_i \cdot (\rho_p - \rho)}{\rho_p} \quad (10)$$

The first term on the right-hand side is the drag force per unit particle mass, in which F_{Di} is defined in Equation 11. The second term is buoyancy/gravitational force per unit particle mass.

$$F_{Di} = \frac{18\mu}{\rho_p d_p^2} \cdot \frac{C_{Di} \cdot Re_i}{24} \quad (11)$$

where Re_i , Reynolds number for a spherical particle, and C_{Di} , drag coefficient are respectively given by:

$$Re_i = \frac{\rho d_p \cdot |v_{pi} - v_i|}{\mu} \quad (12)$$

$$C_{Di} = \frac{K_1}{Re_i} + \frac{K_2}{Re_i^2} + K_3 \quad (13)$$

In Equations 10-13, ρ is the fluid density, ρ_p is particle density, v_i is fluid velocity, v_{pi} is particle velocity d_p is particle diameter, μ is the dynamic viscosity, K_1 , K_2 , K_3 are empirical constants for spherical particles as function of Re_i .

4.7.3 Model Implementation

The methodology of using CFD for analysis comprises three general steps: geometry and mesh generation (pre-processing), setting-up and solving a physical model (processing) and finally, post-processing the modeled data.

This study utilizes FLUENT 12.1 and GAMBIT 2.0 algorithms (Fluent Inc., NH, USA) to perform the CFD analysis. GAMBIT 2.0 is used for solid geometry creation and meshing, while for FLUENT 12.1 for solving the system of time averaged governing equations (RANS-based model) through the numerical method of finite volume difference elements.

4.7.3.1 Geometry and Mesh Generation for Linear and Crenellated Ponds

The physical geometry of the Linear and Crenellated ponds is built in the GAMBIT environment. Particular attention is placed in building elements that can be easily discretized and do not generate eventual meshing abnormalities, such as high skewness and poor aspect ratios. The geometry created in the computational domain represented the volume occupied by the flow. To discretize the geometry, the complex domain of the control volume is spatially subdivided into a set of discrete simple-shaped cells of pre-defined topology. These cells are referred to as mesh elements and are adjacently connected to each other. The mesh generated is completely comprised of tetrahedral elements, which is a non-uniform meshing scheme where the nodes do not reside on a grid. A high quality mesh is important to the accuracy and convergence of the finite element computation and any aberration within the mesh will negatively impact the final result. This mesh is checked to ensure that equiangle skewness and local variations in cell size are minimized to produce a high quality mesh. In addition, several iterations of grid refinement are performed to determine the necessary mesh density that balances the accuracy of the solution with the exponentially increasing demand of computational resources.

Figure 21 shows the isometric views of meshed geometry for both Pond configurations to illustrate the meshing process. The system as a whole is discretized into approximately 3 million cells for FAA linear Pond and 3.5 million cells for Crenellated Pond.

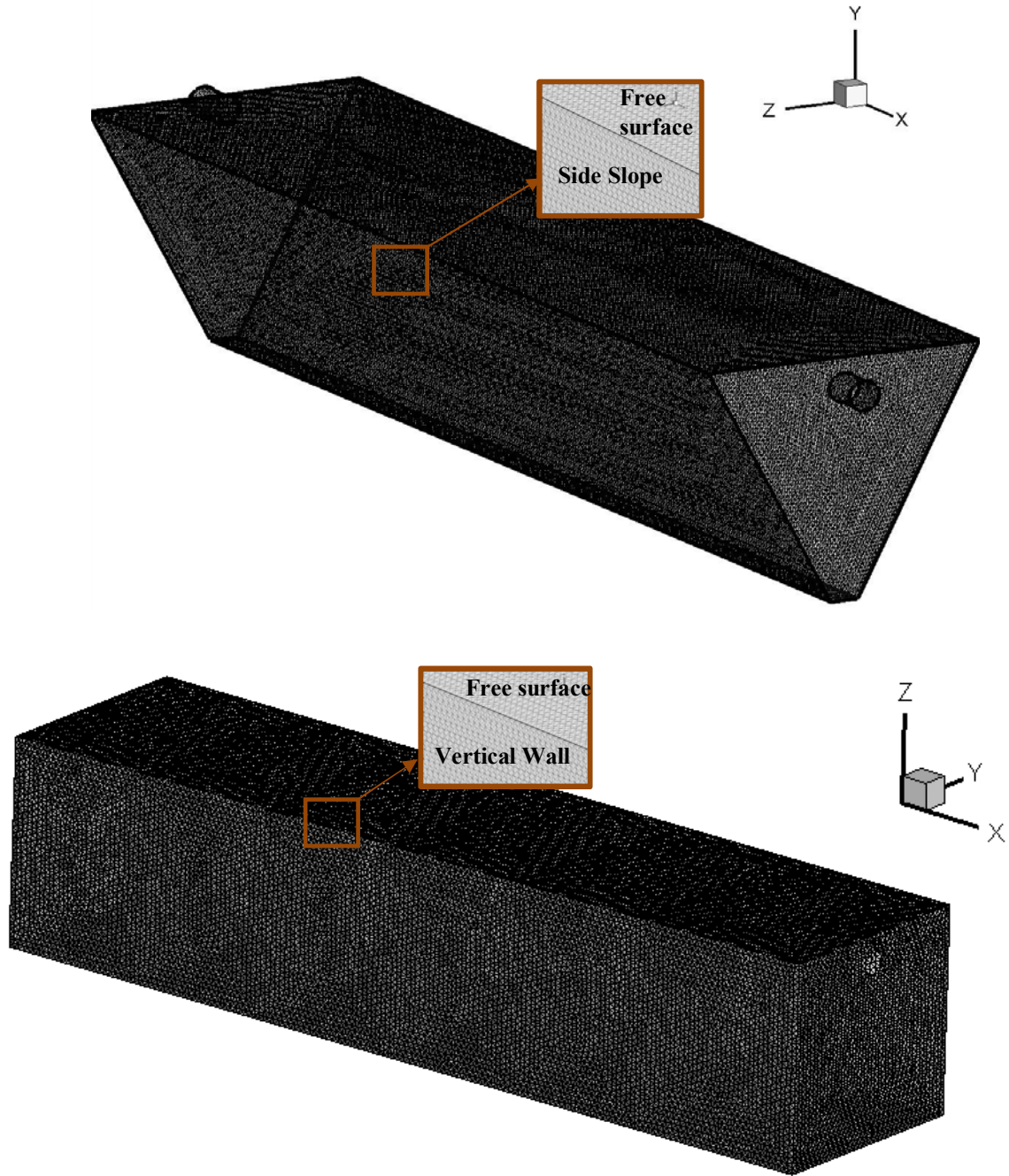


Figure 21 Isometric Section of the Pilot-scale Physical Model of the FAA Linear Pond (A) and Crenellated Configuration (B) Models built in GAMBIT environment.

The figure shows that the mesh used to model this geometrically complex domain is comprised of tetrahedral elements and characterized by a non-uniform meshing scheme. Elements for the FAA Linear Pond Model are 3 millions and Elements for the Crenellated Configuration Model are 3.5 million.

4.7.3.2 Geometry and Mesh Generation for ORL Wet Pond

The construction of the 3D CFD model for the Orlando Executive Airport STB pond requires significant effort with regard to the definition of the pond geometry based on bathymetric data (Figure 22) and generation of a computational grid. The complex domain of the control volume is spatially discretized into a set of discrete tetrahedral cells forming a non-uniform and structured mesh. The mesh generated is completely comprised of tetrahedral elements with a maximum spacing of 0.5 meters. To provide greater resolution in the vicinity of inlet and outlet where higher velocity gradients are anticipated, node spacing is decreased up to 0.05 meters. The completed mesh comprises approximately 4,000,000 cells with an average volume cell of 12 L. A high quality mesh is important to the accuracy and convergence of the finite element computation and any aberration within the mesh will negatively impact the final result. A post-processing check on mesh quality, based on skewness of the generated cells, indicates that the mesh is of high quality and would not compromise solution stability. Figure 23 shows the geometrical model generated in Gambit and Figure 24 illustrates the meshed geometry.

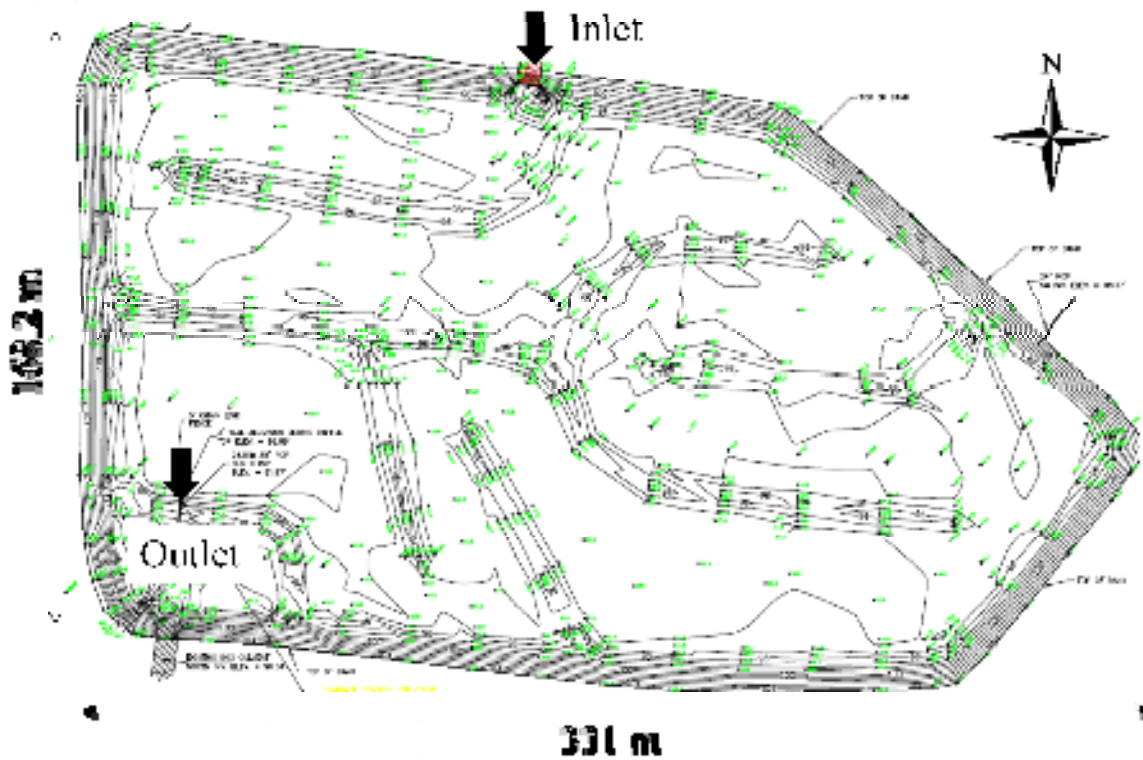


Figure 22 Bathymetry of ORL Pond

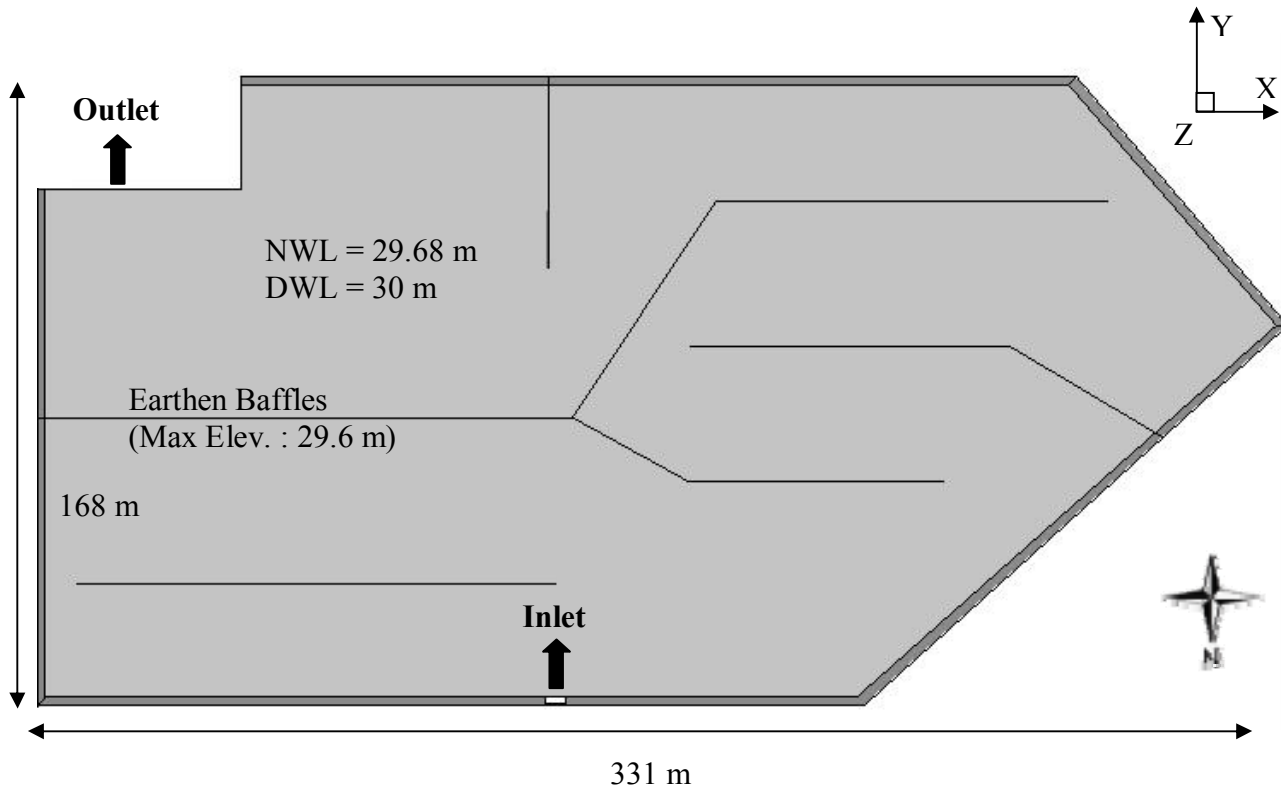


Figure 23 Plan view of the South Wet Pond located at the Orlando Executive Airport

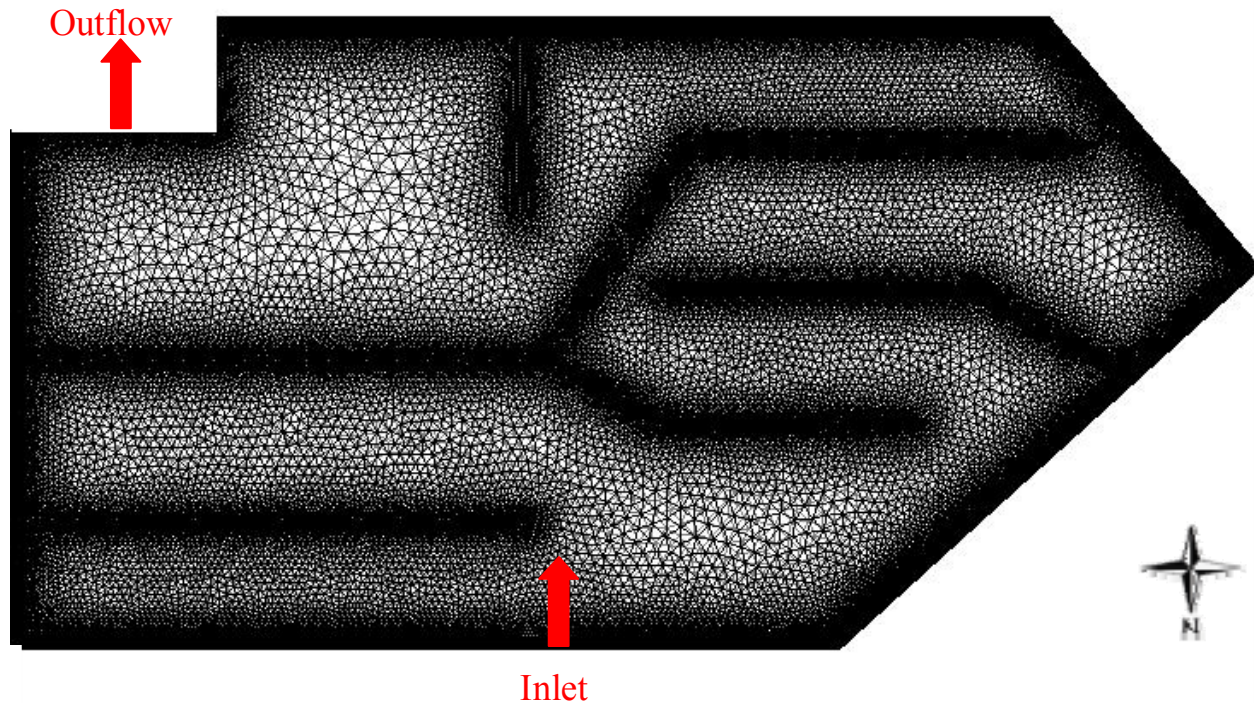


Figure 24 Plan View of the Meshed Geometry for ORL Pond

4.7.3.3 Geometry and Mesh Generation for Triangular and Rectangular Quarry Ponds

Similarly to the ORL Wet Pond, the geometrical model for the Triangular and Rectangular Quarry Ponds was built in Gambit and successively meshed. The meshes generated comprise respectively approximately 700,000 cells and 600,000 for triangular and Rectangular Quarry Ponds. A post-processing check on mesh quality was performed to verify the skewness of the generated cell and to ensure the mesh is of high quality and does not compromise solution stability.

Figures 26-27 show the meshed geometry for both Ponds.

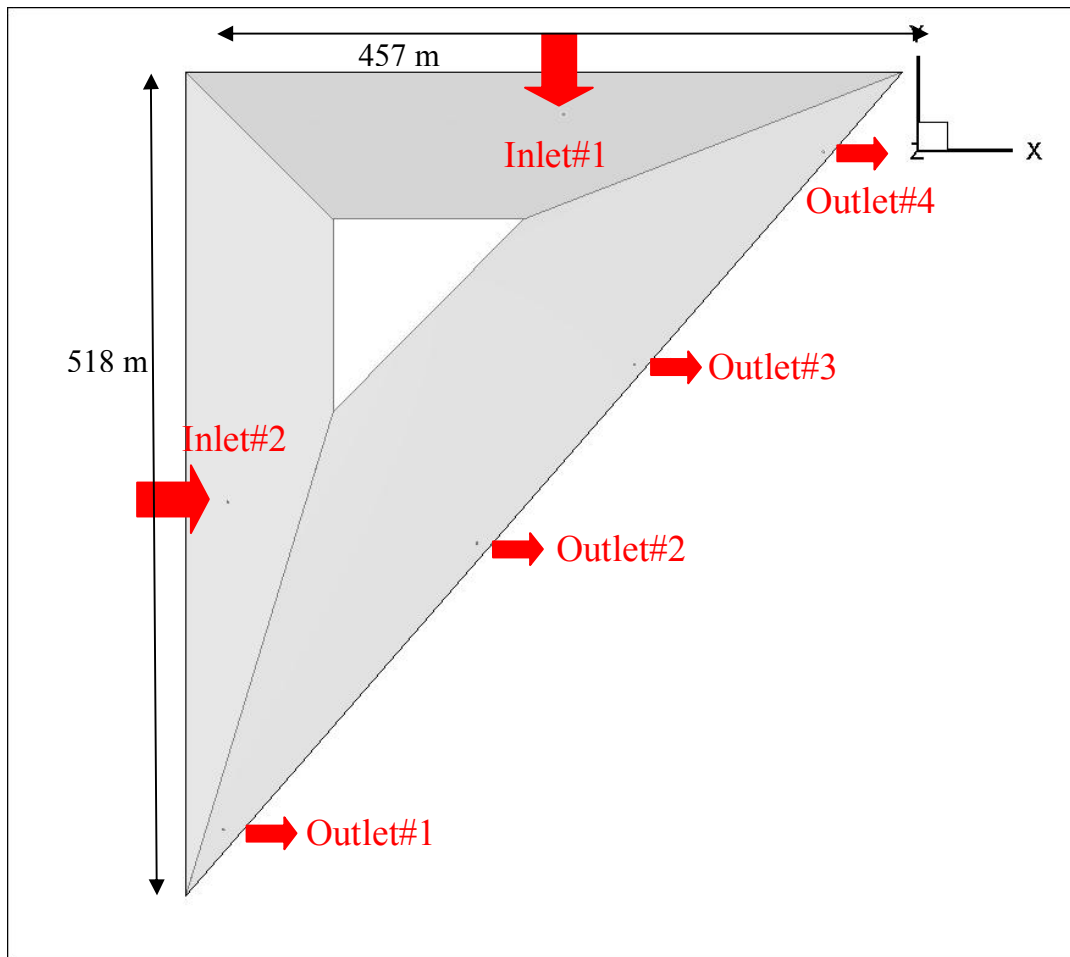


Figure 25 Geometrical model of generic triangular Pond

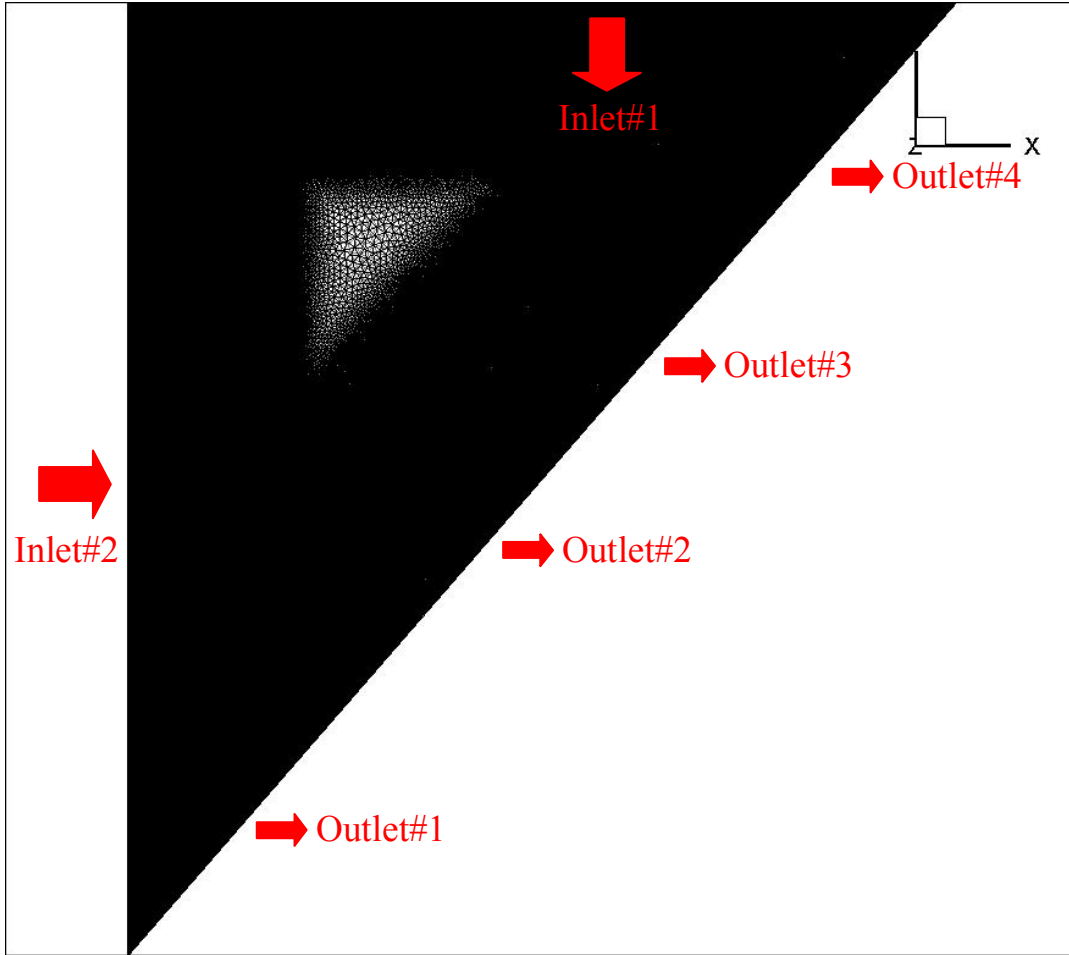


Figure 26 Meshed Geometry for generic triangular quarry Pond

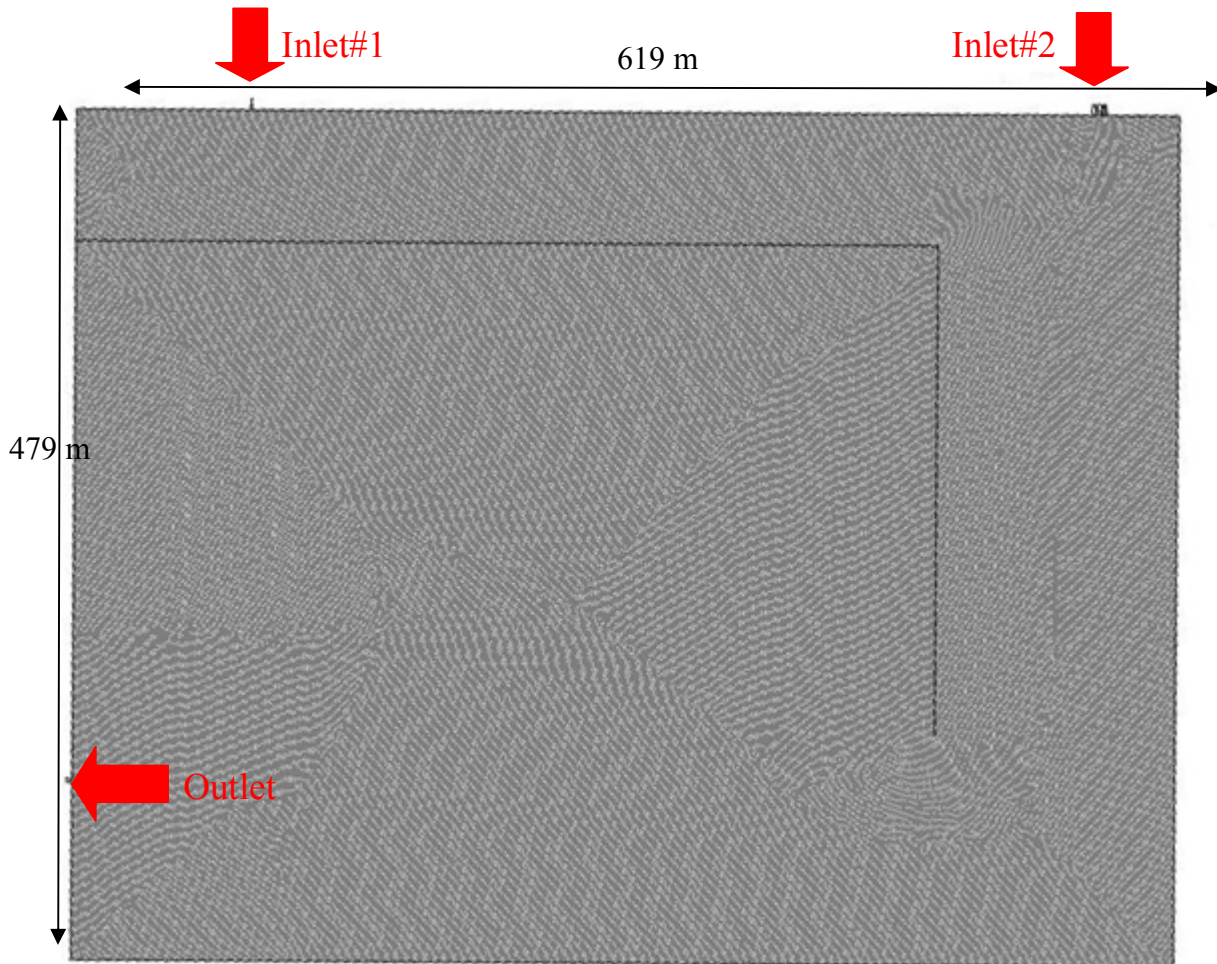


Figure 27 Geometry of generic Rectangular Pond

4.7.4 Boundary and Initial Conditions, Computational Parameters and Assumptions

Boundary conditions are required for the bottom, sides and top of the mesh model. The bottom and sides are specified as wall boundary conditions. The inlet is specified as velocity inlet. The Pond outlet is specified as an outflow boundary. The free surface is approximated as shear free wall with velocity components normal to the surface. PM injections are uniformly released from the inlet section at a temporal frequency of 1 min to ensure a continuous delivery of PM into the system. The PM tracking length is computed in CFD model by tracking trajectories of a tracer, with diameter of 1 micrometer and density of 62.4 lb/ft³ (998.2 kg/m³) (equal to water density) at a lowest flow rates (1% of Q_p). In order to model the time-dependent distribution of effluent particles, a custom subroutine is implemented in CFD. This user defined function records injection time, residence time and particle size of each particle eluted from the computational domain. To model the influent PSD, the PM gradation is discretized into a number of particle classes on a symmetric gravimetric basis on the arithmetic scale. Dickenson and Sansalone (2009) demonstrates that a discretization number (DN) of 16 is generally able to reproduce accurate results for silt gradations under steady conditions. Therefore, in this study a DN equal to 16 is used since a hetero-disperse and fine influent PM gradation is analyzed (Figure 6). The governing equations are solved based on a time step of 10 seconds, which turned out to provide time-independent results.

The method is based on the following assumptions to fully specify and characterize the CFD model:

- The flow regime established within the domain is hypothesized to be turbulent
- Gravity influences fluid flow and PM and is defined as 32 ft/s² (9.81 m/s²).
- Fluid medium is water and is defined to have a density of 62.4 lb/ft³ (998.2 kg/m³) and a kinematic viscosity of 1.1·10⁻⁵ ft²/s (1.004 *10⁻⁶ m²/s) at a temperature of 68 °F (20°C).

4.7.5 Population Balance

A population balance model (PBM) is coupled with CFD to model particle separation. Assuming no flocculation in the dispersed particle phase, the PBM equation (Jakobsen, 2008) and mass per particle, $p_{\xi,\tau,n}$ are as follows.

$$\sum_{\xi_{\min}}^{\xi_{\max}} \sum_{\tau=0}^{t_d} \sum_{n=1}^N (p_{\xi,\tau,n})_{\text{inf}} = \sum_{\xi_{\min}}^{\xi_{\max}} \sum_{\tau=0}^{t_d} \sum_{n=1}^N (p_{\xi,\tau,n})_{\text{eff}} + \sum_{\xi_{\min}}^{\xi_{\max}} \sum_{\tau=0}^{t_d} \sum_{n=1}^N (p_{\xi,\tau,n})_{\text{sep}}$$

(14)

$$p_{\xi,\tau,n} = \left(\frac{M_{\xi,\tau}}{N} \right)_{n=1}^N$$

(151)

$M_{\xi,\tau}$ is PM mass associated with the particle size range ξ as function of injection time τ , N is the total number of particles injected at the inlet section, t_d is the event duration.

4.7.6 Model validation

To evaluate the accuracy of the modeled results, Absolute relative error $\Delta\beta$ is introduced. It represents a measure of the accuracy error of the CFD model results respect to the full scale physical model data. The value of $\Delta\beta$ is computed as follows:

$$\Delta\beta = \left| \frac{\beta_{\text{measured}} - \beta_{\text{modeled}}}{\beta_{\text{measured}}} \right| \cdot \% \quad (16)$$

where β_{measured} and β_{modeled} represent respectively measured and modeled PM separation.

4.7.7 Computational resources

CFD simulations are solved in parallel on a Dell Precision 690 Workstation equipped with two quad core Intel Xeon® 2.33GHz (a total of eight cores), 16 GB of RAM, and a Dell Precision

7400 Workstation equipped with two quad core Intel Xeon® 2.5GHz (a total of eight cores), 32 GB of RAM. The computing times for physical model Pond models are between 6-36 hours. The computing time of ST Pond model is about 1 week.

5 Results and Discussion

5.1 Experimental Results - FAA Linear Pond and Crenellated Pond Configurations

From December 2009 through May 2010, the full-scale model of FAA Linear Pond and Crenellated Pond underwent physical model testing at the “Stormwater Unit Operations and Processes” facility located at University of Florida, Gainesville, FL. A total of 6 physical modeling experimental runs are performed for two Pond Configurations at unsteady influent flow rates (see Figure 7 and 8) and at steady state thermal, granulometric (particle size distribution) and gravimetric (particle concentration) conditions. In this section, monitoring data collected from the tests are reported along with a discussion of the findings. This analysis examines the PM separation of the two Pond Configurations (linear and crenellated) when it is subjected to the influent silt PM gradation. Testing experiments are carried out for the three hydrographs reported in Figure 11 and at influent sediment concentrations of 200 mg/L. The run operational parameters and the treatment run results for three hydrographs are summarized in the following Table 3. This table also correlates a given experimental run to a MBE, which confirms that each accepted run remained within $\pm 10\%$ MBE in order to fulfill the QC protocol. Any physical model run that did not achieve this requirement is reconstructed and rerun.

In order to investigate the influence of particle sizes from a hetero-disperse PSD on the overall PM separation of the system, the physical model results corresponding to the influent concentration of 200 mg/L are reported in terms of temporal variation of effluent PM in the following plot (Figure 28).

As expected, the performance of the FAA Linear Pond unit demonstrates exponentially increasing mass removal as the unsteady flow rate decreases towards low flow. At 2% maximum hydraulic capacity, the unit exhibits PM separation nearly equal to 90%. The PM separation decreases with increased flow up to the flow rate corresponding to 50%-100% of maximum hydraulic capacity. This phenomenon corresponds to the exponentially decreasing settling velocity of PM with respect to particle size. Since the influent PM gradation is hetero-disperse and contains a significant portion of finer particles it is expected that the unit, primarily

using the mechanism of gravitational settling, will not reach high efficiencies unless it is operating at very low flow rates. For the higher flow rates the unit is primarily capturing coarse PM while the fine material is passing through the unit. From the results shown in Table 3 and Figure 28, the PM separation results for the Crenellated Pond are almost doubled with respect to those obtained for the Linear Pond. This suggests that the Crenellated Pond is able to remove the coarser fraction of the influent PM gradation and retain part of finer fraction. This is due to a better utilization of the unit volume. In fact, the formation of dead zones and potential short-circuiting are reduced by the presence of the baffles, which lead to significantly increased detention times inside the system. However, as it is possible to note from Figure 28, for all three hydrographs at high flow rates, the effluent PM eluted from the crenellated Pond, although less than that shown for Linear Pond, is still significantly high. The reason of these findings is that at high flow rates the PM material which accumulates in the system throughout the entire controlled experimental run and that remain in suspension, is washed out from the unit.

Effluent PSD data obtained for each experimental run are compared to investigate the performance of both unit configurations under the loading of a silt gradation. Figure 29 shows PSD ranges related to tested unsteady hydrographs for influent loading concentrations of 200 mg/L. As it is expected, performance of both units increases by capturing finer PM as the flow rate decreases. Furthermore, the graph in Figure 29 provides an insight on the settling behavior of each particle size, showing the ranges of particle sizes which are completely retained within the unit for given flow rates. In addition, the PSD data are compared with the influent silt gradation to evaluate the system performance in terms of PM separation.

Linear FAA Pond

	Q_p	V	T_{tot}	SOR_{50}	d_p	$\beta_{measured}$	MBE
Hydrograph	(gpm)	(gal)	(min)	gal/(min-ft ²)	(μ m)	(%)	(%)
Triangular	450	3,99	44	23.4	23.8	47.1	6.03
July 8 th 2008	806	23,52	110	82.0	35.6	20.6	0.46
25 year - 24 hr	408	67,13	1369	25.6	35.6	32.3	1.76

Crenellated Pond

	Q_p	V	T_{tot}	SOR_{50}	d_p	$\beta_{measured}$	MBE
Hydrograph	(gpm)	(gal)	(min)	gal/(min-ft ²)	(μ m)	(%)	(%)
Triangular	450	3,99	44	10.6	25.2	98.3	10.40
July 8 th 2008	806	23,52	110	50.6	22.4	71.3	0.85
25 year - 24 hr	408	67,13	1369	14.9	28.3	63.7	9.67

Table 3 Summary of run operational parameters and measured treatment performance results based on effluent concentration and separated particulate matter (PM) for Pilot-scale Linear Pond and Crenellated Pond Configurations at UF loaded by hetero-disperse silt particle size gradation for three different hydrological events. Q_p is the peak influent flow rate, V is the Total Influent Volume, T_{tot} is the duration of the hydrological event, SOR_{50} is Surface Overflow Rate at Median Flow Rate, d_p is d_{50} of Recovered PM PSD, and MBE is Mass Balance Error

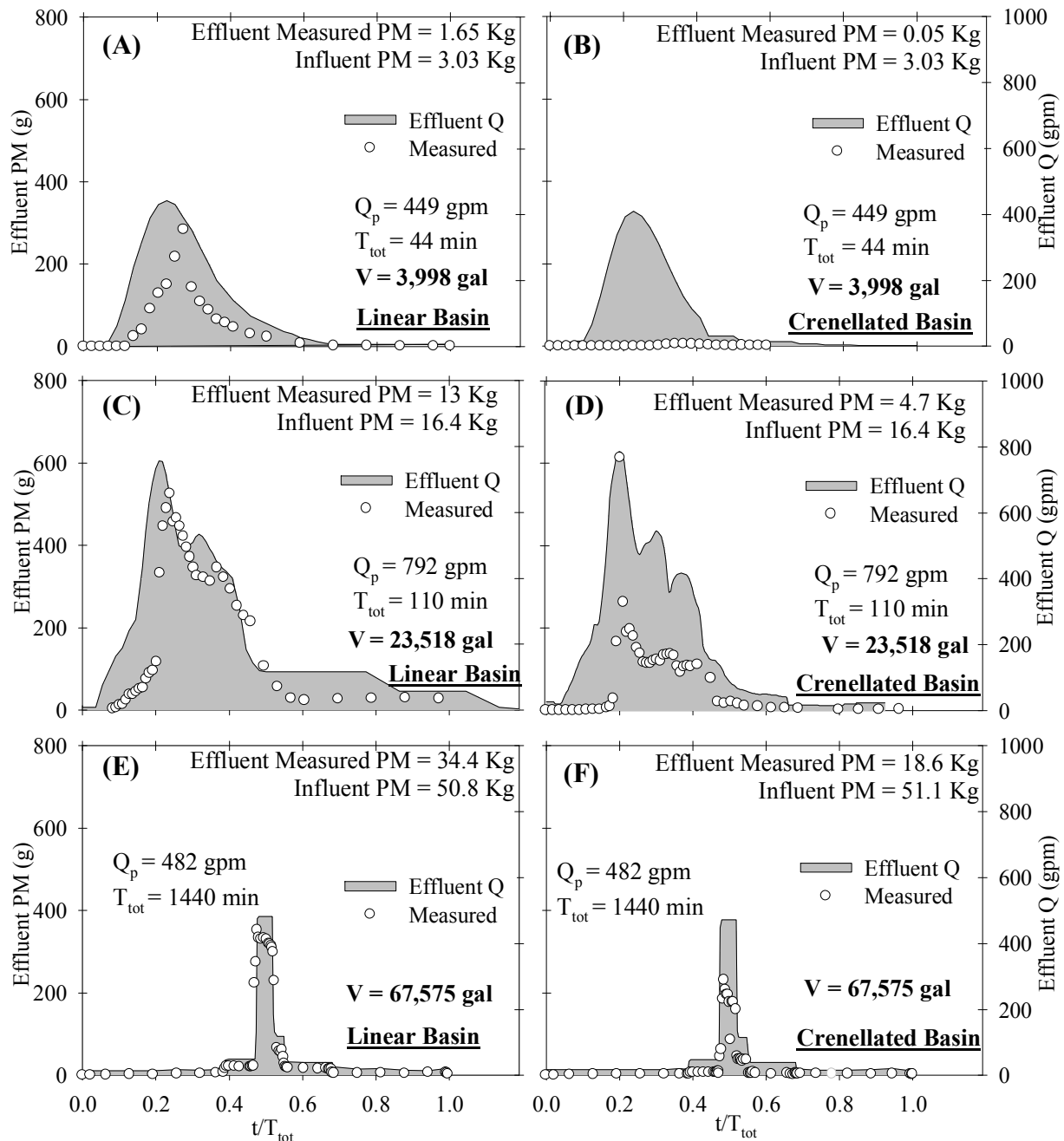


Figure 28 Effluent measured PM results for the Triangular Hyetograph (A, B), the Hydrological Event of July 8th 2008 (C, D) and the Design Storm Event of 24 hour-25 years (E, F) respectively for Pilot-scale Linear and Crenellated Pond Configurations at UF. V is the total influent volume, Q_p is the Peak Influent Flow Rate and T_{tot} is the total duration of the Hydrological Event.

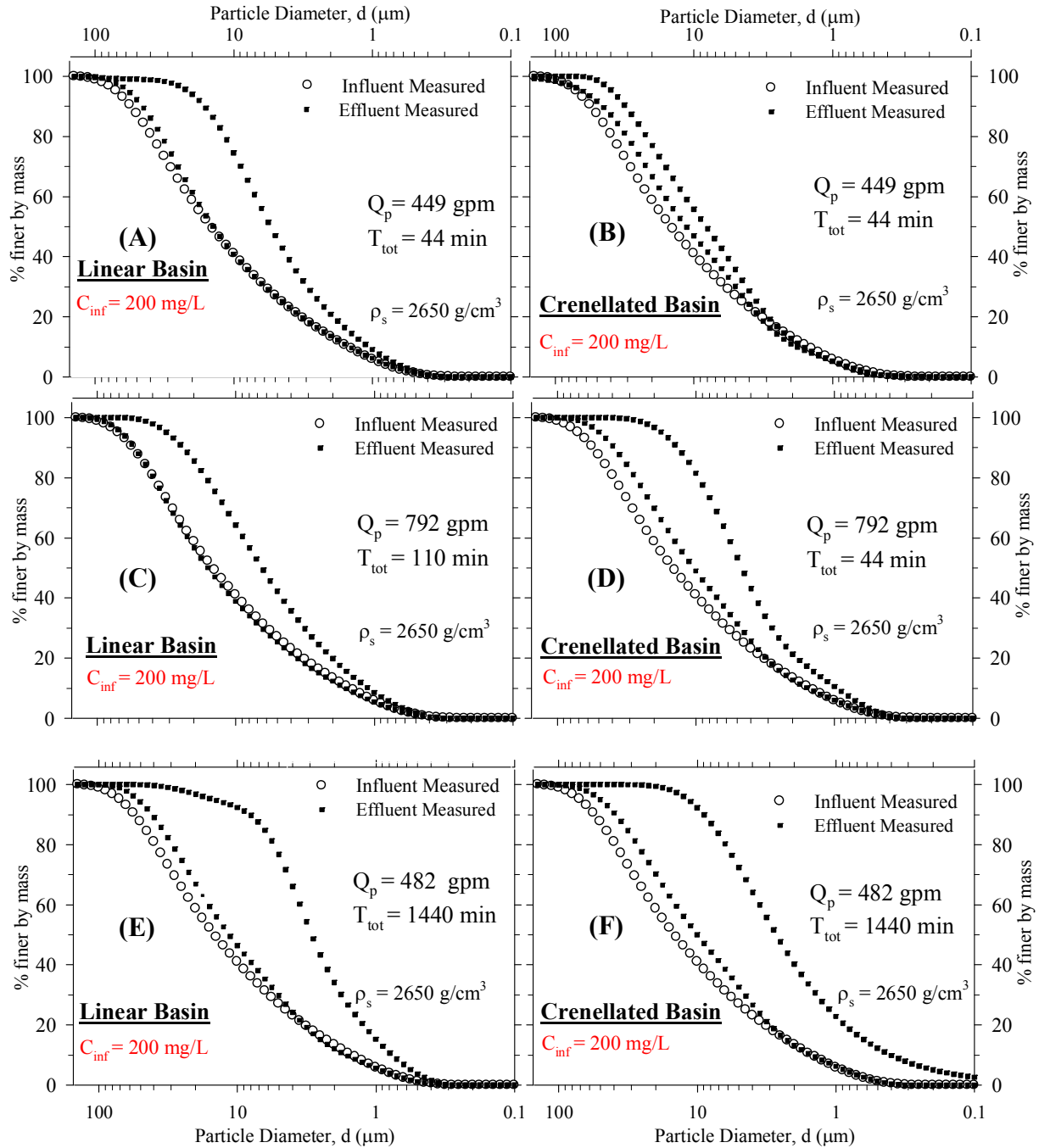


Figure 29 Effluent Measured PSDs for the Triangular Hyetograph (A, B), the Hydrological Event of July 8th 2008 (C, D) and the Design Storm Event of 24 hour-25 years (E, F) respectively for Pilot-scale Linear and Crenellated Pond Configurations at UF. ρ_s is the particle density, Q_p is the Peak Influent Flow Rate and T_{tot} is the total duration of the Hydrological Event.

5.2 CFD Modeling – FAA Linear Pond and Crenellated Pond results

After running the CFD model and solving the flow field, it is possible to analyze the hydrodynamic response of the two systems and visualize the results in terms of pathlines in post-processing. Checking the behavior of the pathlines through the unit operation (UO) in steady state condition confirms the quality of the mesh created in GAMBIT and the validity of the model constructed and consequently processed in CFD. Figure 30 and Figure 31 shows the pathlines for steady state condition obtained for the FAA Linear Pond and Crenellated Pond models for the maximum hydraulic capacity, 1.77 cfs (50 L/s). As it is possible to note from the figure reported below, fluid pathlines follow an acceptable and plausible pattern through both systems. The density of the pathlines can give an indication of the utilization of the treatment volume. At the maximum hydraulic capacity, it is qualitatively apparent that for the FAA Linear Pond the treatment volume is not uniformly fully utilized, showing two lateral stagnant regions and a short circuiting at the middle section of the unit. The presence of these defects in the hydraulic footprint indicates that the geometry of the unit can be modified to increase the utilization of the entire treatment volume and improve the hydraulic response of the system. Conversely, the Crenellated Pond shows a better utilization of the treatment volume due to the presence of the baffles, which constrains the flow to follow a longer path and occupy uniformly the entire cross section of the Pond. Dead zones are still visible at the intersection of the baffles and the lateral walls, but they represent reasonably small entities.

In Table 4 the results obtained from the CFD model are summarized and compared to those retrieved from the experimental testing. To assess the accuracy of the CFD results with the monitoring data, the absolute percentage difference ($\Delta\beta$) is computed. The $\Delta\beta$ s computed range from a minimum of 0.2 to a maximum of 9.7%. The values obtained are therefore within the control limit defined for $\Delta\beta$, which is 10%, demonstrating that the CFD model shows excellent confluence to the experimental data.

Figure 32 shows the CFD model results in terms of Effluent PM as function of time for both configurations and demonstrates physical model data are in accordance with numerical model outcomes. Figure 33 depicts the effluent PM PSDs variation over time for the set of six simulations performed. As before, the CFD modeled PSDs are in good agreement with measured

PSD results. In particular, in the figure the range of effluent measured and modeled PSDs (grey shaded) are shown, knowing that the PSDs vary throughout the event according to the unsteady flow rate.

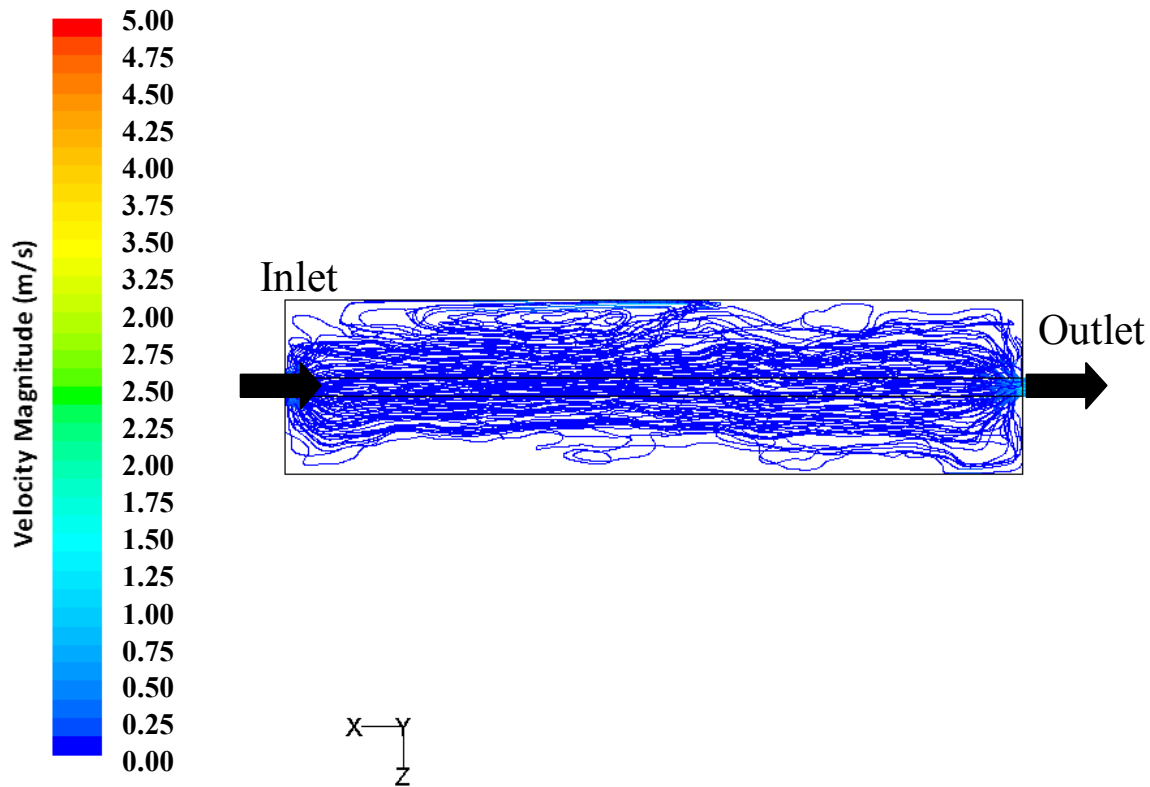


Figure 30 Fluid pathlines at maximum hydraulic capacity of 1.77 cfs (50 L/s) from FAA Linear Pond model developed in CFD, respectively. The pathlines are colored by Velocity Magnitude expressed as m/s.

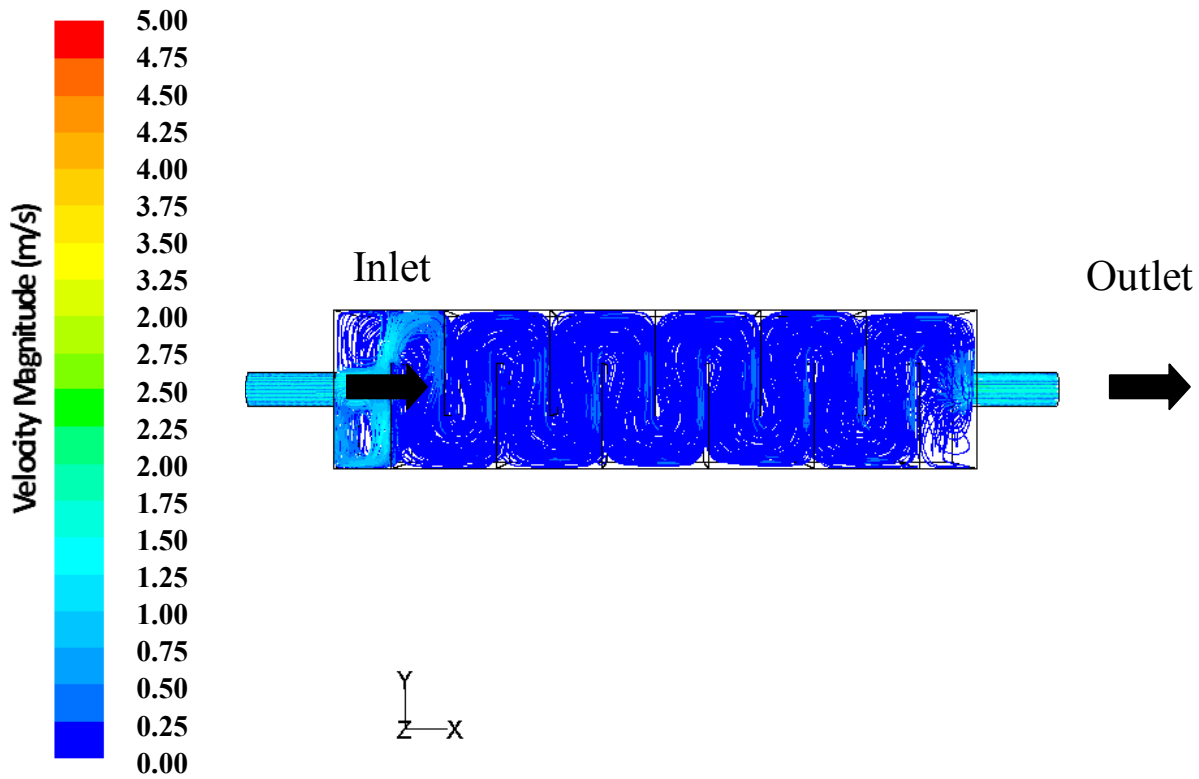


Figure 31 Fluid pathlines at maximum hydraulic capacity of 1.77 cfs (50 L/s) from Crenellated Pond model developed in CFD, respectively. The pathlines are colored by Velocity Magnitude expressed as m/s.

FAA Linear Pond

	Q_p	V	T_{tot}	$\beta_{measured}$	$\beta_{modeled}$	$\Delta\beta$
Hydrograph	(gpm)	(gal)	(min)	(%)	(%)	%
Triangular	450	3,99	44	47.1	47	0.20
July 8 th 2008	806	23,52	110	20.6	19	8.0
25 year - 24 hr	408	67,13	1369	32.3	29.2	9.7

Crenellated Pond

	Q_p	V	T_{tot}	$\beta_{measured}$	$\beta_{modeled}$	$\Delta\beta$
Hydrograph	(gpm)	(gal)	(min)	(%)	(%)	%
Triangular	450	3,99	44	98.3	98	0.3
July 8 th 2008	806	23,52	110	71.3	68	4.7
25 year - 24 hr	408	67,13	1369	63.7	67	5.2

Table 4 Summary of Experimental and Measured treatment performance results based on effluent concentration and separated particulate matter (PM) for Pilot-scale Linear and Crenellated Pond Configurations at UF loaded by hetero-disperse silt particle size gradation for three different hydrological events. V is the Total Influent Volume, Q_p is the peak influent flow rate, T_{tot} is the duration of the hydrological event and $\Delta\beta$ is Absolute Percentage Error.

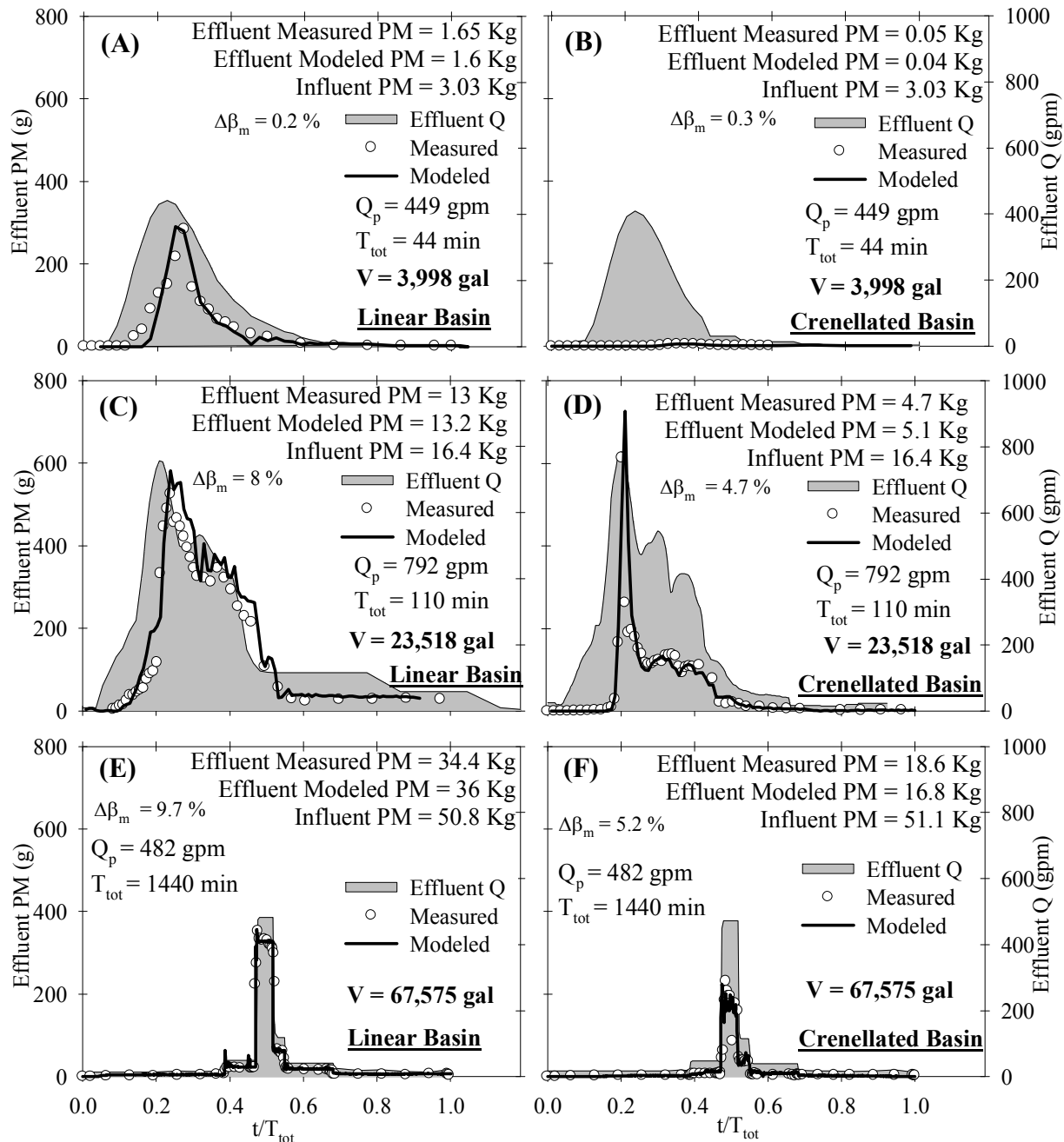


Figure 32 Effluent measured and CFD modeled PM results for the Triangular Hyetograph (A, B), the Hydrological Event of July 8th 2008 (C, D) and the Design Storm Event of 24 hour-25 years (E, F) respectively for pilot-scale Linear and Crenellated Pond Configurations at UF. $\Delta\beta$ represents the Absolute Percentage Error, V is the total influent volume, Q_p is the Peak Influent Flow Rate and T_{tot} is the total duration of the hydrological Event.

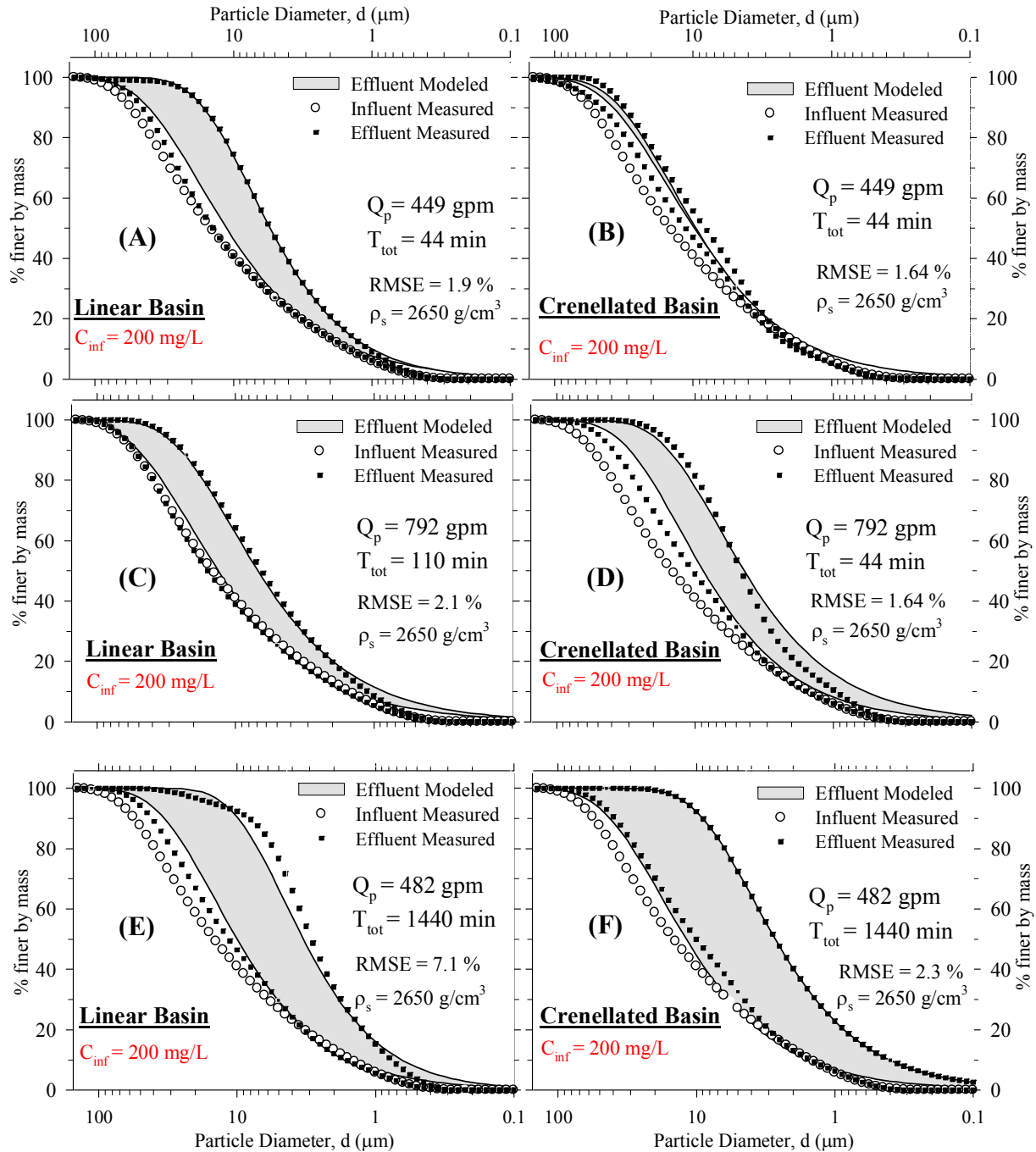


Figure 33 Effluent Measured and CFD Modeled PSDs for the Triangular Hyetograph (A, B), the Hydrological Event of July 8th 2008 (C, D) and the Design Storm Event of 24 hour-25 years (E, F) respectively for Pilot-scale Linear FAA and Crenellated Pond Configurations at UF. The shaded area indicates the range of variation of effluent PSDs throughout the hydrological events. RMSE is the Root Mean Squared Error between Effluent Average Measured and Modeled PSDs, ρ_s is the particle density, Q_p is the Peak Influent Flow Rate and T_{tot} is the total duration of the Hydrological Event.

5.3 CFD Modeling – ORL Wet Pond Results

The flow field, consisting of pressure and velocity data, is solved for selected hydrographs and the DPM model is applied for the influent silt gradation. The behavior of the pathlines within the system is shown at flow rates of 3.53 cfs (100 L/s) (1.5 % of Q_p), 26.48 cfs (750 L/s) (11% of Q_p), 106 cfs (3000 L/s) (50% of Q_p) and 238 cfs (6750 L/s) (100% of Q_p) in Figure 34. As it is possible to note from the pathlines as the flow rate increases the short-circuiting toward to the outlet of the Pond increases. This is due to the fact that up to a flow rate of 3.53 cfs (100 L/s) the presence of baffles has a strong influence on the flow path and constrains it to follow the longest trajectories, since the water level in the ST Pond is lower or at most equal to the maximum elevation of the earthed baffles. When flow rate values are above 3.53 cfs (100 L/s), the water level in the Pond, increases and becomes higher than the height of the baffles of 3 feet (0.9 m). This means while some of the pathlines still follow the path delimited by the baffles, others overpass the baffle structures and reach the outlet section faster. The effect of the baffles therefore is reduced for flow rates higher than 3.53 cfs (100 L/s), without playing any further their role in the treatment unit. The plot reported below (Figure 35) explicates this concept. Figure 36, Figure 37 and Figure 38 show also that for flow rates higher than 3.53 cfs, a portion of flow path lines, in the inlet zone, impinge against the horizontal baffle and turn in a vortex on the left side. The other portion of the flow does not encounter the baffle and turns toward to the right side following the pressure gradients toward to the outlet and partially the path delimited by the baffles. Selected PM sizes utilized to discretize the influent PSD and to evaluate the performance of the system are below included for visualization purposes as standard sizes. The following figures (Figure 39-42) show the particle trajectories obtained from CFD simulations at a peak flow rate of 238 cfs (6750 L/s) and represent a qualitative visualization of the particle dispersion behavior within the treatment system. As expected, 5 μm particles at the peak flow rate are uniformly dispersed within the system and are partially eluted from the system. Greater particle sizes are able to settle and the percentage of retained particles increases with the weight of the specific PM particle.

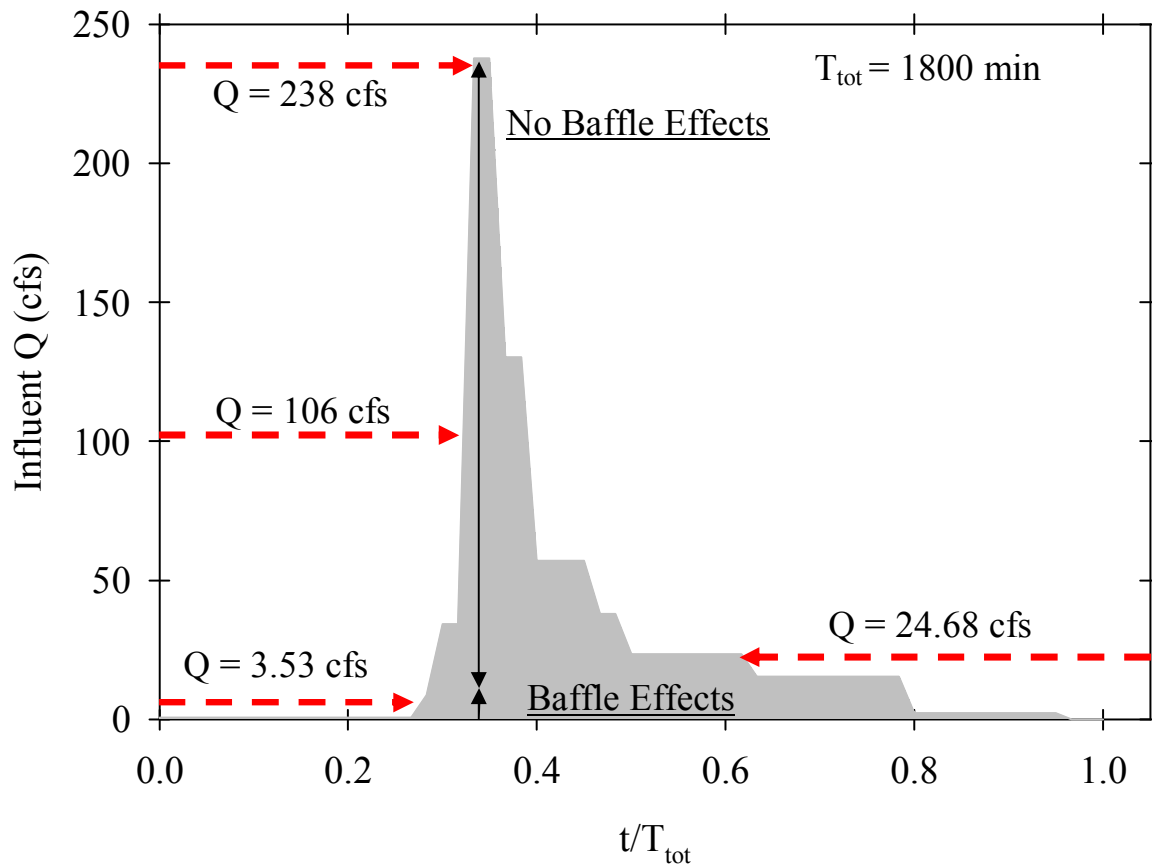


Figure 34 25 yr-24 hr Design Storm for ORL Wet Pond. The Q_p is 238 cfs (6750 L/s). The red arrows indicate the flow rates at which the pathline visualization is performed in the following figures. Five flow rates are highlighted: 3.53 cfs (100 L/s) which represents 1.5 % of Q_p , 26.48 cfs (750 L/s) which represents 10% of Q_p , 106 cfs (3000 L/s) which represents 50% of Q_p and 238 cfs (6750 L/s) equal to the peak flow rate. Based on the hydraulic condition established in the ORL Wet Pond, the water level at 1.5 % of Q_p reaches the height of the earthed baffles. In this case the baffles influence the flow path, avoiding short-circuiting. At higher flow rates than 1.5% of Q_p the water level increases and a portion of the flow overpasses the baffles. In this case, baffles partially exert their function and their effect on the flow path is significantly reduced.

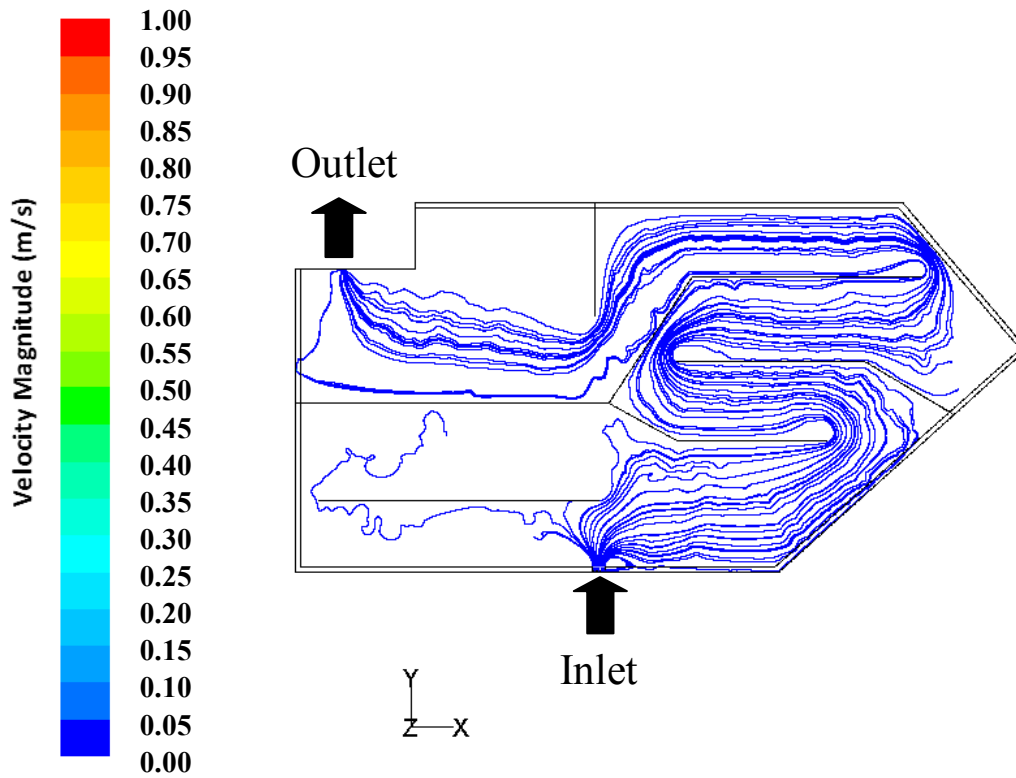


Figure 35 Fluid pathlines respectively at $Q = 3.53$ cfs (100 L/s) from ST ORL Pond model developed in Fluent 12. The pathlines are colored by Velocity Magnitude expressed as m/s

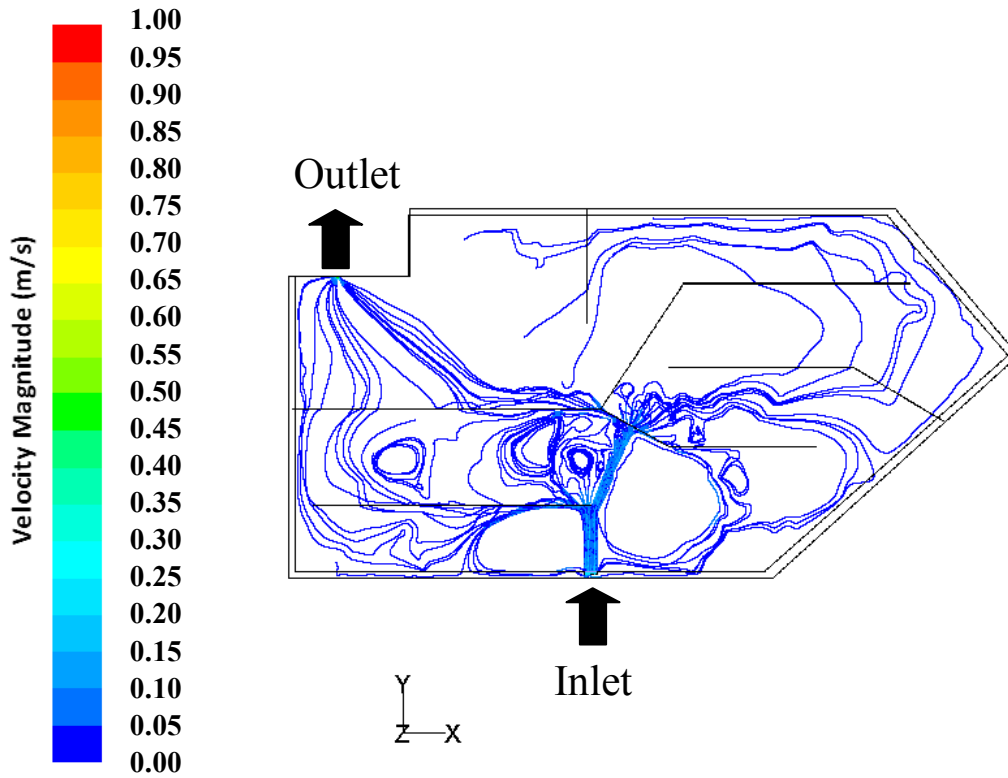


Figure 36 Fluid pathlines respectively at $Q = 26.48$ cfs (750 L/s) from ST ORL Pond model developed in Fluent 12. The pathlines are colored by Velocity Magnitude expressed as m/s

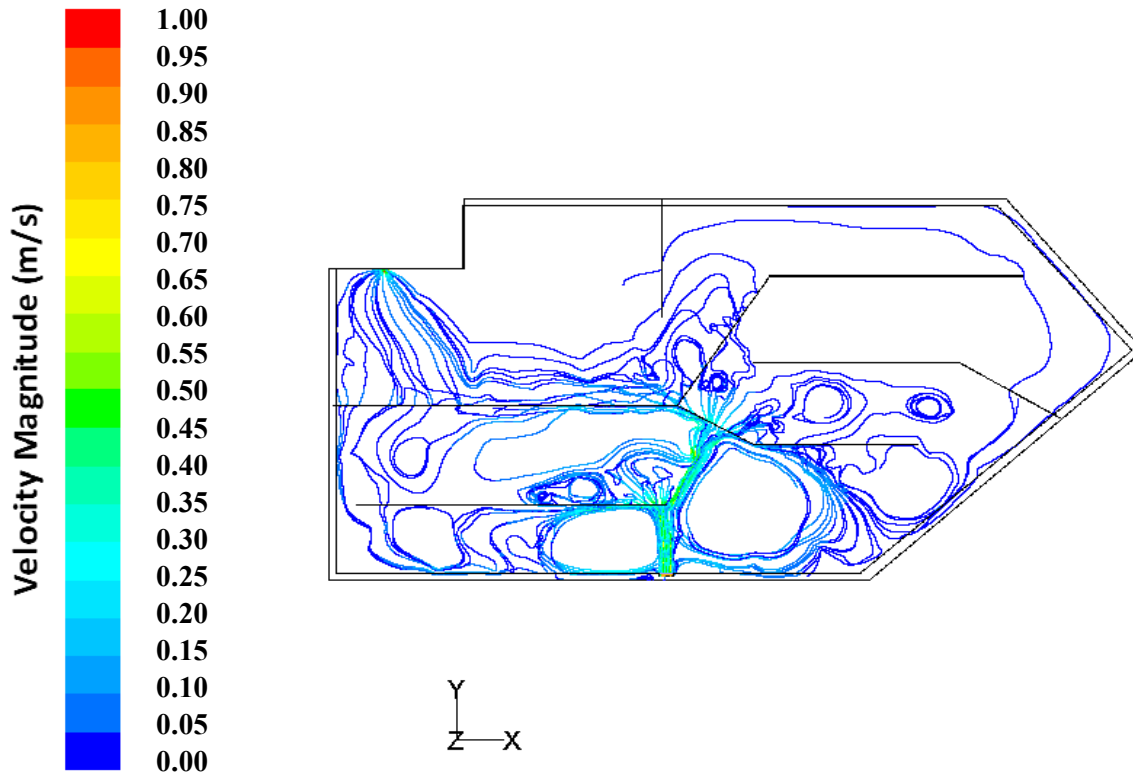


Figure 37 Fluid pathlines respectively at $Q = 106$ cfs (3000 L/s) for ORL Pond model developed in Fluent 12. The pathlines are colored by Velocity Magnitude expressed as m/s.

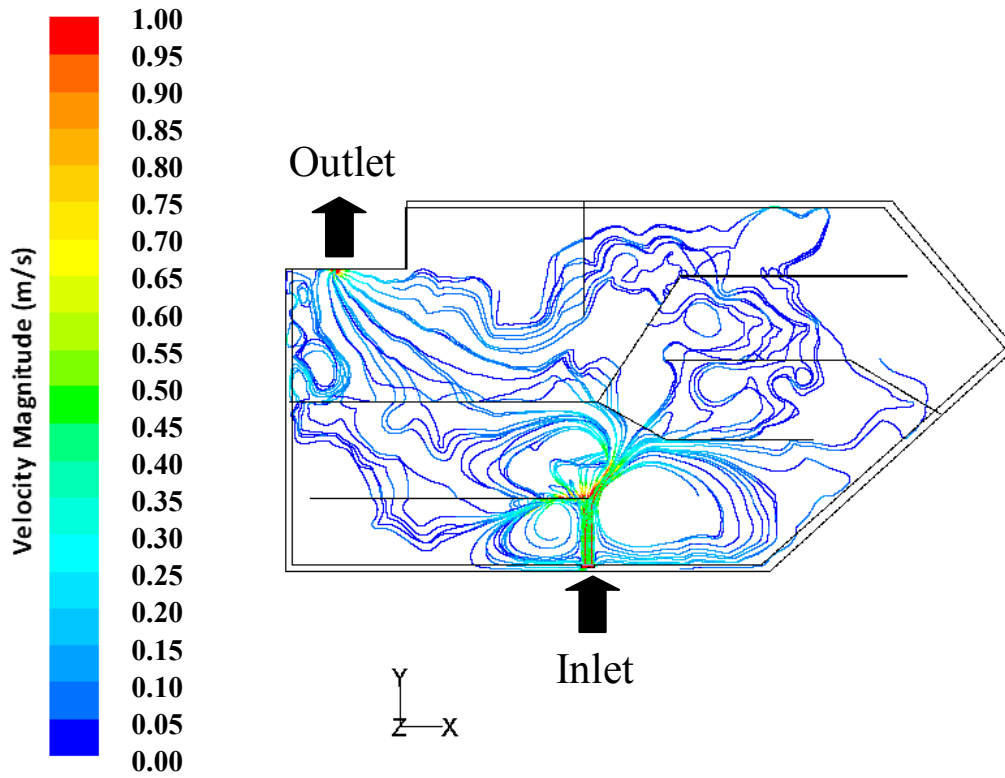


Figure 38 Fluid pathlines respectively at $Q = 238$ cfs (6750 L/s) for ORL Pond model developed in Fluent 12. The pathlines are colored by Velocity Magnitude expressed as m/s.

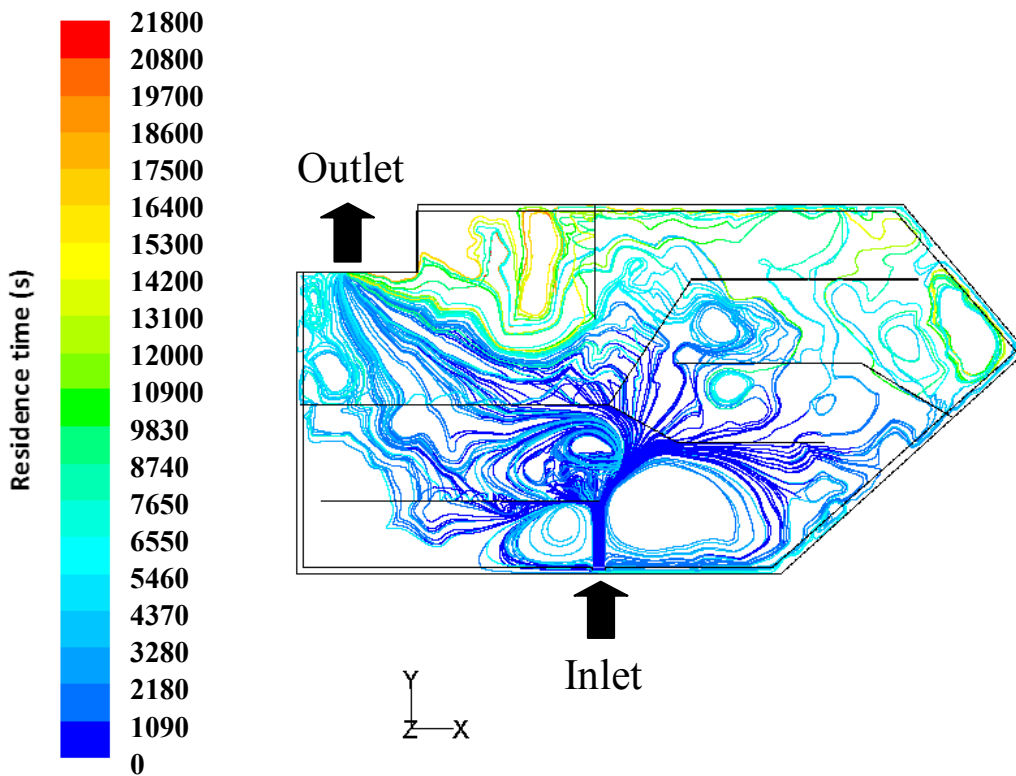


Figure 39 Discrete particle tracks for 5 μm PM ($\rho_s=2.650 \text{ g/cm}^3$) for $Q= 238 \text{ cfs}$ (6750 L/s). Particle tracks are colored by particle residence time. In the figures, dark blue and red correspond to the shortest and longest residence times, respectively. However, the color gradation refers to different value range for each picture; therefore, the figure provides only a qualitative representation of the particle tracks as function of residence time expressed in seconds

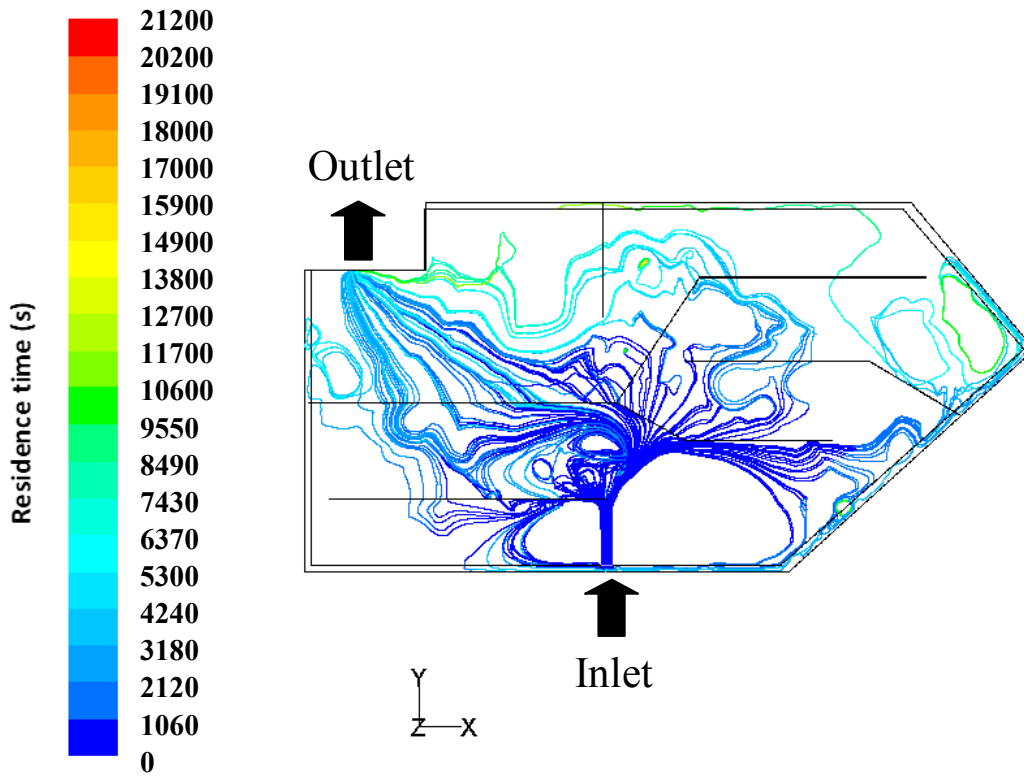


Figure 40 Discrete particle tracks for 35 μm PM ($\rho_s=2.650 \text{ g/cm}^3$) for $Q= 238 \text{ cfs}$ (6750 L/s). Particle tracks are colored by particle residence time. In the figures, dark blue and red correspond to the shortest and longest residence times, respectively. However, the color gradation refers to different value range for each picture; therefore, the figure provides only a qualitative representation of the particle tracks as function of residence time expressed in seconds.

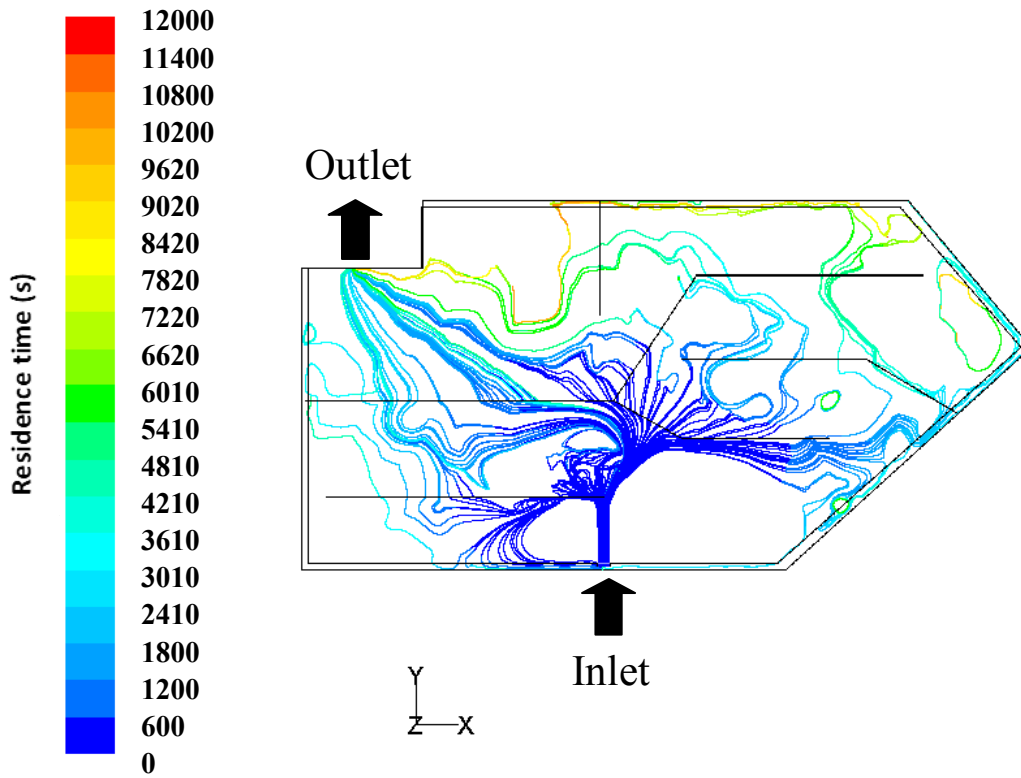


Figure 41 Discrete particle tracks for 55 µm PM ($\rho_s=2.650 \text{ g/cm}^3$) for $Q= 238 \text{ cfs}$ (6750 L/s). Particle tracks are colored by particle residence time. In the figures, dark blue and red correspond to the shortest and longest residence times, respectively. However, the color gradation refers to different value range for each picture; therefore, the figure provides only a qualitative representation of the particle tracks as function of residence time expressed in seconds.

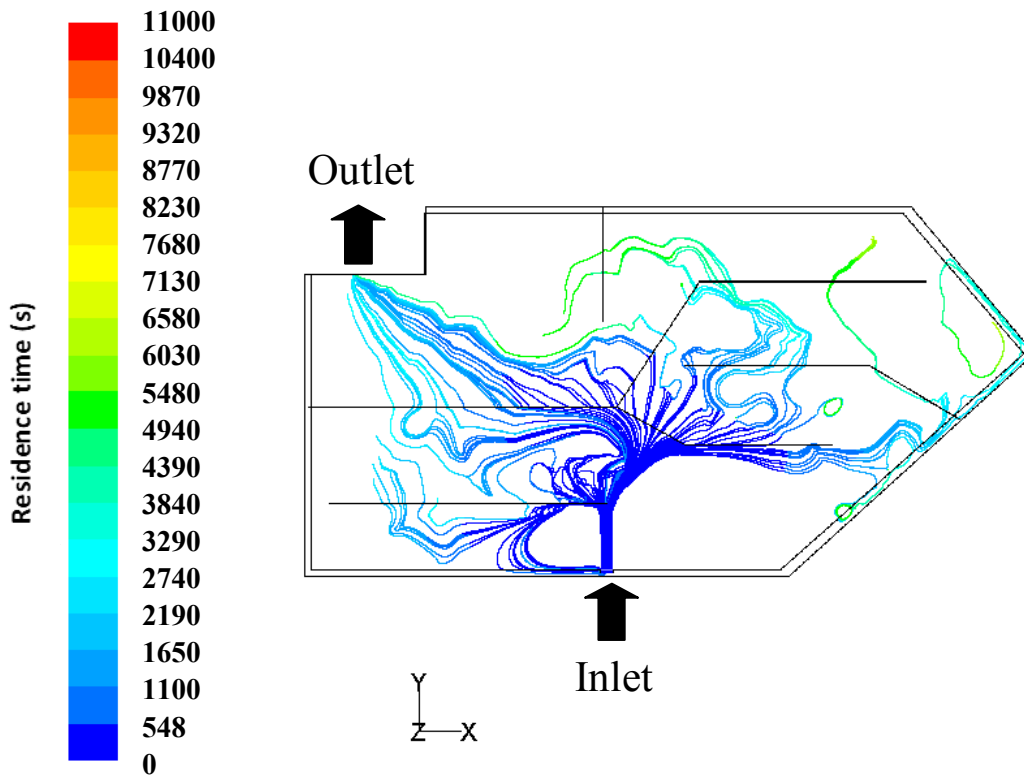


Figure 42 Discrete particle tracks for 85 μm PM ($\rho_s=2.650 \text{ g/cm}^3$) for $Q= 238 \text{ cfs}$ (6750 L/s). Particle tracks are colored by particle residence time. In the figures, dark blue and red correspond to the shortest and longest residence times, respectively. However, the color gradation refers to different value range for each picture; therefore, the figure provides only a qualitative representation of the particle tracks as function of residence time expressed in seconds.

Finally, the CFD modeled results under unsteady condition are shown for the ST ORL Pond. In particular, the PM separation and the temporal variation of effluent PM eluted from the system are depicted in Figure 43.

Figure 43 shows the results obtained for the 25 year-24 hour Design Storm generated from the SWMM model previously described in Section 3.4 at a constant influent silt concentration of 100 mg/L. The overall PM separation for the Design Storm is approximately 53 %. In Figure 44 CFD modeled results in terms of temporal variation of effluent PSDs are shown. Note the PSD with a d_{50} of 25 μm that delineates the lower limit of the shaded area is coarser than the influent PSD. This is due to the fact the coarser fraction of influent PM accumulates in the first part of the event and at the peak flow rate it is rapidly stirred up and flushed from the system.

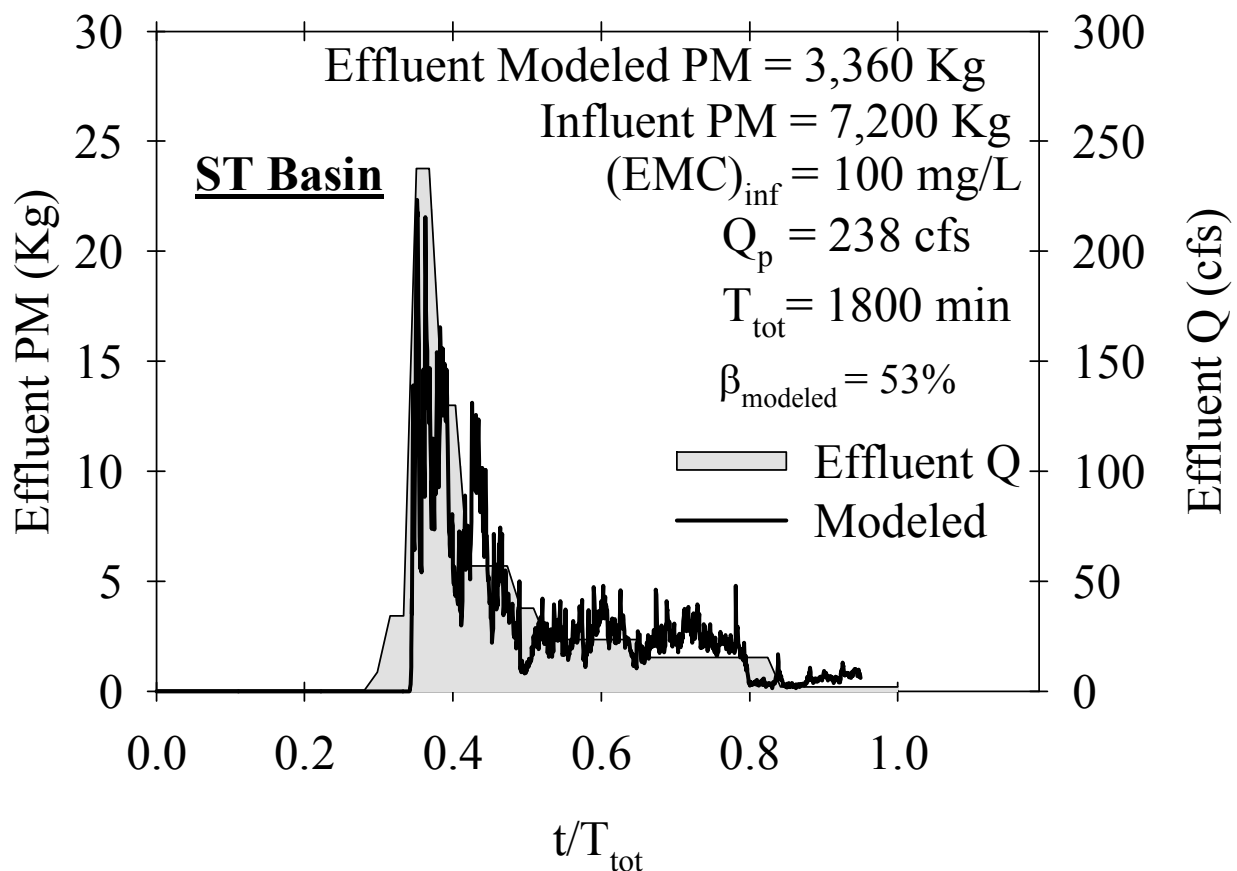


Figure 43 CFD Modeled Effluent PM for 25 year-24 hour Design Storm for ST ORL Pond. $(EMC)_{inf}$ represents the Influent Event Mean Concentration; Q_p is the peak flow rate, equal to 6750 L/s (238 cfs), T_{tot} is the total duration of the hydrograph; β_{max} is the modeled PM separation

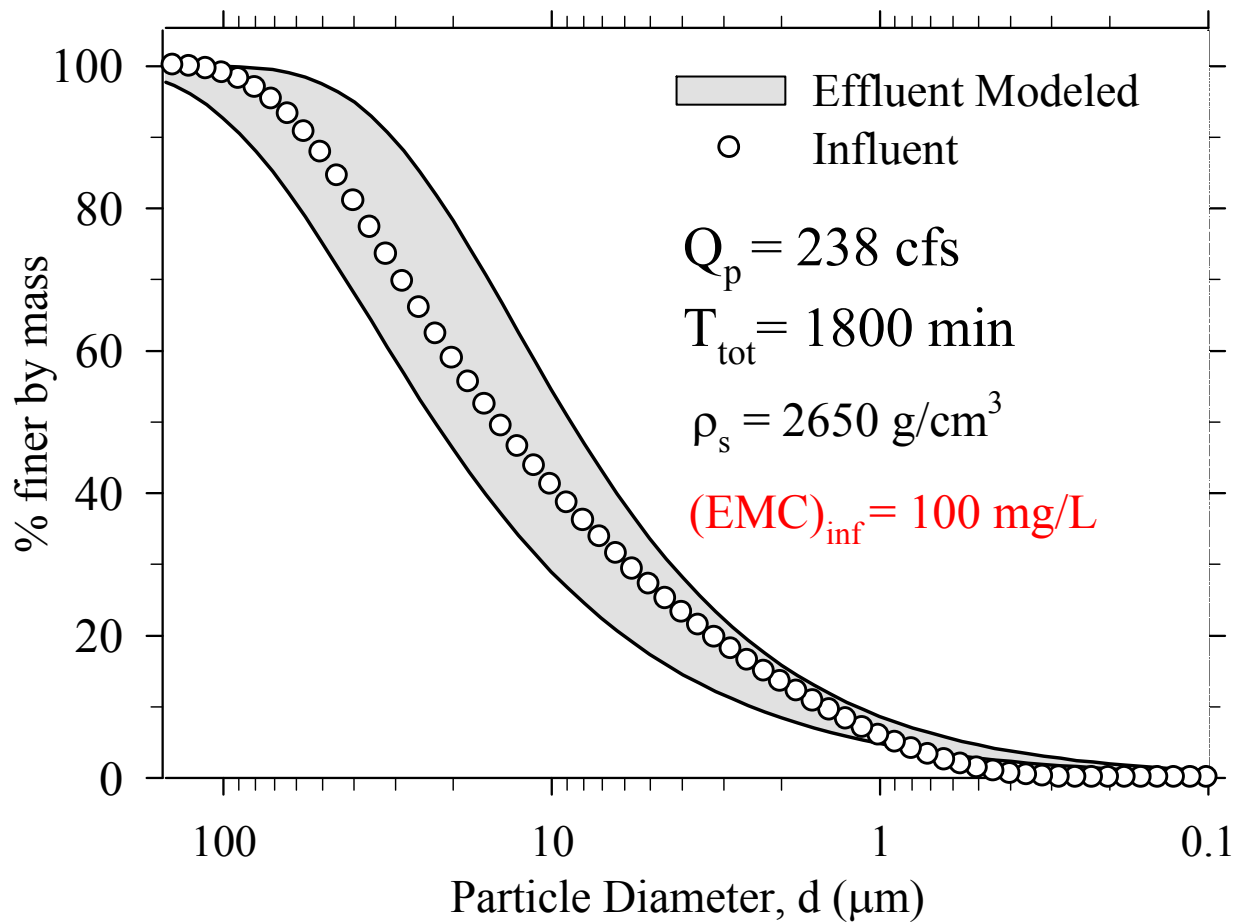


Figure 44 CFD Modeled Effluent PSD. The shaded area indicates the range of variation of effluent PSDs throughout the 25 year-24 hour Design Storm. $(EMC)_{inf}$ represents the Influent Event Mean Concentration; Q_p is the peak flow, equal to 6750 L/s (238 cfs), T_{tot} is the total duration of the hydrograph

5.4 CFD Modeling - Triangular and Rectangular Quarry Ponds Results

In this section the CFD modeled results are reported for the Triangular and Rectangular Quarry Ponds. In particular, the flow pathlines and particle tracks for 25 μm particle diameter are shown in Figure 45 and Figure 46. The modeled results demonstrate the hydraulic volume available is partially utilized, showing the presence of short-circuiting. The fluid pathlines coming out from the inlet #2 follow the slope along the right side wall and successively, reach the outlet along the south vertical wall.

The use of such an extended surface area is pointless since a large amount of space is occupied without providing any additional treatment performance advantage.

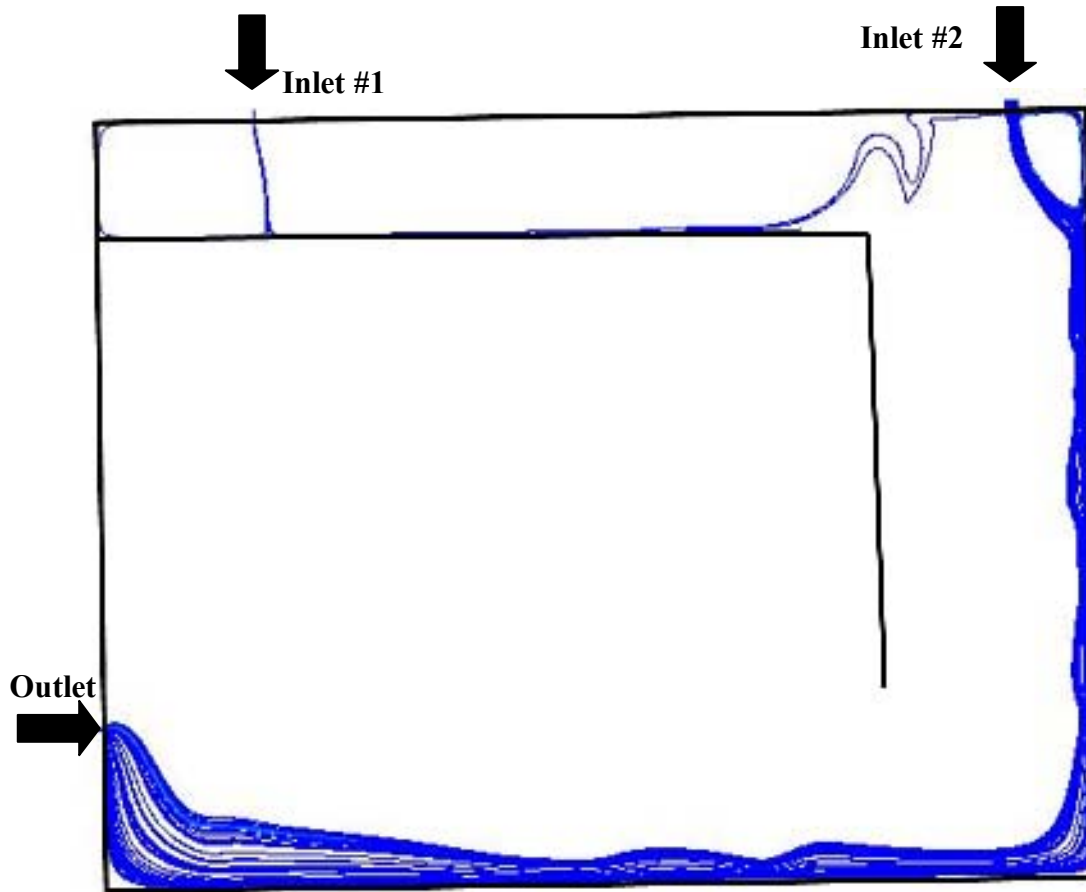


Figure 45 Fluid pathlines respectively at $Q = 821$ cfs for generic Rectangular Pond model developed in Fluent 12. The pathlines are colored by Velocity Magnitude.

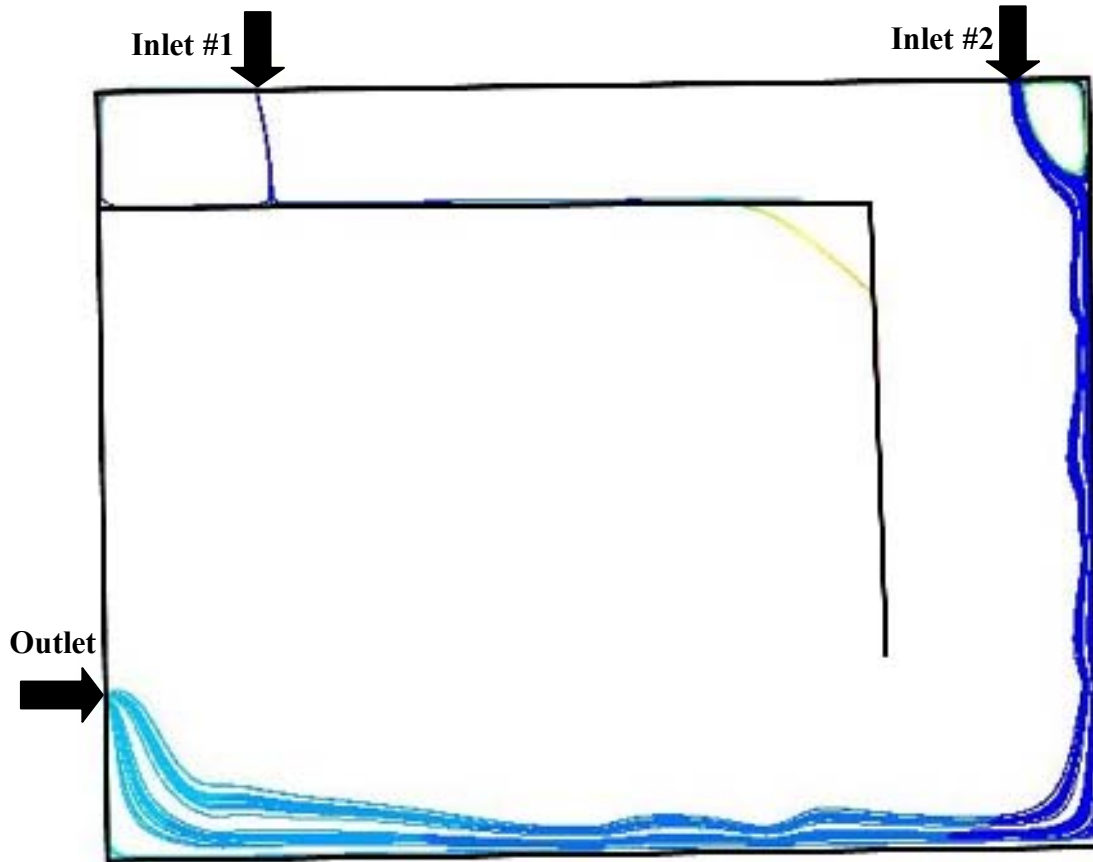


Figure 46 Pathlines for particles with diameter of 25 μm in generic Rectangular Pond Simulation.

The effluent PM PSD at $Q = 821$ cfs is depicted in the plot below, showing a fraction of the coarse material is removed. The overall PM separation is 51%.

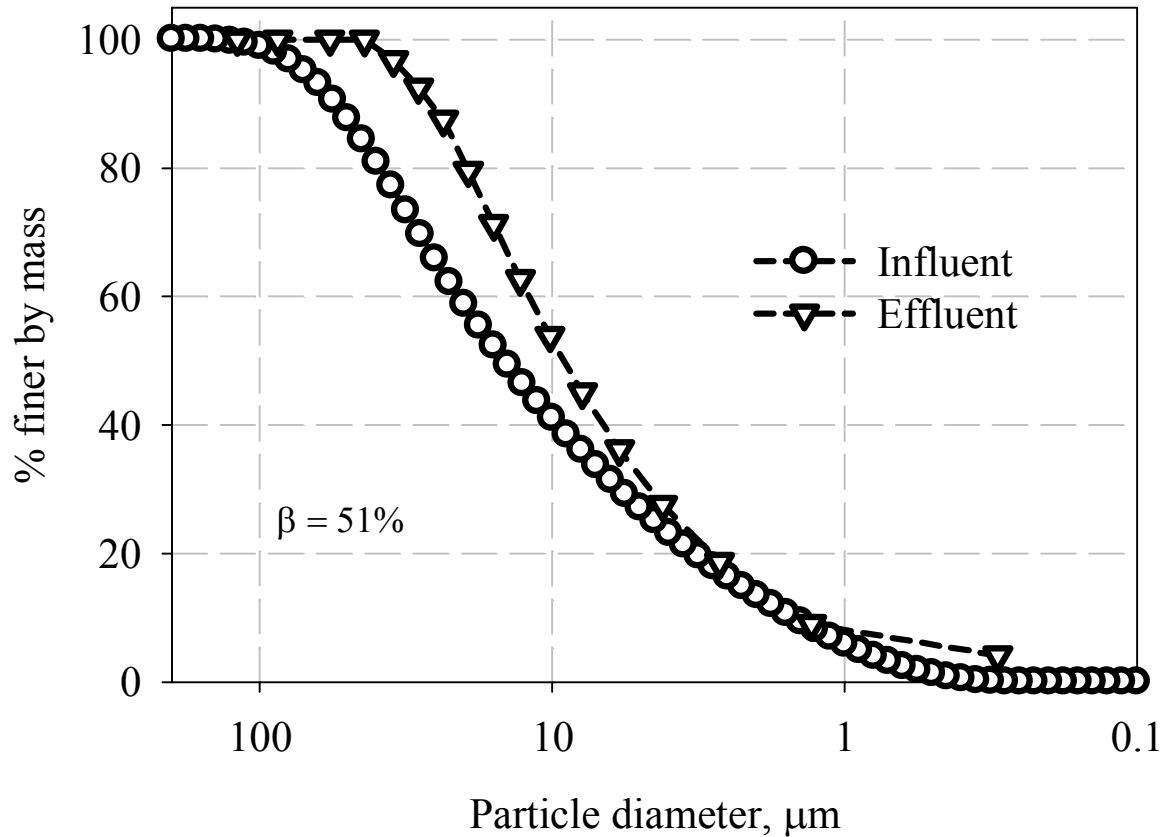


Figure 47 Particle size distribution (PSD) for influent and effluent particles in generic Rectangular Pond Simulation. Overall Separation (β) is 51 %.

In Figure 48 and Figure 49 the flow pathlines and particle tracks for 25 μm particle diameter are respectively shown for the Triangular Quarry Pond. The pathlines show the actual path followed by the flow to escape the system is relatively short, in comparison to the extended dimension of the unit. At the peak flow rate the finer fraction of the PM PSD is completely eluted from the system. The effluent PM PSD at $Q = 236$ cfs is depicted in the plot below. The overall PM separation is 21% for the Triangular Quarry Pond at the peak flow rate.

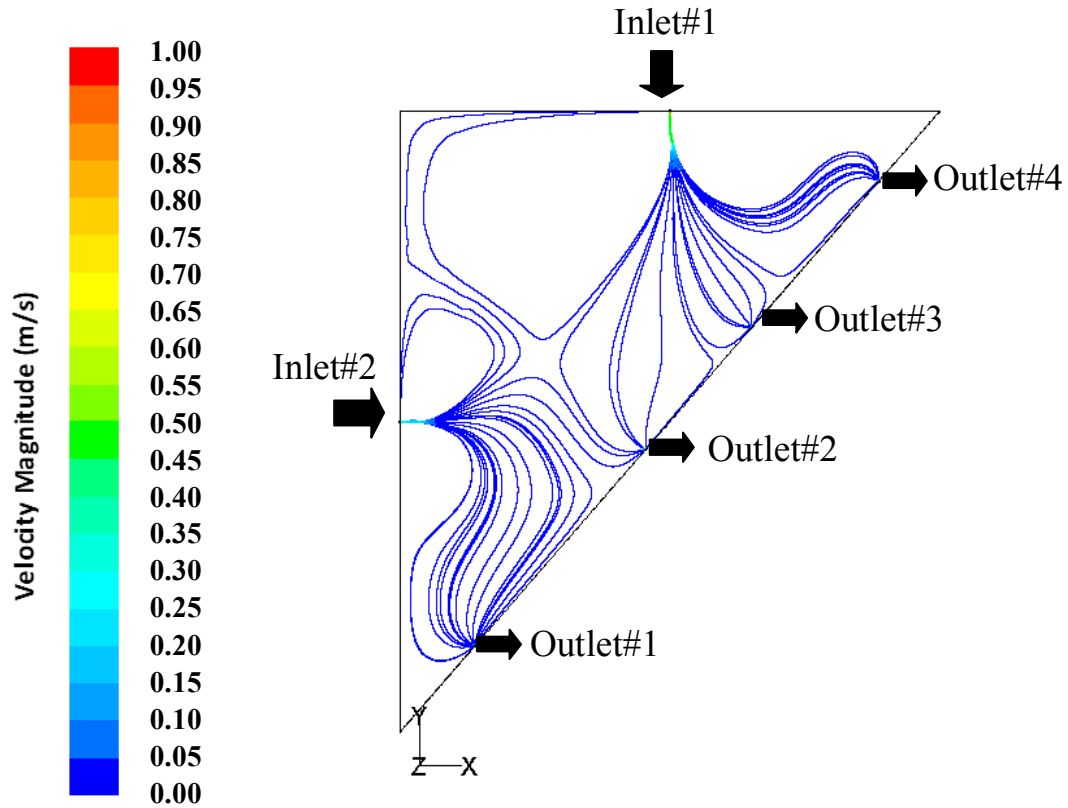


Figure 48 Fluid pathlines at maximum hydraulic capacity of 236 cfs (6682.6 L/s) for generic triangular Pond model developed in CFD, respectively. The pathlines are colored by Velocity Magnitude.

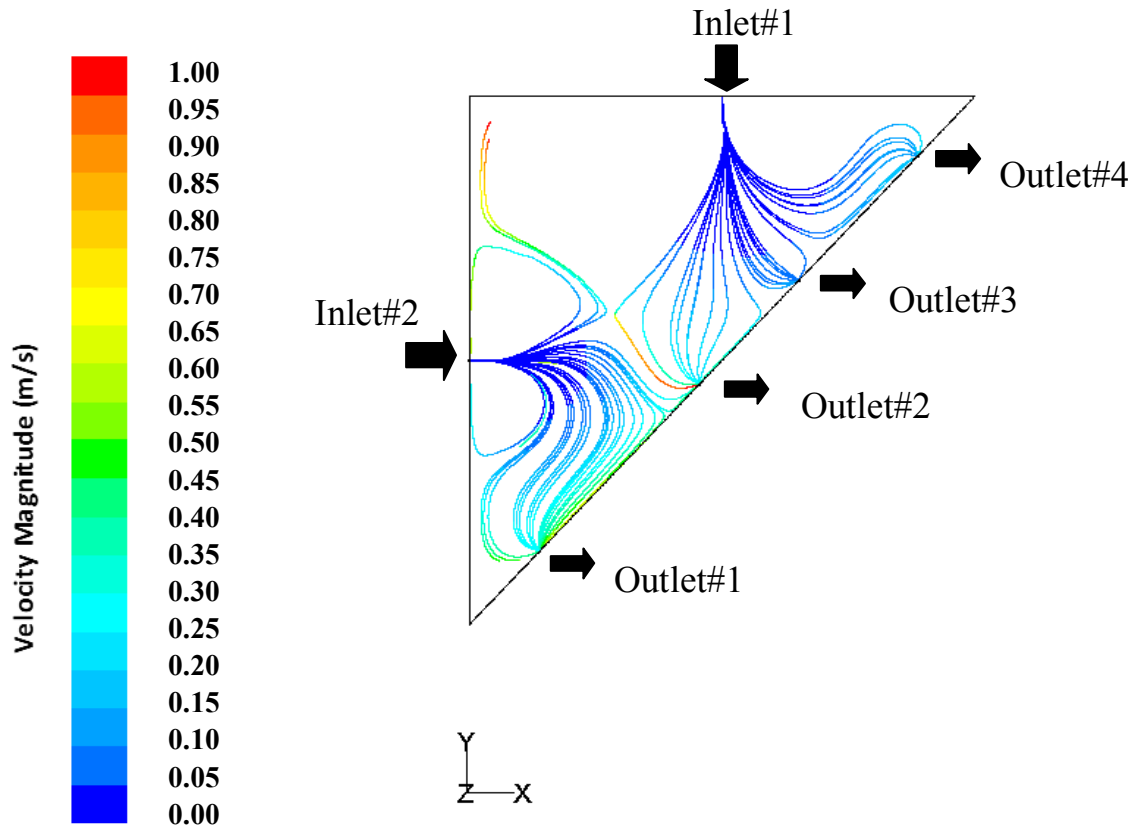


Figure 49 Discrete particle tracks for 25 μm PM ($\rho_s=2.650 \text{ g/cm}^3$) for 236 cfs (6682.6 L/s) for generic triangular Pond model. Particle tracks are colored by particle residence time. In the figures, dark blue and red correspond to the shortest and longest residence times, respectively. However, the color gradation refers to different value range for each picture; therefore, the figure provides only a qualitative representation of the particle tracks as function of residence time.

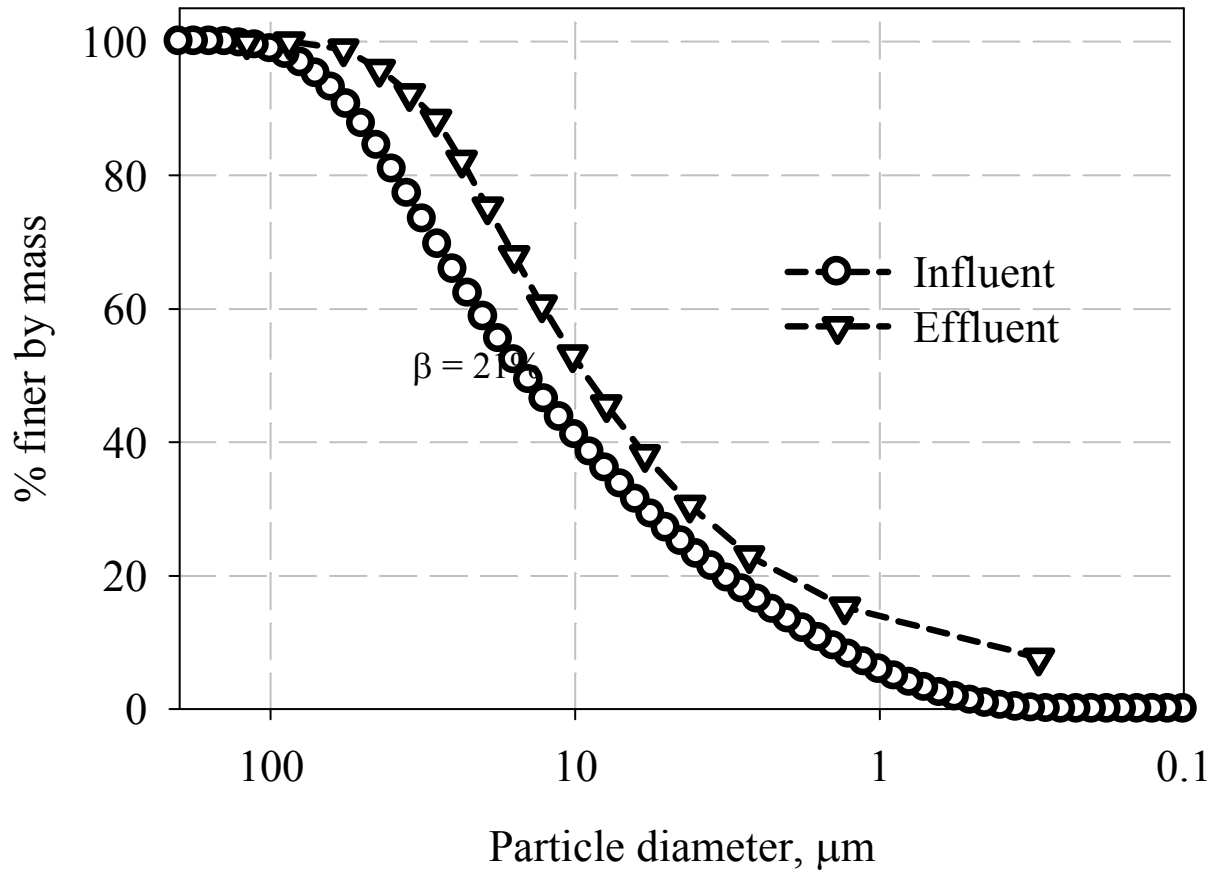


Figure 50 Particle size distribution (PSD) for influent and effluent particles for generic triangular quarry Pond. Overall Separation (β) is 21 %.

6 Conclusions and Recommendations

1. This analysis demonstrates the ability of CFD to model effluent mass and PSDs of PM as well as the overall PM separation of the Ponds investigated through achieving a high level of agreement between measured and modeled results. This level of agreement is accomplished by combining a validated CFD model and representative measurements of flow and granulometric quantities coupled with mass balance checks. Post-processing results provided insight into the mechanistic Pond behavior by means of three dimensional hydraulic profiles and particle trajectories.

2. The very large triangular and rectangular pond models demonstrate that the generic application of volume and depth (permanent pools having a mean residence time) without hydrodynamic isolation between inflow and outflow and also hydrodynamic control within the pond results in highly inefficient utilization of a pond volume. This is aggravated during extreme events. While such ponds have very low volumetric utilization and treatment effectiveness (for example, PM separation), they may represent a good repository for non-hazardous and non-reactive constituents that do not impact the overall water chemistry.

3. Modeled results for the FAA Linear Pond in companion with experimental data indicate that PM separation is fairly low varying from 48 to 20 % when the system is loaded with a silt PSD. However, this performance range is for relatively intense storms whose intensity will be exceeded less than 20% of the time on an annual basis for the least intense storm or only once every 25 years for the more intense storms modeled. Average annual performance should be expected to be better. Based on prior modeling (FDOT 2007) the expected average annual performance would exceed traditional presumptive ponds currently incorporated in Florida rules. Since treatment effectiveness (for example, PM separation or solute reduction) is based on average annual performance and not extreme events, this does not eliminate an FAA linear pond as a viable water management option, but suggests a modified form of the pond is likely a better option. For the FAA Linear Pond, the silt PSD used in this report, as representative of the fine

yet non-colloidal fraction of a PSD is recommended for use with Newton's Law (Stoke's law in the laminar settling regime) to establish the appropriate effluent discharge rate.

4. The treatment effectiveness (as PM separation) of a FAA Linear Pond is significantly improved using a Crenellated Pond with a series of internal baffles for the same surface area and volume. This has been identified as the best treatment performance within a given footprint that can be built with features that minimize wildlife attraction. The Crenellated Pond is characterized by the same surface area of the FAA Linear Pond. By comparing the modeled flow patterns with those for the case without baffles, it is evident that flow conditions are significantly improved. In particular, short-circuiting is considerably mitigated and velocity distribution within the Pond are more evenly distributed and drastically reduced in magnitude. Additionally, the volume is fully utilized avoiding the presence of dead zones. These factors significantly favor PM clarification, increasing the overall PM separation by a factor of 2. For the FAA Linear Pond, the silt PSD used in this report, as representative of the fine yet non-colloidal fraction of a PSD is recommended for use with Newton's Law (Stoke's law in the laminar settling regime) to establish the appropriate SOR. The baffle number and spacing could be based on the study results, but improved guidance will be developed following full scale pond testing recognizing that design guidance will be also be guided by individual site conditions. Major advantages for airport use include minimizing pond surface area to reduce the attractiveness to hazardous wildlife, minimizing the land required for water management, designing more maintainable pond systems and still maintaining a high PM separation per unit volume utilized. Furthermore, the effect of different layouts and numbers of baffles for given airport constraints can be investigated in CFD to verify which design best satisfies pre-set requirements in terms of cost, maintenance and overall performance.

5. The CFD models for the existing ORL pond indicate even baffled Ponds require spacing and top elevations consistent with a defined performance level during extreme events. The recommendation is to design the height elevation of the baffles based on the water level established at the peak flow rate (or at least 75% of Q_p) in the 25 year-24 hour

storm. The baffles placed in the Pond should be appropriately armored to avoid erosion of the baffles. The location of the baffles may be also improved in order to avoid the generation of dead zones and to dissipate completely the impinging jet coming from the inlet pipe. CFD model can be used to investigate different layouts. Potentially, fine PM and chemicals have a high potential to re-suspend and re-partition during intense events.

6. Periodic preventative maintenance is recommended to lower this potential adverse effect. The selection of the maintenance frequency should be based on a combination of rainfall frequency analysis, sediment buildup, and CFD predicted performance of the pond system. The crenellated pond will likely have the most infrequent maintenance needs to maintain a satisfactory level of water treatment performance based on the modeling results reported.

7 References

- ASTM Standard D 3977, 1997 (2002). Standard Test Methods for Determining Sediment Concentration in Water Samples. ASTM International, West Conshohocken, PA, www.astm.org
- Brennen, C. (2005). Fundamentals of Multiphase Flow. New York: Cambridge University Press
- Chow, V., Maidment D., Mays L.W. (1988). Applied Hydrology. New York, NY: McGraw-Hill
- Cristina, C.M. and Sansalone, J.J. (2003). First flush, power law and particle separation diagrams for urban storm-water suspended particulates. *Journal Environmental Engineering*, 129(4), 298–307
- Dickenson J. A. and J. J. Sansalone (2009). Discrete Phase Model Representation of Particulate Matter (PM) for Simulating PM Separation by Hydrodynamic Unit Operations. *Environmental Science Technology*, 43(21), 8220–8226
- EPA, 2000. National Water Quality Inventory. National Water Quality Report to Congress under Clean Water Act Section 305(b), retrieved from <http://www.epa.gov/305b/2000report/>
- FAA, 2007, Advisory Circular 150/5200-33B *Hazardous Wildlife Attractants On or Near Airports*
- FDOT, 2010, Drainage Manual
- FDOT, 2005 : Technical Report for the Florida Statewide Airport Stormwater Study
- FDOT, 2007 Application Assessment for the Florida Statewide Airport Stormwater Study

- Ferziger, J., Peric, M. (2002) Computational Methods for Fluid Dynamics. Springer: Berlin
- Fluent Inc., (2006). *Fluent 12 User's Guide*, Lebanon, New Hampshire, USA
- He, C., Wood, J., Marsalek, J., Rochfort, Q. (2008). Using CFD Modeling to Improve the Inlet Hydraulics and Performance of a Storm-Water Clarifier. *Journal of Environmental Engineering*, 134(9), 722-730
- Jakobsen, H.A. (2008). Chemical Reactor Modeling: Multiphase Reactive Flows. Springer Berlin: Heidelberg
- Jilavenkatesa A., Dapkunas S.J. and Lum L.S.H. (2001). Particle Size Characterization. National Institute of Standards and Technology, Special Publication 960-1, DC Washington
- Ma J., Ying G., and Sansalone J. J. (2010). Transport and Distribution of Particulate Matter Phosphorus Fractions in Rainfall-Runoff from Roadway Source Areas. *Journal of Environmental Engineering*, 136 (11), 1197-1205
- Magill N., Sansalone J. (2010). Distribution of Particulate-Bound Metals for Source Area Snow in the Lake Tahoe Watershed. *Journal of Environmental Engineering*, 136(2), 185-193
- Metcalf and Eddy (2003). Wastewater Engineering Treatment and Reuse. Boston: McGraw-Hill
- Pathapati S., Sansalone J.J. (2009a). CFD Modeling of a Storm-Water Hydrodynamic Separator. *Journal of Environmental Engineering*, 135(4), 191-202
- Pathapati S., Sansalone J.J. (2009b). CFD Modeling of Particulate Matter Fate and Pressure Drop in a Storm-Water Radial Filter. *Journal of Environmental Engineering*, 135(2), 77-85

- Sansalone, J. J., and S.-S. Pathapati (2009c). Particle dynamics in a hydrodynamic separator subject to transient rainfall-runoff. *Water Resources Research*, 45
doi:10.1029/2008WR007661
- Sansalone J.J., Ying G. and Lin H. (2010). Distribution of Metals for Particulate Matter Transported in Source Area Rainfall-Runoff. *Journal Environmental Engineering*, 136(2), 172-184
- Ranade, V. V. (2001). Computational Flow Modeling for Chemical Reactor Engineering. 1st ed., London: Academic
- Shih, T.-H.; Liou, W. W.; Shabbir, A.; Yang, Z.; Zhu, J. (1995). A new κ - ϵ eddy-viscosity model for high Reynolds Number turbulent flows- model development and validation. *Computational Fluids*, 24 (3), 227–238.
- St. Johns river management District, Technical publication SJ 88-3: Rainfall analysis for Northeast Florida, 1988
- Teng, Z. and Sansalone, J.J. (2004). In-situ storm water treatment and recharge through infiltration: Particle transport and separation mechanisms. *Journal of Environmental Engineering*, 130(9), 1008-1020
- Wu, J.S., Holman, R. E., Dorney, J.R. (1996). Systematic Evaluation of Pollutant Removal by Urban Wet Detention Ponds. *Journal of Environmental Engineering*, 122(11), 983-988

8 Abbreviations and Symbols

- AC: Advisory Circular
- C_{Di} : Drag coefficient
- C_{inf} : influent concentration [mg/L]
- C_1, C_2 : Empirical constants in the standard k- ϵ model
- CFD : Computational fluid dynamics
- d_p : particle diameter (μm)
- DN : Discretization number
- DHL : Dynamic Head Level (ft)
- DPM : Discrete particle model
- $(EMC)_{inf}$: Influent Event Mean Concentration [mg/L]
- FAA : Federal Aviation Administration
- FDEP : Florida Department of Environmental Protection
- F_{Di} : Buoyancy/gravitational force per unit particle mass
- g_i : sum of body sources in the i th direction (m s^{-2})
- GF : Gamma Function
- GNV : Gainesville Regional Airport
- GPM : Gallons per minute
- HDPE : High-density polyethylene
- HP : Horse Power
- I : Inflow
- k : turbulent kinetic energy per unit mass ($\text{m}^2 \text{s}^{-2}$)

- K1, K2, K3 : empirical constants as function of particle Re_i
- LPM : Liter per minute
- $M_{\xi, \tau}$: PM mass associated with the particle size range ξ as function of injection time τ
- MB : Mixing Pond
- MBE : Mass Balance Error
- N : Number of particles injected at the inlet section
- NB : North Pond
- NRCS : National Resource Conservation Service
- N-S : Navier-Stokes
- NWL : Normal Water Level (ft)
- O : Outflow
- ORL : Orlando Executive Airport
- $P_{\xi, \tau, v}$: Mass per particle (Kg)
- PFR : Plug Flow Reactor
- PM : Particulate matter (Kg)
- PSD : Particle size distribution
- Q_p : Peak flow rate ($L s^{-1}$, cfs, gpm)
- Q : Flow rate ($L s^{-1}$, cfs, gpm)
- p_j : Reynolds averaged pressure ($Kg m^{-2}$)
- $P_{25\text{year}, 24\text{ hour}}$: Rainfall precipitation with return period of 25 year and duration of 24 hour
- PBM : Population Balance Model

- PLC : Programmable Logic Control System
- QA : Quality Assurance
- QC : Quality Control
- RANS : Reynolds Averaged Navier Stokes
- Re_i : Reynold number for a particle
- RMSE : Root Mean Squared Error
- S : Storage
- SCS : Soil Conservation Service
- SIMPLE : Semi-Implicit Method for Pressure-Linked Equations
- SOR : Surface Overflow Rate
- SOR_{50} : Surface Overflow Rate at median flow rate
- SSC : Suspended sediment concentration ($mg L^{-1}$)
- STB : South Treatment Pond
- SWMM : Storm Water Management Model
- t_a : Time to peak rainfall (min)
- T_d : Total rainfall duration (min)
- t_p : Time of peak flow rate (min)
- T_{tot} : Duration of runoff event
- u_i : Reynolds averaged velocity in the ith direction ($m s^{-1}$)
- u_j : Reynolds averaged velocity in the jth direction ($m s^{-1}$)
- UO : Unit operation
- USDA : United States Department of Agriculture
- v_i : fluid velocity ($m s^{-1}$)

- v_{pi} : Particle velocity ($m\ s^{-1}$)
- V : Event Total Volume (L, gal)
- VF : Volume fraction
- VFD : Variable Frequency Driver
- x_m : modeled variable
- x_i : i th direction vector (m)
- α : Gamma distribution scale factor
- $\beta_{measured}$: Measured PM Separation
- $\beta_{modeled}$: Modeled PM Separation
- γ : Gamma distribution shape factor
- $\Delta\beta$: Absolute percentage difference between measured and modeled PM separation
- ε : Turbulent energy dissipation viscosity ($m^2\ s^{-2}$)
- μ : dynamic viscosity ($Kg\ m^{-1}\ s^{-1}$)
- ν : Fluid viscosity ($m^2\ s^{-1}$)
- ν_T : Eddy viscosity $m^2\ s^{-1}$
- ξ : Particle size range (μm)
- ρ : fluid density ($Kg\ m^{-3}$)
- ρ_p : particle density ($Kg\ m^{-3}$)

Computational and fluid constants are available in Dickenson and Sansalone (2009).